PLACE IN RETURN BOX to remove this checkout from your record. TO AVOID FINES return on or before date due. MAY BE RECALLED with earlier due date if requested.

DATE DUE	DATE DUE	DATE DUE
	,	

6/01 c:/CIRC/DateDue.p65-p.15

INTERFACIAL ENGINEERING OF THE INTERPHASE BETWEEN CARBON FIBERS AND VINYL ESTER RESIN

By

Lanhong Xu

A DISSERTATION

Submitted to
Michigan State University
in partial fulfillment of the requirements
for the degree of

DOCTOR OF PHILOSOPHY

Department of Chemical Engineering and Materials Science

2003

ABSTRACT

INTERFACIAL ENGINEERING OF THE INTERPHASE BETWEEN CARBON FIBERS AND VINYL ESTER RESIN

By

Lanhong Xu

Vinyl ester resins have been extensively used for the manufacture of low cost high performance composites. Carbon fibers are important reinforcement materials. The use of vinyl ester composites reinforced with carbon fibers requires an improvement in the fiber/matrix adhesion levels. The objectives of this study were to gain an understanding of the factors controlling interfacial adhesion between carbon fibers and vinyl ester resin; to model the contributions of the factors controlling fiber/matrix adhesion; and to provide an engineered and optimized interface between carbon fiber and vinyl ester for tailoring structurally efficient carbon fiber/vinyl ester composites. This work consists of three parts.

Part I: a partially cross-linked DGEBA epoxy polymer sizing placed onto carbon fiber surface was found to be a beneficial interphase between the carbon fiber and vinyl ester resin resulting in an increase in fiber-matrix adhesion. The adhesion was evaluated as interfacial shear strength (IFSS) with micro-indentation. Nano-indentation and nano-scratch technique were used to investigate the gradient between this epoxy sizing and vinyl ester resin. An optimized thickness of this sizing was found and the mechanism by which this sizing improved adhesion was also investigated. A set of 2-D non-linear finite element models was set up for simulation of the micro-indentation process and consistent results were found between the experimental data and numerical results. It was found

that the epoxy sizing formed more chemical bonds with the surface of the carbon fiber reinforcement and an interpenetrating interphase with the vinyl ester resin. The resulting interphase between vinyl ester matrix and epoxy sizing reduced the residual stress caused by the volume shrinkage of the vinyl ester after curing.

Part II: since it is known that the carbon fiber surface can interfere with the vinyl ester polymerization, the effects of preferential adsorption of the catalysts and styrene on the carbon fiber surface on fiber/matrix adhesion have been investigated. It was found that although the adsorption of the promoter and accelerator does occur on the carbon fiber surface, it does not substantially affect the fiber/matrix adhesion. The vinyl ester monomers and styrene monomers interact differently in the interphase. Optimum fiber-matrix adhesion can be obtained by selecting the initiator and adjusting the amount of initiator.

Part III: vinyl ester resins undergo significant volume shrinkage upon cure. Cure volume shrinkage was measured by a lab-made dilatometer. The cure volume shrinkage was found to reduce fiber/matrix adhesion as a result of residual stress. A 3-D non-linear finite element model was used to analyze the residual stress distribution at the fiber/matrix interphase. Higher von Mises effective stress was found for large cure volume shrinkage which is consistent with the experimental results.

Copyright by Lanhong Xu 2001 To my dear parents: Ruren Xu and Xuelin Zhao

ACKNOWLEDGMENT

I would like to express my sincere gratitude to my advisor, Professor Lawrence T. Drzal, for his valuable academic guidance, continuous spiritual encouragement and financial support throughout the time taken to complete this work. Without his help, I would not have reached this point today.

Special thanks also go to Dr. Ahmed Al-ostaz and Dr. Tom Mase for their intellectual contributions in finite element analysis and Dr. Richard Schalek for his assistance in nano-indentation test as well as their friendship.

I am thankful to the members of my committee—Dr. Ronald Averill, Dr. Phillip Duxbury, Dr. Krishnamurthy Jayaraman, Dr. Andre Lee, and Dr. Dashin Liu for their careful help in resolving my problems and the time they dedicated to my PhD study.

My thanks are also due to all the faculty, staff and students of the Composite Materials and Structures Center at Michigan State University who have helped me in many countless ways during my PhD study, especially, Mike Rich, Kelby Thayler, Hiroyuki Fukushima.

Finally, I thank my husband Ben Cai for his love and support in enabling me to complete this work.

TABLE OF CONTENTS

List of Tables	iv
List of Figures	v
CHAPTER 1 INTRODUCTION	1
CHAPTER 2 BACKGROUND	8
2.1 CARBON FIBER REINFORCEMENT	8
2.1.1 Manufacture Process	10
2.1.2 Topography and Morphology	10
2.1.3 The Surface Chemistry and Energetics	13
2.1.4 Carbon Fiber Surface Treatment	15
2.2 VINYL ESTER MATRIX RESINS	19
2.2.1 Introduction to DERAKANE Epoxy Vinyl Ester Resin	19
2.2.2 Cure Kinetics of Vinyl Ester Resin	22
2.2.3 Phase Separation and Microgel	26
2.2.4 Influence of Styrene Monomer Content	26
2.2.5 Cure Shrinkage of Vinyl Ester	29
2.3 CARBON FIBER- VINYL MATRIX INTERPHASE	31
2.3.1 General Introduction to Fiber/Matrix Interphase	31
2.3.2 Evaluation the Strength of the Fiber-Matrix Interphase	35
2.3.3 Low Adhesion between Carbon Fiber and Vinyl Ester Resin	35
2.3.4 Improvement of Adhesion between Vinyl Ester and Carbon Fiber	41
2.4 REFERENCES	42

CHAPTER 3 STATEMENT OF THE PROBLEM	49
CHAPTER 4 EXPERIEMNTAL METHODS	53
4.1 FIBER SIZING	53
4.1.1 Sizing Materials	53
4.1.2 Sizing Process	57
4.1.3 Sizing Thickness Measurement (TGA)	57
4.1.4 Environmental Scanning Electron Microscope (ESEM)	61
4.2 MEASUREMENTS OF MECHANICAL PROPERTIES OF MATERIALS	61
4.2.1 Dynamic Mechanical Thermal Analysis (DMTA)	61
4.2.2 United Testing System (UTS)	65
4.2.3 MTS Nano-indentation and Nano-scratch Test	65
4.2.3.1 Nano-Indentation Test 4.2.3.2 Nano-Scratch Test	66 69
4.3 MEASUREMENT OF THE ADHESION BETWEEN CARBON FIBER AND VINYL ESTER RESIN	71
4.4 REFERENCES	75
CHAPTER 5 IMPROVEMENT OF ADHESION BETWEEN CARBON FIBERS AND VINYL ESTER RESIN WITH EPOXY SIZING	77
5.1 INTRODUCTION	78
5.2 EXPERIMENTAL MATERIALS AND METHODS	80
5.3 RESULTS AND DISCUSSIONS	89
5.3.1 The Thickness of Sizing can be Controlled by the Concentration of Sizing Solution	89

5.3.2	Improvement of carbon fiber/vinyl ester adhesion with DGEBA sizing and the optimum sizing thickness for the best Interfacial Shear Strength (IFSS)	93
5.3.3	The role DGEBA sizing material played between carbon fiber and vinyl ester	94
5.4 CON	CLUSIONS	104
5.5 REFI	ERENCES	106
CHAPTER 6	INFLUENCES OF THE COMPONENT CHEMISTRY TO THE ADHESION BETWEEN VINYL ESTER AND CARBON FIBER	108
6.1 INTRO	DDUCTION	109
6.2 EXPE	RIMENTAL MATERIALS AND METHODS	112
6.3 RESU	LTS AND DISCUSSIONS	116
6.3.1	Influence of the Catalyst Concentration on the Properties of the Matrix Material	116
6.3.2	The Effect of Catalyst Concentration on the Interfacial Shear Strength (IFSS)	120
6.3.3	The Contribution of Vinyl Ester and Styrene Monomer of the D411-C50 to the Adhesion	125
6.4 CON	CLUSIONS	129
6.5 REFI	ERENCES	131
CHAPTER	7 CURE VOLUME SHRINKAGES OF VINYL ESTER RESINS AND THEIR INFLUENCES ON THE ADHESIONS BETWEEN CARBON FIBERS AND VINYL ESTER MARIX RESINS	133
7.1 INTRO	ODUCTION	134
7.2 EXPE	RIMENTAL MATERIALS AND METHODS	135
7 3 RFSI I	LTS AND DISCUSSIONS	145

7.3.1	Cure Shrinkage of Vinyl Ester Matrices	145
7.3.2	Influence of Cure Volume Shrinkage of Matrix Resin on the Adhesion between Carbon Fiber and Vinyl Ester	152
7.3.3	Interphase between DGEBA Epoxy Sizing and Vinyl Ester of Different Volume Shrinkage	155
7.3.4	Finite Element Analysis of the Residual Stress Caused by Cure Volume Shrinkage	159
7.4 MODI	ELLING INTERPHASE STRENGTH	162
7.5 CONC	CLUSIONS	166
7.6 REFE	RENCES	168
CHAPTER 8	CONCLUSIONS AND RECOMMENDATIONS	170
APPENDICE	CS:	
APPENDIX I	EVALUATION OF FIBER/MATRIX ADHESION	175
APPENDIX I	C++ PROGRAM FOR NANO-SCRATCH TEST	197
APPENDIX I	II RELATIONSHIP BETWEEN LINEAR SHRINKAGE AND VOLUMETRIC SHRINKAGE	202

LIST OF TABLES

Table 2.1	Selected Properties of AS4 Carbon Fiber	
Table 2.2	A Comparison of the Selected Properties to the Styrene Monomer Content for D411 Vinyl Ester Resin	28
Table 2.3	Volume Shrinkage of Vinyl Ester Resins	28
Table 2.4	Selected Properties of D411-C50 vinyl ester	30
Table 4.1	Selected Properties of DGEBA-T403	55
Table 4.2	The resolution and the ranges of MTS nano-scrach XP head and nano-indentation DCM Head	66
Table 5.1	Materials mechanical properties for finite element model	88
Table 6.1	Cure Formulations	115
Table 7.1	Property comparison of D411-C50 to Fuchem 891 vinyl ester	137
Table 7.2	The cure formulations for the investigation of the cure volume shrinkage	141
Table 7.3	Themomechanical properties for finite element model	144

LIST OF FIGURES

Figure 2.1	Manufacturing process of PAN based carbon fiber	9
Figure 2.2	Schematic draws of a three-dimensional model of a part of carbon fiber	11
Figure 2.3	Surface chemistry of AS4 carbon fiber	12
Figure 2.4	A schematic representation of the electrochemical oxidative surface treatment of the carbon fibers	14
Figure 2.5	Vinyl ester resin are produced from epoxy resin	20
Figure 2.6	Catalysts for cure of vinyl ester resin	23
Figure 2.7	(a) Chemical structure of typical DGEBA-based VE-ST resin system components, (b) a schematic representation of the VE-ST network formation showing the cross-linking capacity of the difunctional VE monomer, and (c) reactions encountered during the free radical bulk copolymerization of VE resin systems (draw not to the scale	24
Figure 2.10	Fiber-Matrix Interphase	32
Figure 2.11	Schematic diagram of the micro-indentation method for measuring fiber/matrix adhesion	36
Figure 2.12	Interfacial shear strength measured with the single fiber fragmentation test over a series of carbon fibers in an epoxy matrix, Epon 828-mPDA, two vinyl ester matrices, the Derakane 411-C50 and 8084	38
Figure 2.13	Interfacial shear strength of micro-droplet with polymers and as-received carbon fibers	39
Figure 4.1	Molecular of Diglycidy Ether of Bisphenol A (DGEBA) and Jeffamine T 403	54
Figure 4.2	Using a pre-impregnation machine to simulate the application of sizing in an industrial process	56
Figure 4.3	Using TGA to measure the sizing thickness	59

Figure 4.4	Using DMTA to measure the storage modulus at certain temperature and the glass transformation temperature	63
Figure 4.5	Use UTS to measure the tensile modulus	64
Figure 4.6	A hypothetic set of continuous load-displacement data of nano-indentation	67
Figure 4.7	Coefficient of friction (COF)	70
Figure 4.8	Interfacial Testing Systems (ITS) used for performing micro-indentation tests on fiber reinforced composites	72
Figure 4.9	ITS images for fiber before and after test	73
Figure 5.1	Effect of fiber sizing on the interfacial shear strength and composite mechanical properties	79
Figure 5.2	Molecular Structures for the chemicals used in this chapter	82
Figure 5.3	Cure formulation and cure process	83
Figure 5.4	The effect of the tip size to an interface with infinitesimal wideness	84
Figure 5.5	Four-phase model (drawing not to the scale) for finite element analysis	88
Figure 5.6	The sizing thickness versus the concentration of sizing solution	90
Figure 5.7	Sizing quality assessed with Environmental Scanning Electron Microscope (ESEM)	91
Figure 5.8	The interfacial shear strength (IFSS) related to the sizing thickness	92
Figure 5.9	Potential chemical reactions between carbon fiber surface and epoxy/amine system	95
Figure 5.10	Nano-indentation test	97
Figure 5.11	Nano-indentation results for the DGEBA/Vinyl ester interphase	98

Figure 5.12	Nano-scratch test traces for vinyl ester/DGEBA interphase	99
Figure 5.13	Comparison of the nano-scratch data between DGEBA sizing/vinyl ester interphase and reference interphase	100
Figure 5.14	Model for the interphase between carbon fiber and vinyl ester resin with epoxy sizing	103
Figure 6.1	Comparison of the interfacial shear strength between Panex carbon fiber/Derekane 411-C50 vinyl ester adhesion with different initiator	111
Figure 6.2	Influence of the amount of CHP-5 to the properties of cured D411-C50 resin	117
Figure 6.3	Influence of the amount of CoNap to the properties of cured D411-C50 resin	118
Figure 6.4	Influence of the amount of DMA to the properties of cured D411-C50 resin	119
Figure 6.5	The influence of the amount of CHP-5 to the IFSS between D411-C50 and AS4/Coated AS4 fibers	121
Figure 6.6	The influence of the amount of CoNap to the IFSS between D411-C50 and AS4/Coated AS4 fibers	122
Figure 6.7	The influence of the amount of DMA to the IFSS between D411-C50 and AS4/Coated AS4 fibers	123
Figure 6.8	Moduli comparison between vinyl ester, D411-C50 and styrene	126
Figure 6.9	The IFSS of vinyl ester, D411-C50 and styrene with AS4 and coated AS4 fibers	127
Figure 7.1	The setup used for the cure volume shrinkage measurements	138
Figure 7.2	A transversely isotropic array of composite fibers with the representative volume element indicated by a dashed line	143
Figure 7.3	The silicone oil level in the pipette of the lab-mad dilatometer versus time	146
Figure 7.4	The volume shrinkage observed from the lab-made dilatometer according to time	147

Figure 7.5	Influence of Cure Process to the Cure Volume Shrinkage of Vinyl Ester	150
Figure 7.6	One of the DMTA Measurement for Room Temperature Cured Fuchem 891	151
Figure 7.7	Influence of vinyl ester cure volume shrinkage on the bulk moduli	153
Figure 7.8	Influence of vinyl ester cure volume shrinkage on the Interfacial shear strength	154
Figure 7.9	Nano-scratch trace for the interphase of DGEBA epoxy sizing/Fuchem 891-MEKP	156
Figure 7.10	Comparison of nano-scratch data for the interphase of DGEBA epoxy sizing/Fuchem 891-MEKP and the interphase of DGEBA epoxy sizing/D411-CHP	157
Figure 7.11	Indenter force time history	159
Figure 7.12	von Mises stress for a point in the matrix at the interphase-matrix boundary located approximately 18 μm from the free surface	160
Figure 7.13	von Mises Stress Distribution at 5 g Indenter Load	161
Figure 7.14	The interphase property presented by interfacial shear strength(IFSS) plot	163

CHAPTER 1

INTRODUCTION

Advanced polymer composite with carbon fiber as reinforcement are extremely strong and light—around 10 times the strength to weight ratio of most metals. Carbon fiber composites started out in the 1950s and became a mature structural material in the 1980s. Vinyl ester resins were introduced in the late 1960s, originally were developed for their superior toughness and chemical resistance in comparison to unsaturated polyester, now find a wide range of applications. Carbon fibers have mainly been used in aerospace applications together with epoxy or high temperature thermoplastics, whereas vinyl ester resins have found use in large-volume and low-cost applications with primarily glass fiber as reinforcement. More recently, the availability of lower cost carbon fibers is improving the potential for the manufacture and application of carbon fiber reinforced composites in segments previously seemed too expensive, such as automobiles and infrastructures [1,2]. However when carbon fibers are combined with vinyl ester, the mechanical properties of the resulting composites are lower than desirable comparing with carbon fiber reinforced epoxy composite material [3,4].

Low adhesion between carbon fibers and vinyl ester resins was extensively reported ^[4-11]. It is well known that fiber/matrix adhesion can be a significant reason for lowering the mechanical properties of a composite material ^[12-15]. The interfacial shear strength of carbon fiber/vinyl ester system measured by single fiber fragmentation is only 50% of

that of the carbon/epoxy system ^[3,4]. Previous study found that the application of a lightly cross-linked, epoxy polymer onto the carbon fiber surface provides a beneficial interphase between the carbon fiber and vinyl ester resin matrix resulting in an increase in fiber-matrix adhesion and mechanical properties of the composites as well ^[4,16]. However, the exact mechanism by which this sizing improved adhesion remained unknown and the epoxy-amine sizing need to be optimized for compatibility and thickness. The first part of this study focused on the investigation of the effects of the thickness and gradient of the epoxy sizing on the adhesion between carbon fiber and vinyl ester resin.

Typical vinyl ester resins contain 35-50wt% styrene monomer as reactive diluents. The copolymerization between styrene monomer and vinyl ester monomer is a heterogeneous, free radical, chain-growth, and cross-linking reaction. The wetting condition to the carbon fiber surface of styrene monomer could be different from that of vinyl ester monomer because the surface energy of styrene monomer would be smaller than that of vinyl ester resin (refer: 40(epoxy) ^[17]; 26.7(benzene) ^[18]). In addition, a previous investigation by Weitzsacker, Drzal et al. ^[19] investigated the reactions of the catalyst and/or promoters to determine if they were competing with the vinyl ester matrix resin for reactive sites at the carbon fiber surface. Cobalt was detected at 2.6% at the surface of the AS4 carbon fiber exposed to cobalt naphthenate (CoNap) and a minor change was also noted in the surface chemistry of the fiber exposed to dimethyl aniline (DMA) which are the promoters and accelerators for the free radical copolymerization respectively. The influences of the reaction catalysts and the two components of vinyl

ester resin, the vinyl ester monomer and styrene monomer on the interface properties between carbon fiber and vinyl ester was the second interest of this study.

Residual stress can be another factor that lowers the adhesion if it creates a transverse tensile stress of sufficient magnitude at the fiber-matrix interphase. Since it is known that vinyl ester resin can undergo as much as 9% volume shrinkage with cure while typical epoxy system undergo only 3-4% shrinkage during cure [20,21]. This shrinkage can induce significant stresses in the composite already before loading. On the other hand, composite materials have residual stress from the fabrication. In the case of carbon fibers, the coefficient of thermal expansion (CTE) is quite small and can actually be negative [22]. The fiber is anisotropic and the radial and longitudinal thermal expansions can be quite different. The polyester is isotropic but has a CTE a factor of 80×10⁻⁶/K ^[23] (compare with Epoxy: $60\times10^{-6}/K$ [21], $127\times10^{-6}/K$ [24]). This disparity becomes increasingly significant as higher processing temperatures are reached with the absolute difference between the glass temperature and the use of temperature determining the magnitude of these residual thermal stresses. In addition, the difference of thermal conductivities of materials can introduce unevenly distributed temperature during process and application can also result in residual stresses even defects [25]. The final part of this study focused on the cure volume shrinkage of vinyl ester resin and its influences on the adhesion between carbon fiber and vinyl ester resin.

Finite element methods have been widely used to predict the effective elastic properties and the elastic response of fibrous composites under mechanical and/or thermal loading. Finite elements are particularly useful for detail studies of the stress distributions in the fiber and surrounding matrix as a function of the actual fiber

arrangement, matrix properties, loading condition and application temperature ^[23, 26-29]. Using IDEAS for the pre-processing and ABAQUS for processing and post-processing, a set of non-linear contact finite element models were set up to find out the influence of the thickness of sizing material and the results were compared with the experimental data in the first part of the research. LS-DYNA, one of the most powerful non-linear finite element analysis methods, was used for the simulation of the cure volume shrinkage and the stress brought by the shrinkage in the third part of the research.

The research has been organized into three major sections as described above and is represented by Chapter1 through Chapter 8. Chapter 1 and 2 detail the driving principles behind the research undertaken in this study. Chapter 3 is the objectives of this study. The experimental methods are covered in Chapter 4. Chapter 5, Chapter 6, and Chapter 7 provide the experimental works covering the summary, introduction, experimental procedures, results and discussions of the three major sections of the researches. Chapter 5: the influence of sizing thickness and gradient on the adhesion between carbon fiber and vinyl ester matrix; Chapter 6: the influence of the component chemistry on the adhesion between carbon fiber and vinyl ester matrix; Chapter 7: the influences of resin cure volume shrinkage on the adhesion between carbon fiber and vinyl ester matrix. Chapter 8 contains the conclusions and the ideas for future works.

REFERNECES:

- 1. High Preformance Composites, Vol. 4, pp 11, 1996
- 2. Zoltek Companies, Inc., Annual Report, pp 6, 1995
- 3. D. Hoyns. and L. T. Drzal, "Hydrothermo-mechanical Response and Surface Treated and Sized Carbon Fiber/Vinyl Ester Composites", **ASTM Symposium on the Fiber Matrix and Interface Properties**, Nov., 1994
- 4. S. M. Corbin, **M.S. Thesis**, Department of Chemical Engineering, Michigan State University, 1998
- 5. V. Rao and L. T. Drzal, **Polym Compos**, Vol. 12, No. 48, 1991
- 6. L. H. Peebles, Carbon Fibers, CRC Press, Boca Raton, 1990
- 7. T.H. Yoon, H. M. Kang, M. Bump, and J. S. Riffle, "Effect of solubility and miscibility on the adhesion behavior of polymer-coated carbon fibers with vinyl esterresins", J. App. Poly. Sci. (USA), vol. 79, no. 6, pp. 1042-1053, 2001
- 8. Kim, I.C., Yoon, T.-H., "Enhanced interfacial adhesion of carbon fibers to vinyl ester resin using poly(arylene ether phosphine oxide) coatings as adhesion promoters", Journal of Adhesion Science and Technology (Netherlands), vol. 14, no. 4, pp. 545-559, Feb. 2000
- 9. Derakane 411-45 (Vinyl Ester Resin), Alloy Digest (USA), pp. 2, Aug. 1991
- M. J. Reis, M. J., M. Botelho Do Rego, and J. D. Lopes Da Silva, J. Mater.Sci., Vol. 30, No. 118, 1995
- 11. M. J. Rich, S. Corbin, and L. T. Drzal, "Adhesion of carbon fibers to vinyl ester matrices", Proceedings of the 12th International Conference of Composite Materials, 1999
- 12. M. J. Pitkethly, J. P. Favre, U. Gaur, J. Jakubowski, S. F. Mudrich, D. L. Caldwell, L. T. Drzal, M. Nardin, H. D. Wagner and et al., "A Round-robin Program on Interfacial Test Methods", Compos. Sci. Technol., 48, 205-214, 1993
- 13. Yu. A. Gorbatkina, Adhesive Strength of Fiber-Polymer Systems, Ellis Horwood, New York, 1992

- 14. L. T. Drzal and M. Madhukar, "Fiber-Matrix Adhesion and Its Relationship to Composite Mechanical Properties" J. Matr. Sci., 28, 569-610, 1993
- 15. Hoecker, K. Friedrich, H. Blumberg and J. Karger-Kocsis, Comp. Sci. Tech., Vol.54, pp.317, 1995
- 16. L. Xu, L. T. Drzal, "Influence of interphase chemistry on the adhesion between vinyl ester resin and carbon fibers", **Proceedings of the 23rd Annual Meeting of "Adhesion Science for the 21st Century"**, 2000
- 17. L. T. Drzal, "The Epoxy Interphase in Composites", review chapter in Advances in Polymer Science II, 75, K. Dusek, ed., Spring-Verlag, pp. 16, 1985
- 18. L. Xu, **Mater Thesis**, School of Mechanics and Materials Science, Washington State University, 1998
- 19. L. Weitzsacker, M. Xie and L. T. Drzal, "Using XPS to Investigate Fiber/Matrix Chemical Interactions in Carbon Fiber Reinforced Composites", Surf. Interf. Anal. 25, 53-63, 1997
- 20. M. B. Launikitis, "Vinyl Ester Resin", Hand Book of Composite, pp.38-49
- 21. L. S. Penn and T. T. Chiao, "Epoxy Resins", Hand Book of Composite, pp.57~88
- J. M. Whitney and L. T. Drzal "Three Dimensional Stress Distribution Around An Isolated Fiber Fragment", ASTM STP 937, Toughened Composites, 179-196, 1987
- 23. A. ten Busschen, **Ph.D thesis**, Delft University of Thechnology, the Netherlands, 1996
- 24. D. K. Hadad, "Physical and chemical characterization of epoxy resins", **Epoxy** Resins_Chemistry and Technology, 2nd edition, edited by C. A. May, pp. 1089-1172, 1988
- 25. V. Rao and L. T. Drzal, "The Temperature Dependence of Interfacial Shear Strength for Various Polymeric Matrices Reinforced with Carbon Fibers", J. Adhesion, 37, 83-95, 1992
- 26. L. Zhang, **Ph. D thesis**, Delft University of technology, the Netherlands, 1995
- 27. H. Ho and L. T. Drzal, "Non-linear Numerical Study of the Single-Fiber Fragmentation Test, Part I: Test Mechanics", Composites Engineering, 5, No. 10-11, 1231-1244, 1995

- 28. H. Ho and L. T. Drzal, "Non-linear Numerical Study of the Single-Fiber Fragmentation Test, Part II: A Parametric Study", Composites Engineering, 5, No. 10-11, 1245-1259, 1995
- 29. H. Ho and L. T. Drzal, "Evaluation of Interfacial Mechanical Properties of Fiber Reinforced Composites Using the Microindentation Method", accepted for publication in Composites, Part A, 1998

CHAPTER 2

BACKGROUND

This chapter details the background of this study in regard of understanding the chemical and physical nature of carbon fiber, vinyl ester, and carbon fiber/vinyl ester interphase.

2.1 CARBON FIBER REINFORCEMENT

The purpose of fiber reinforcement is different for different classes of matrix materials. For ceramics, it is to introduce a measurement of toughness, for metals, it is to inhibit plastic deformation and for polymers, it is to impart stiffness and strength [1]. Fiber reinforced polymeric composite technology is based on taking advantage of the high strength and high stiffness of fibers. Graphite or carbon fibers are the most widely used advanced fiber. Graphite fibers normally have at least 99% of carbon while carbon fibers typically are less than 95% carbon [2]. The term "carbon" instead of "graphite" is used to denote these fibers, since they are composed of crystalline graphite, and also of non-crystalline material and areas of crystal misalignment [3].

Figure 2.1 Manufacturing process of PAN based carbon fiber [4]

2.1.1 Manufacture Process

Carbon fibers are usually produced by carbonization of organic precursor fibers followed by graphitization at high temperature, Figure 2.1 ^[4]. A number of precursors can be used for making fibers, such as polyacrylonitrile (PAN), rayon (cellulose) and mesosphere pitch. The majority of the commercial carbon fibers currently produced are based on PAN ^[5]. PAN- based carbon fiber can be grouped into type A (low modulus) and type HM (high modulus). Type A fibers were graphited at approximately at 1500°C while type HM fibers were graphited at 2600°C ^[6]. AS4 carbon fiber (Hercules Incorporated) is type of A, Surface treated, PAN based carbon fiber. The tow size of the fiber used in this study is 12K filaments.

2.1.2 Topography and Morphology

So-called carbon fiber is made of carbon which is a very light element. Carbon can exist in a variety of crystalline forms. Beside the well-known covalent diamond structure, graphite structure wherein the carbon atoms are arranged in the form of hexagonal layers is another main structure of crystalline carbon. Carbon fiber is of graphite structure. The properties of a carbon fiber are a direct reflection of the structure of graphite which is highly anisotropic on a nanoscopic scale. The basic structure of the carbon fibers is the graphite crystallites which are composed of turbostatically layered basal planes or graphite ribbon [5-8] as shown in Figure 2.2. The ribbons increase in size with increasing graphitization temperature. The ribbons undulate and twist along the

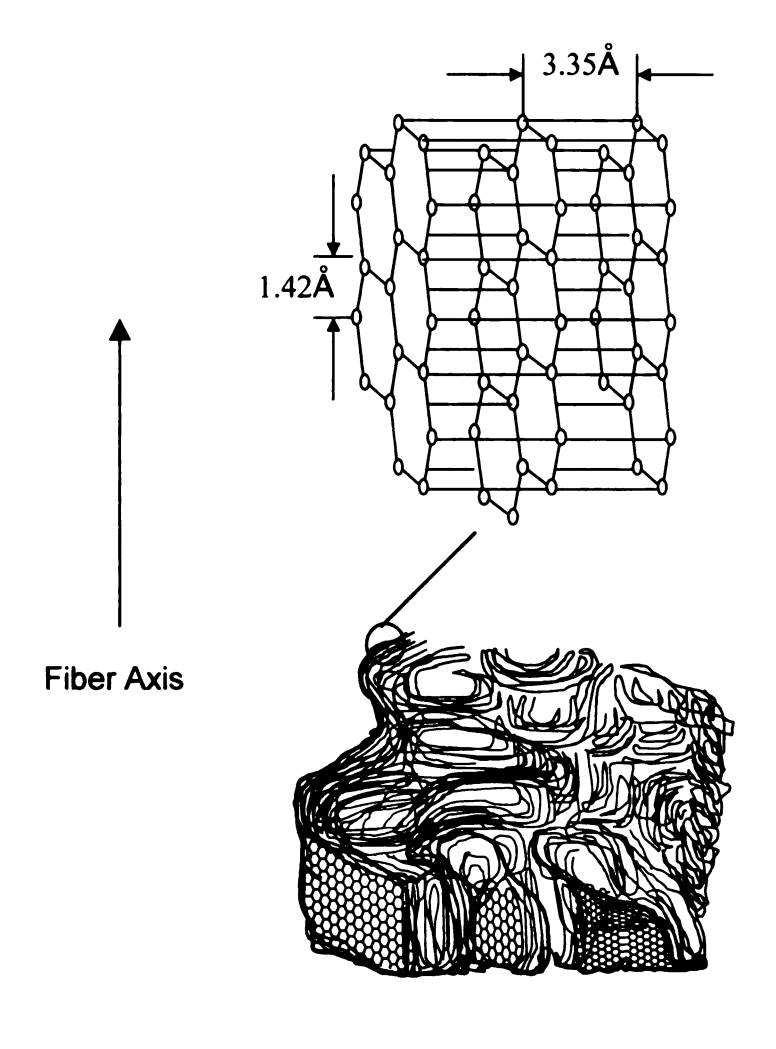


Figure 2.2 Schematic draws of a three-dimensional model of a part of carbon fiber

Figure 2.3 Surface chemistry of AS4 carbon fiber

fiber axis and the degree of alignment varies with graphitization temperature. Type A fiber has graphitic basal planes plus edges and corners which are highly reactive comprising the fiber surface while the more graphite type HM fiber has a surface composed mostly of graphitic basal plane. The proportion of the surface composed of edge and corner areas would change with fiber modulus. The high bond strength between the carbon atoms in the basal plane gives an extremely high modulus along the fiber axis, while the weak van der Waals type of bonding between the neighboring layers produces a low modulus along the edge plane.

Another aspect of topographical feature of the carbon fiber is the surface area. In fiber reinforced composites where the fiber diameter is on the order of 5 to 10 microns, at a 50 volume percent loading, the actual interfacial surface area between fiber and matrix can be on the order of 5,000 to 10,000 square meter per cubic centimeter of composite^[43].

2.1.3 The Surface Chemistry and Energetics

The quantity and the type of chemical group present on the fiber surface is a function of the type of fiber, i.e. its graphitization temperature, and the type of surface treatment used, i.e. gaseous, liquid or catalytic oxidation ^[19]. Boehm et al ^[20] have attempted to identify the type of chemical function groups present on the carbon surface. They have shown that the oxygen present on the carbon surface can be in as many as four different chemical groups. Carboxylic acid, lactone, carbonyl and alcoholic oxygens. It was also found that the Nitrogen in the form of amine or cyano groups is almost always on the low heat treatment temperature fiber surface ^[21]. Trace amounts or elements such as silicon,

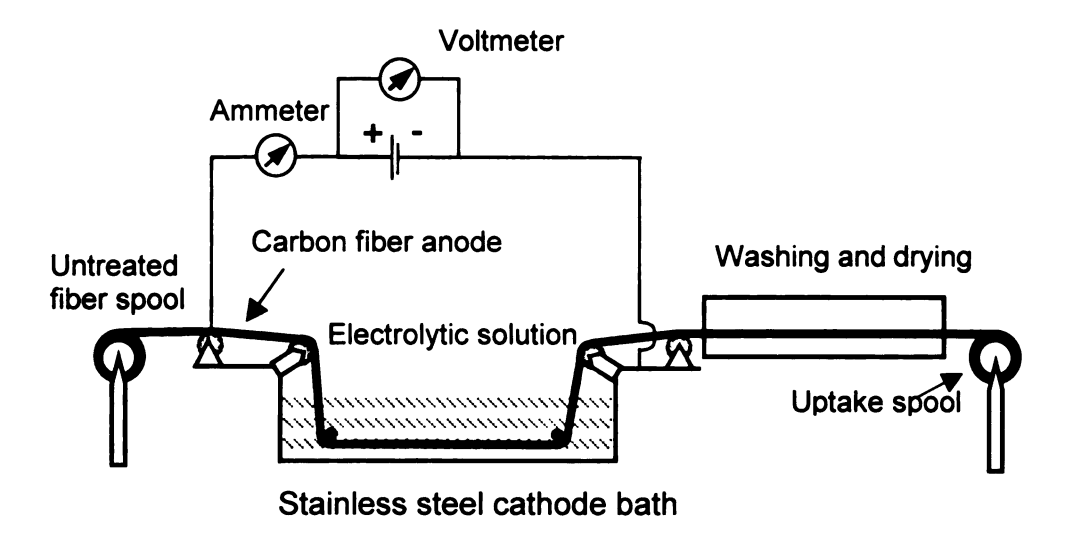


Figure 2.4 A schematic representation of the electrochemical oxidative surface treatment of the carbon fibers [27]

from the earlier polymer fiber spinning steps, as being on the fiber surface has shown that the sodium has the ability to diffuse to the fiber surface from the bulk of the fiber at moderate elevated temperatures.

A necessary condition for fiber and matrix compatibility is thermodynamic wetting. The thermodynamic criterion for wetting of the fiber by the matrix is in general that the surface free energy of the fiber surface must be greater than that of the matrix ^[23]. The surface free energy of AS4 carbon fiber has been measured and reported by Drzal ^[6] by contact angle technique based on the method proposed by Kaelble ^[24]. The total surface free energy is range from 39 mJ/m² to 57 mJ/m² which were contributed by both polar and dispersive component.

2.1.4 Carbon Fiber Surface Treatment

Carbon fibers are subject to post treatments including surface treatments and/or application of organic sizing. Surface treatment of carbon fibers can in general be classified into oxidative and non-oxidative treatments. Oxidative treatments are further divided into dry oxidation in the presence of gases, plasma etching and wet oxidation. In the process of dry oxidation, the carbon surface layers simply burn away unevenly to create pits in line that coalesce into channel resulting a high surface rigidity. The fundamental principle of a plasma treatment is to induce the formation of active species in a gas by a suitable energy transfer. The result of this treatment is that many chemical bonds on the surface are broken forming very reactive species [28].

One of the wet oxidation surface treatments is electrochemical oxidation. The fibers are the electrical anode in a circuit as they are continuously drawn through a solution of electrolyte in water as shown in Figure 2.4. The voltage in the circuit is maintained constant, while the current and the residence time in the electrolytic bath are varied to change the degree of surface treatment.

The total surface free energy is increased for both type A surface treated (AS) and type HM surface treated (HMS) by surface treatment. The measured change is primarily in the polar component of the surface free energy and directly related to Interfacial shear strength between fiber and matrix [14, 28, 25]. The dispersive part of surface free energy is virtually insensitive to surface treatment, probably due to the chemically inert graphitic basal planes [26,29-30].

In addition to the use of surface treatment which are primarily chemical in natural, surface finishes or coatings are also used to affect fiber-matrix adhesion. Organic coating or sizing or finishes in an amount of 0.5~7 wt% are typically applied in order to improve their compatibility with the resin, protect the fiber surface from damage, protect fiber surface reactivity and/or their "handle ability" [31.32]. These coatings are applied to both untreated and surface treated fibers by passing the fibers through a sizing bath filled with organic solution. The sizing agents most commonly employed are polyvinyl alcohol, epoxy, polyimide and etc [31]. The mechanism by which sizing operates is fundamentally different than the surface treatment mechanism. The sizing layers are hundreds of nanometers thick. The properties of this sizing layer itself are imparted to the interphase and can control the adhesion between fiber and matrix.

AS4 carbon fibers are PAN based, type A carbon fibers which have intermediate axial tensile modulus. They are surface treated with electrochemical oxidation process which optimizes the adhesion to epoxy. Firstly, the treatments remove a weak out fiber layer initially present on the fiber. Secondly, surface chemical groups are added which increase the interaction with the epoxy. On the carbon fiber surface, Oxygen reactive groups in the forms of carboxylic acid, lactones, carbonyl and alcoholic hydroxyl and Nitrogen reactive groups in the form of amine and cyano on are potential chemical reactive sites to epoxy group and amine group of epoxy resin. Some of the properties of AS4 carbon fibers are list in Table 2.1.

Properties	AS4
E ₁ , GPa (Msi)	241(35)
E ₂ , GPa (Msi)	21 (3)
E ₃ , GPa (Msi)	21 (3)
ν ₁₂	0.2
ν ₁₃	0.2
ν ₂₃	0.25
G ₁₂ , GPa (Msi)	21 (3)
G ₁₃ , GPa (Msi)	21 (3)
G ₂₃ , GPa (Msi)	8.3 (1.2)
α ₁ (10 ⁻⁶ /°C)	-0.11
α ₂ (10 ⁻⁶ /°C)	8.5
α ₃ (10 ⁻⁶ /°C)	8.5
ρ (g/m ³)	1.77
Surface Energy γ (mJ/m²)	39~57
Tow size	12,000
Diameter (10 ⁻⁶ m)	7~8

Note: E: Tensile Modulus

v: Poisson's Ratio G: Shear Modulus

α: Thermal Expansion Coefficient Direction 1: Fiber Axis Direction

Direction 2 and 3: Fiber Transverse Direction

Table 2.1 Selected Properties of AS4 Carbon Fiber

18

2.2 Vinyl Ester Matrix Resins

The matrix holds the fiber together in a structural unit and protects them from external damage, transfer and distributes the applied loads to the fibers, and in many cases contributes some needed property such as ductility, toughness, or electrical insulation.

In the early 1960s scientists from both Shell Oil and Dow Chemical were attempting to expand the epoxy market. They discovered that polymeric bisphenol A epoxies could be reacted with acrylic acids yielding a structure with pendant vinyl groups. These resins could be reacted with styrene to yield very resilient thermoset structures. This chemistry has been extended to other epoxy structures to give "vinyl esters" with special properties. Chemists at ICI Americas soon discovered that the propoylated bisphenol intermediate used to make the Atlas polyesters could be reacted with an isocyanate and then used to form a urethane modified vinyl ester.

2.2.1 Introduction to DERAKANE Epoxy Vinyl Ester Resin

Epoxy vinyl ester resins were commercially introduced by Shell Chemical Company under the trade name of EPOCRYL Resins in 1965. In 1966 Dow Chemical Company coined the DERAKANE epoxy vinyl ester resins destination with the introduction of a similar series of resin for molding applications. DERAKANE 411 epoxy vinyl ester

$$\begin{array}{c}
O \\
CH_{2}-CH-CH_{2} \\
R-CH_{2}-CH-CH_{2}
\end{array}$$

$$\begin{array}{c}
O \\
R-CH_{2}-CH-CH_{2}
\end{array}$$

Diglycidy Ether Bisophenol A (DGEBA)

+
$$HO - C - C = C$$
 Catalysts Heat

Methacrylic Acid or Acrylic Acid

DGEBA Epoxy Based Vinyl Ester

+ Styrene (as reactive diluent) + Inhibitors

where n=0~3, R=0
$$\stackrel{\text{CH}_3}{\stackrel{|}{-}}$$
 O , and R' = H or $-\text{CH}_3$

Figure 2.5 Vinyl ester resins were produced from epoxy resins

resins are produced by the addition of unsaturated carboxylic acids (methacrylic or acrylic acid) to an epoxide resin, such as Diglycidy Ether of Bisphenol A (DGEBA), as shown in Figure 2.5 and appropriate diluents, normally styrene, and polymerization inhibitors are added during or after esterification.

DERAKANE epoxy vinyl ester resins have outstanding resistance to corrosion. Chemical attack on these types resin occurs through hydrolysis of the ester groups or the splitting of unreacted carbon-to-carbon double bond through actions such as oxidation or halogenations. The number and arrangement of ester linkage and carbon-to-carbon double bond on DERAKANE epoxy vinyl ester resins make them less polar than polyester^[33], see Figure 2.7. In cured bisphenol A fumaric acid polyester and isophthalic polyesters, the ester linkages occur throughout the molecular chain, making the chain more susceptible to attack by hydrolysis. In addition to ester linkage, carbon-to-carbon double bonds also occur randomly throughout the bisphenol A fumaric acid polyester and isophthalic polyester chains, and not all of those double bonds react during polymerization. Those unreacted double bond are susceptible to chemical attack. In DERAKANE epoxy vinyl ester resins, the carbon-to-carbon double bonds are at the ends of the molecular chain that make them exceptional active. As a result, DERAKANE epoxy vinyl ester resins cure rapidly and consistently to give fast green strength and superior creep resistance. The second hydroxyl groups on the vinyl ester molecule also have a beneficial effect on the adhesion to the glass fibers which is rich in hydroxyl groups on their surfaces. DERAKANE epoxy vinyl ester resins can be used to fabricate a wide range of corrosion-resistant fiber reinforced polymeric (FRP) applications by all conventional fabricating techniques. For example, DERAKANE 411 resins are medium

viscosity materials widely used for contact molding, pultrusion, matched die molding, continuous laminating, and filament winding. DERAKANE 411-C50 resins are lower viscosity versions, primarily used for resin transfer molding, centrifugal casting, and other applications requiring extremely fast wet-out.

2.2.2 Cure Kinetics of Vinyl Ester Resin

In thermosetting polymers, the liquid resins are converted into hard brittle solids by chemical cross-linking, curing, which leads to the formation of a tightly bound three-dimensional networks of polymer chains. Curing can be achieved at room temperature but it is usual to use a cure schedule, process, which involves heating at one or more time temperatures to achieve optimum cross-linking and hence optimum properties [37]. A relatively high temperature final post-cure treatment is often given to minimize any further cure and change in properties during service. The gel time can also be varied with careful control of the amount of catalysts such as initiator, promoter and/or accelerator. Initiators are chemicals to initiate the chemical reaction that cause the resin to cross-link and cure. Commonly employed initiators include organic peroxides and organic hydro peroxides. Promoters and accelerators are used to speed up and enhance the cross-link reaction. The basic molecular structure for the initiators, promoters and accelerators are shown in Figure 2.6.

DERAKANE 411-C50 epoxy vinyl ester resin (D411-C50) is a mixture of DGEBA based vinyl ester monomer (VE) and styrene monomer (ST) [33-35]. Using nuclear magnetic resonance (NMR), Palmese and et al found that the average molecular weight

$$\begin{array}{c} \text{HO} - \text{O} - \text{C} - \text{O} - \text{O} - \text{C} - \text{O} - \text{OH} \\ \text{C}_2\text{H}_5 & \text{C}_2\text{H}_5 & \text{C}_2\text{H}_5 & \text{C}_0^{+2} \end{array}$$

$$\begin{array}{c} \text{Methyl Ethyl Ketone Peroxide (MEKP)} \\ \text{C} + \text{C}_3 & \text{Cobalt Napthanate (CoNap)} \\ \text{C} + \text{C}_3 & \text{Cobalt Napthanate (CoNap)} \\ \text{C} + \text{C}_3 & \text{C}_{\text{H}_3} & \text{C}_{\text{H}_3} \\ \text{Cumene Hydroperoxide (CHP)} & \text{C}_{\text{H}_3} & \text{C}_{\text{H}_3} \\ \text{C} + \text{C}_3 & \text{C}_{\text{H}_3} & \text{C}_{\text{H}_3} \\ \text{C}_{\text{H}_3} & \text{C}_{\text{H}_3} & \text{C}_{\text{H}_3} \\ \text{C}_{\text{H}_3} & \text{C}_{\text{H}_3} & \text{C}_{\text{H}_3} \\ \text{C}_{\text{H}_3} & \text{C}_{\text{H}_3} & \text{C}_{\text{H}_3} \\ \text{C}$$

Figure 2.6 Catalyst for cure of vinyl ester resin

(Initiators)

Derekane 411 DGEBA Epoxy Based Vinyl Ester (VE)

Styrene (ST) (a)

$$I \rightarrow 2R \bullet \qquad \text{Initiator decay}$$

$$R \bullet + VE \rightarrow VE \bullet \qquad \text{Radicals attack monomer}$$

$$VE \bullet VE \rightarrow VE \rightarrow VE \bullet \qquad VE \text{ homopolymerization}$$

VE• VE \rightarrow (VE-VE)• VE homopolymerization VE• ST \rightarrow (VE-ST)• VE, ST copolymerization ST• VE \rightarrow (ST-VE)• VE, ST copolymerization VS• ST \rightarrow (ST-ST)• ST homopolymerization

(c)

Figure 2.7 (a) Chemical structure of typical DGEBA-based VE-ST resin system components, (b) a schematic representation of the VE-ST network formation showing the cross-linking capacity of the difunctional VE monomer, and (c) reactions encountered during the free radical bulk copolymerization of VE resin systems [36] (draw not to the scale)

of VE is 908g/mol (compare the molecular weight of ST: 104g/mol) and the resin was found to contain 45.0wt% of styrene [37]. The mixture of vinvl ester and styrene contain double bonds that react and cross-link into network structure. During network formation, the vinyl-ester monomer provides cross-linking capacity and branch points for the network, while the styrene monomer provides linear chain extension. Upon cure, the two reactive vinyl end groups, while styrene has only one are all gone. Thus, the vinyl ester monomer styrenated vinyl ester resin exhibits excellent resistance to acids, bases, and solvents. The reaction between styrene (ST) and vinvl ester (VE) is a heterogeneous free-radical chain cross-linking copolymerization. As shown in Figure 2.7(a) [36], the vinyl-ester monomer has provides a cross-linking capacity and branch points for the formation of a network, as shown schematically in Figure 2.7(b), while the styrene monomer provides linear chain extension during cure. Figure 2.7(c), reactions that contribute to the cross-linked network include homopolymerization of vinyl ester monomer, homopolymerization of styrene, and copolymerization of vinyl-ester with styrene.

The reaction competition between VE and ST monomer was investigated by Palmese and et al as well ^[36]. The results indicate that the rate of fractional conversion of styrene double bonds is initially less than that of vinyl-ester vinyl groups. However, styrene monomer continues to react after conversion of vinyl ester double bonds has ceased. In addition, the overall extent of conversion was found to increase with increasing isothermal cure temperature.

2.2.3 Phase Separation and Microgel

An important feature of free-radical crosslinking copolymerization of styrene and unsaturated polyester (UP) is the formation of a heterogeneous through strong intermolecular reactions and phase separation. The cure of unsaturated polyester resins has been found to result in heterogeneous morphologies characterized by the presence of spherical structures ranging in size from 10 to 200 nm [36-40]. Brill found closely packed microgels on the order of 100 nm in diameter for VE resin cured at 90°C and washed with acetone, which attests to the formation of microgel structures in VE systems^[41]. Many investigators have shown that curing of UP resins results in the formation of microgels during the initial stages of reaction [42-47]. They define microgels as localized microregions with a higher crosslink density than the surrounding medium. It has also been suggested that the size and number of microgels depend on cure temperature and resin formulation (i.e., styrene content and degree of unsaturation), and that these factors may affect material behavior [45-47]. Such structure affects not only the cure behavior and morphological changes of the resin but also the physical properties of the final products.

2.2.4 Influence of Styrene Monomer Content

The mechanical properties of thermosetting polymer depend on the molecular units making up the network and on the length and density of the cross-link. The former is mined by the initials, promoters and accelerator are used and the later by the control of

the cross-link processes which are involved in the cure, especially cure temperature. It was found that the initial cure temperature significantly affects the mechanical behavior of vinyl ester resin systems in particular, value of strength and fracture toughness for 125°C postcured samples initially cured isothermally at 30°C are much higher than those obtained for sample initially cured isothermally at 90°C [37]. Thermosetting polymers are normally considered as brittle. Cross-linking makes sliding of molecules past one and another difficult thus making the polymer strong and rigid but often do not have much elongation before break. It was also found that low temperature cured, 30°C cured, D411-C50 vinyl ester resin exhibits ductile behavior, other case such as 125°C postcured after low temperature curing, 90°C cured and 125°C postcured after 90°C curing, however, show typical brittle behavior [37]. The properties of cured vinyl ester also depend strongly on the concentration of styrene monomer, as reactive diluents, in the original resin, see Table 2.2.

Styrene Content (wt%)	0	15	50
Heat Distortion Temp. (°C)	149	138	116
Tensile Modulus GPa (Mpsi)	4.1 (0.59)	3.7 (0.53)	3.3 (0.48)
Elongation (%)	2.0	2.3	4.5

Table 2.2 A Comparison of the Selected Properties to the Styrene Monomer Content for D411 Vinyl Ester Resin [48]

inul Ester St	Styrono	Double Bond Content (eq/100g)	Volume Shrinkage (%)	
inyl Ester Resin Molecular Weight	Styrene Content (%)		From Gel Point to Full Cure	From Liquid Resin to Full Cure
500ª	0	0.40	4.3	5.4
500ª	25	0.55	6.8	7.6
500°	50	0.70	9.1	10.3
900 _p	50	0.61	-	7.0
1200°	50	0.58	-	5.4

Note: a: EPOCRYL Resin 12; b: EPOCRYL Resin 321; c: EPOCRYL Resin 322.

Table 2.3 Volume Shrinkage of Vinyl Ester Resin [48]

2.2.5 Cure Shrinkage of Vinyl Ester

Upon cure, the volume shrinkage of vinyl ester resin is generally lower than that of unsaturated polyester resin but higher than that of their parent epoxy resin. Vinyl ester resin can undergo as much as 5-10% volume shrinkage with cure depends on the molecular weight of vinyl ester monomer and the content of styrene, see Table 2.3 ^[48], while typical epoxy system undergo only 3-4% shrinkage during cure ^[48,49]. Shrinkage can induce significant stresses in the composite already before loading. While when the material in the liquid state, no stress will be build up. Even when the material in one region is solidified, the surrounding material can still flow and shrinkage induced stress is limited. Stress caused by volume shrinkage begins to build up at a certain point of volume shrink. The cure shrinkage of some of the vinyl ester resin are listed Table 2.3.

The curing stage and volume shrinkage rate are not yet available, the determination of the so-called certain point of cure volume shrink is till a problem. According to Ten Busschen [50], among the total volume shrinkage of 9.3%, about 2.7% occurs in the solid state. Also when cured vinyl ester experience elevated temperature, it will expense just like other resins. The most characteristic property of thermosetting resin is in response to heat since, unlike thermoplastics, they do not melt on heating. However, they lose their stiffness properties at the distortion temperature and this defines an effective upper limit for the use in structure components. Some of the properties of D411-C50 vinyl ester resin are list in Table 2.4.

Properties	D411-C50
Tension Modulus, E, GPa (Msi)	3.38 (0.49)
Poisson Ratio, v ₁₂	0.36
Shear Modulus, G, GPa (Msi)	1.25 (0.181) [*]
Coefficient of Thermal Expansion (CTE), α , (10 ⁻⁶ /°C)	80 ^[28]
Density, ρ, (g/m ³)	1.12
Surface Energy, γ, (mJ/m²)	40(epoxy) ^{[43]**} ; 26.7(benzene) ^[77] **

Note: *Measured by Cobin [18] for and the Poisson ratio is based on the measurement

Table 2.4 Selected Properties of D411-C50 vinyl ester

^{**}Surface Energy of vinyl ester should be close to that of epoxy while the surface energy of styrene closes to that of benzene

Most recently, Shanghai Fuchem has developed a new-type epoxy vinyl ester resin featured with very low cure volumeshrinkage together with an improved elongation rate & impact resistance performance, refer Chapter 7 for details.

2.3 Carbon Fiber- Vinyl Matrix Interphase

2.3.1 General Introduction to Fiber/Matrix Interphase

Topography and Morphology of Interphase: the combination of fiber and matrix creates inevitable interface or interphase, Figure 2.8. The concept of interface thickness keeps developing from 0 (interface) to 500nm [52-54], up to 1000nm[57], a three dimensional interphase [52-56]. The boundaries of the interphase are defined as extending from the point in the matrix where the local properties start to change from the bulk properties to the point in the fiber where the local properties are those of the bulk matrix. This region includes matrix that may have chemical and morphological features different from the bulk matrix. It can include impurities, unreacted polymer components, non-polymerized matrix additives, sometimes polymer transcrystallites [58-61], layer of sizing and etc. On the fiber side, topographic, morphological and chemical features can be different from the bulk. At the interface, not only can there be chemical and physical interactions between fiber and matrix, but also voids, adsorbed gas and surface chemical groups can be concentrated.

Strength of the Interphase: Adhesion between fiber and matrix can also be considered as the strength of the interphase. The interphase is where the fiber and matrix bonded

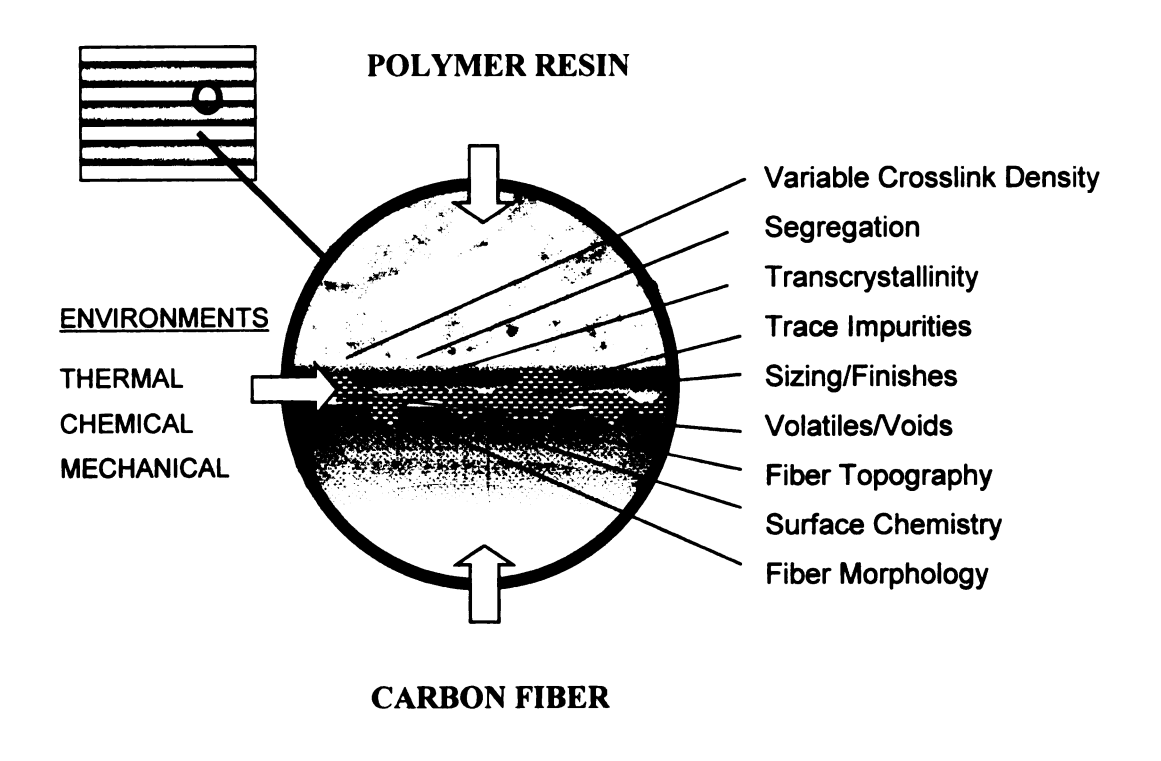


Figure 2.8 Fiber-Matrix Interphase [Drzal]

matrix, or van der Waals force, electrostatic attraction, acid-base interaction including H-together. The bond strength often refers to adhesion which can be evaluated by the work of adhesion, W_A, refer to Appendix I. For fibers without sizing, the contributions to the adhesion could be chemical reaction or inter-diffusion of element between fiber and bond, or mechanical interlock. For fiber with organic coating the situation is rather complex. Beside the interactions mentioned above, the entanglement between the molecules of the polymer sizing and polymer matrix and the inter-diffusion^[62-65] between compatible sizing and matrix polymers could be one of the important contributions to the adhesion. On the other side, voids, contaminates, etc., and thermal residual stress could be negative contribution to the adhesion.

Thermal Residual Stress at Interphase: In addition to chemical and structure consideration, the state of stresses, which result from the process of the composite material itself, can influence the degree of fiber-matrix adhesion. The coefficient of thermal expansion (CTE) of carbon fiber is quite small and can actually be negative while the matrix has a CTE of thirty times larger [27-30.58.83.84]. The fiber is anisotropic and the radial and longitudinal thermal expansions can be quite different. The polyester is isotropic but has a CTE a factor of 80×10⁻⁶/K [50] (compare with Epoxy: 60×10⁻⁶/K [49], 127×10⁻⁶/K [66]). This disparity become increasingly significant as higher processing temperatures are reached with the absolute difference between the glass temperature and the use of temperature determining the magnitude of these residual thermal stresses. In addition, the difference of thermal conductivities of materials can introduce unevenly distributed temperature during process and application can also result in residual stresses even defects [67].

Interphase thermodynamics: a necessary condition for fiber and matrix bond is thermodynamic wetting. Wetting can be described thermodynamically as the creation of an interface whose free energy decreases. If contact angles are used as a measure of wettability this means that the contact angles should be less than 90° for wetting to occur. This happens when the surface energy of the wetting liquid is less than that of surface which it is placed. Carbon fibers, as mentioned in Section 2.1.3, generally are high in surface energy and the porosity and micro-topography present on their surface aid the wetting of the substrate. In the case of carbon fiber with D411-C50 resin which is a mixture of vinyl ester resin and styrene monomer, the Vinyl ester resins have a surface free energy high than the styrene monomer. This might imply that styrene potentially predominate on the surface of the carbon fiber.

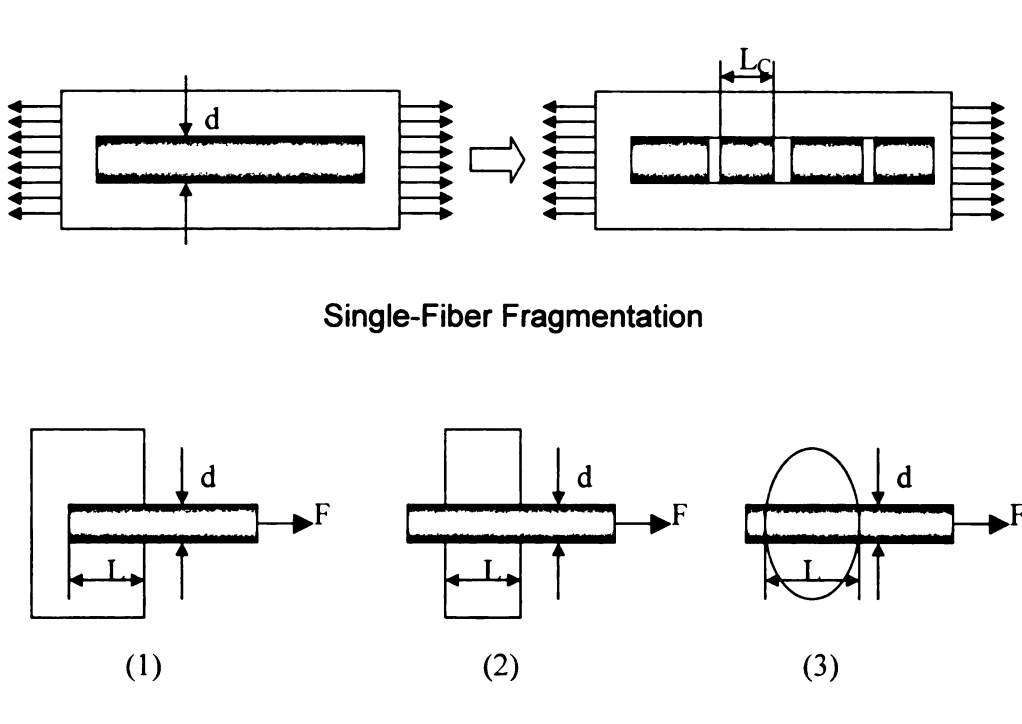
Interphase Engineering with Fiber Sizing: With fiber sizing, the interphase could be controlled and designed. Usually these sizings, sometimes called coatings or finishes, are 100-500 nm thick ^[54]. Some of the properties of the sizing materials were imparted on the fiber surface after sizing process. The sizings protect the fiber surface from damage, improve the wetting of fiber by matrix and protect fiber surface reactivity ^[54]. The sizing should be designed to adhere well to the fiber surface and should partially diffuse into the matrix resin during cure. The interphase design could be design of the sizing chemistry, sizing molecular structure and/or sizing thickness. Sizing could increase the strength of the interphase by introducing more chemical reactive site and/or more surface area ^[23, 66, 68-70]

2.3.2 Evaluation the Strength of the Fiber-Matrix Interphase

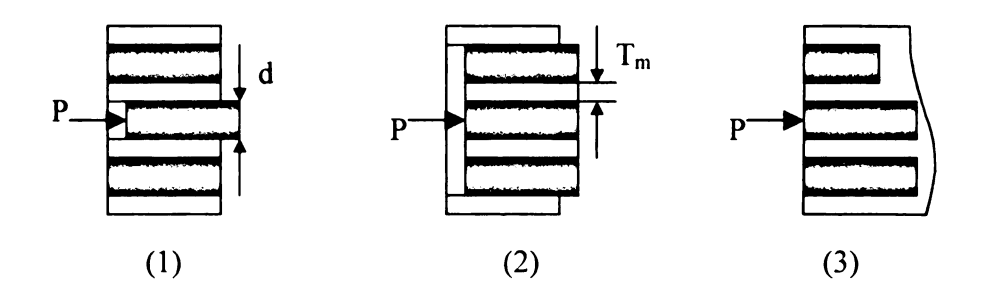
Direct measurement of the interphase strength, normally refers to adhesion, is very difficult. Therefore, the level of adhesion is assessed practically by the interphase strength value, the interfacial shear strength (IFSS), obtained from destructive mechanical tests. These tests could be classified into three groups, fiber pullout test, single fiber fragmentation test and microindentation test [79], shown in Figure 2.9, for details see Appendix I. The microindentation test has attracted much attention because it is an in situ testing method conducted on a real composite, thus allowing for evaluation of the processing or environmental exposure encountered either during manufacturing or in service. The interfacial shear strength value obtained by these tests for a given system is consistent with the mechanical properties of macrocomposites [71-74]. A strong correlation has also been found between the interfacial shear strength and such thermodynamic parameters as surface free energy [75-77] or specific enthalpy of adsorption [77,78]. Therefore, it seems to be possible to obtain information about fiber-matrix adhesion from micro-mechanical experiments.

2.3.3 Low Adhesion between Carbon Fiber and Vinyl Ester Resin

Low adhesion was extensively reported between vinyl ester and carbon fiber ^[51, 80-87]. One example was measured by single fiber fragmentation shown in Figure 2.10^[51]. The carbon fibers used were Panex 33 fiber –100% electrochemical surface treated. The



Single-Fiber Pull-Out



Microindentation



Figure 2.9 Schematic diagram of the microindentation method for measuring fiber-matrix adhesion [79]

interfacial shear strength of a carbon fiber/vinyl ester system, measured with single fiber fragmentation method, possessed only 50% of that of a carbon fiber/epoxy system. Not only when compared with epoxy, another measurement from drop pull-out tests shown in Figure 2.11^[83], carbon fiber/ vinyl ester adhesion was tested to be fairly lower than all the other tested polymer matrixes.

One of the reasons lows adhesion between vinyl ester and carbon fibers could be the chemical nature of the constituents of vinyl ester polymer, the catalysts and the monomers. A previous investigation by Weitzsacker, Drzal et al. [88] has investigated the reactions of the catalyst and/or promoters to determine if they were competing with the vinyl ester matrix resin for reactive sites at the carbon fiber surface. Drzal and et al found that as little as 3% of chemical bonding accounts for a 25% increase in the Interfacial Shear Stress (IFSS) [89]. Cobalt was detected at 2.6% at the surface of the AS4 carbon fiber exposed to cobalt naphthenate (CoNap) and a minor change was also noted in the surface chemistry of the fiber exposed to dimethyl aniline (DMA) which are the promoters and accelerators for the free radical copolymerization respectively. Adsorption of catalysts on the fiber surface resulting less reactive site to form strong chemical bonding could be one of the reason that lowers the adhesion between carbon fiber and vinyl ester. Besides, the preferential adsorption of any of the catalysts would change the stoichiometry. Further more the fiber/matrix interphase also could be changed since removal of even a small amount of the initiator or promoter from the vinyl ester to the carbon fiber surface has the potential to greatly affect the free radical copolymerization, and further more effects such as micro-gel, micro-structure, and phase

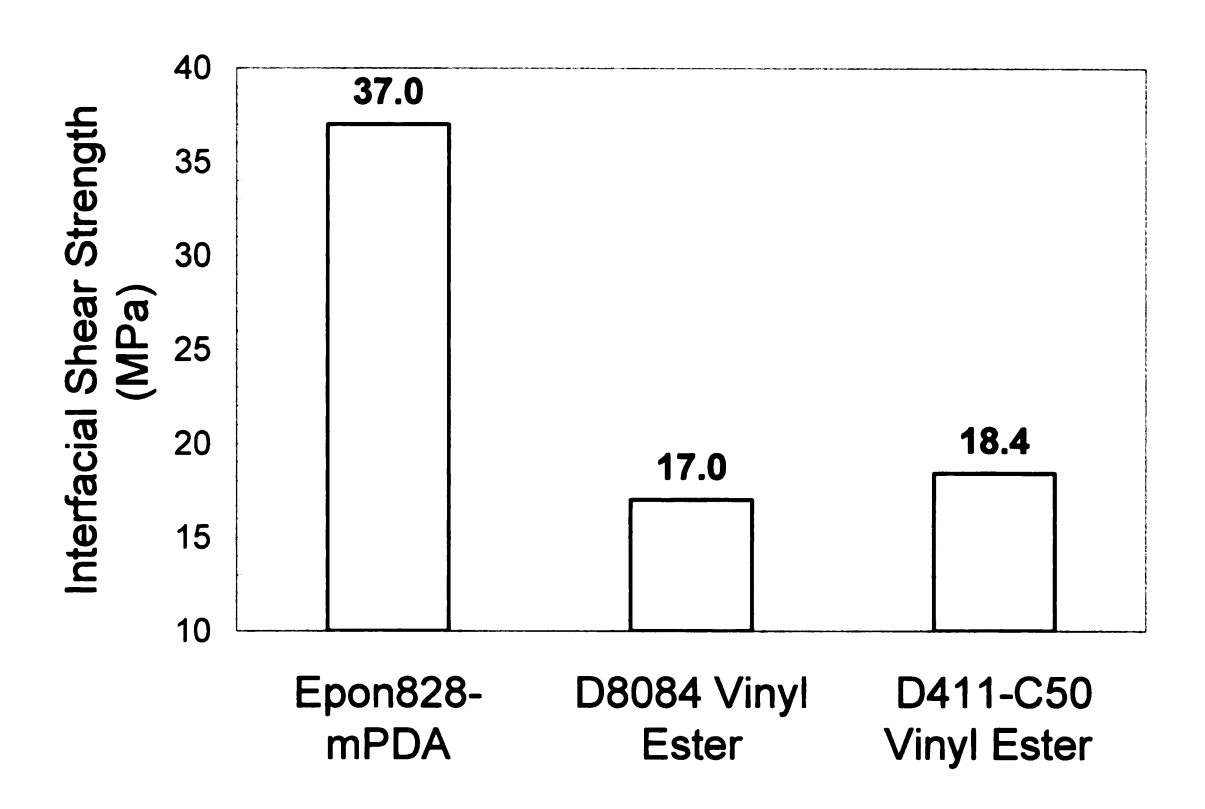


Figure 2.10 Interfacial shear strength measured with the single fiber fragmentation test over a series of carbon fibers in an epoxy matrix, Epon 828-mPDA, two vinyl ester matrices, the Derakane 411-C50 and 8084 [51]

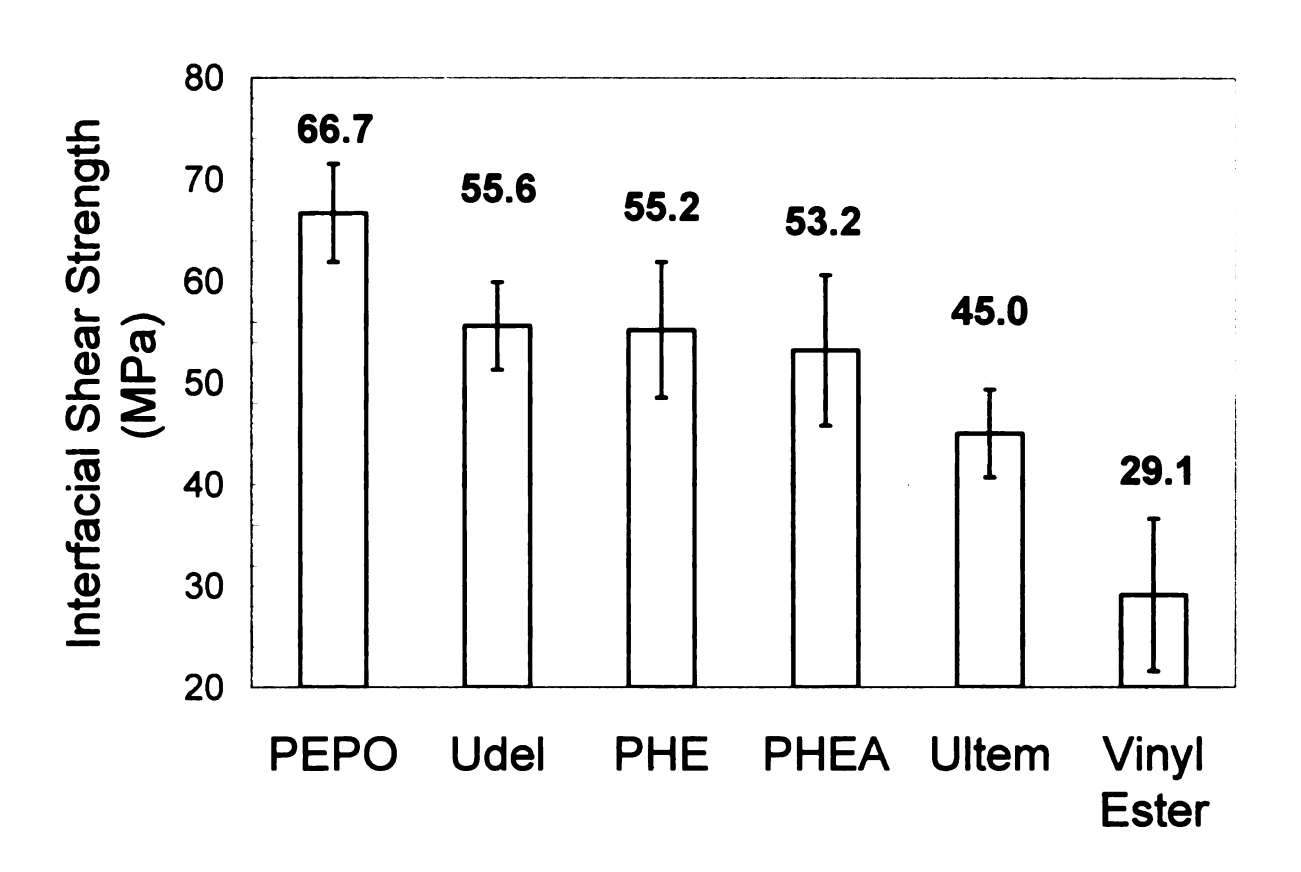


Figure 2.11 Interfacial shear strength of micro-droplet with polymers and asreceived carbon fibers [83]

separation of the vinyl ester material close to fiber surface were mentioned in section 2.2. Typical vinyl ester resins contain 35-50wt% styrene monomer as reactive diluents.

The copolymerization between styrene monomer and vinyl ester monomer is a heterogeneous, free radical, chain-growth, and cross-linking reaction. The wetting condition to the carbon fiber surface of styrene monomer could be different from that of vinyl ester monomer because the surface energy of styrene monomer would be smaller than that of vinyl ester resin (refer: 40(epoxy) [90]; 26.7(benzene) [91]). A potential styrene rich layer on the fiber surface could be another reason that lows the fiber/matrix adhesion.

Residual stress caused by significant cure volume shrinkage of vinyl ester can be another factor that lowers adhesion. Refer to Table 2.3, vinyl ester resin can undergo as much as 5-10% volume shrinkage with cure depends on the molecular weight of vinyl ester monomer and the content of styrene, while typical epoxy system undergo only 3-4% shrinkage during cure [52-54]. On the other hand, composite materials have thermal residual stress from the fabrication. In the case of carbon fibers, the coefficient of thermal expansion (CTE) is quite small and can actually be negative ^[92]. The fiber is anisotropic and the radial and longitudinal thermal expansions can be quite different. The polyester is isotropic but has a CTE a factor of 80×10^{-6} /K ^[50] (compare with Epoxy: 60×10^{-6} /K ^[49], 127×10^{-6} /K ^[66]). This disparity become increasingly significant as higher processing temperatures are reached with the absolute difference between the glass temperature and the use of temperature determining the magnitude of these residual thermal stresses. In addition, the difference of thermal conductivities of materials can

introduce unevenly distributed temperature during process and application can also result in residual stresses, even defects which would lower the fiber/matrix adhesion [67].

2.3.4 Improvement of Adhesion between Vinyl Ester and Carbon Fiber

One strategy to improve adhesion is to interfacially engineer the interphase through the use of a fiber sizing. Sizing could increase the adhesion by introducing more chemical reactive site and/or more surface area [23, 66, 68-70]. Previous data has shown that the application of a lightly cross-linked amine-cured epoxy sizing to the carbon fiber surface creates a beneficial interphase between the carbon fiber and vinyl ester resin matrix resulting in a substantial increase in fiber-matrix adhesion and the mechanical properties of carbon fiber/vinyl ester composites as well [51.87, 93]. Corbin found that with epoxy sizing, the interfacial shear strength measured with single fiber fragmentation increased about 30%. The mechanical properties of the composite material, flexural strength and interlaminate shear strength, also increased 34% and 25% respectively [51,87]. This results showed that the use of fiber epoxy sizing to interfacially engineer the interphase offers a potential avenue for improve the carbon fiber/vinyl ester adhesion. It also should be noted that, the exact mechanism by which this sizing improved adhesion is not known and the interaction between the epoxy sizing and the vinyl ester has to be optimized for compatibility and thickness.

2.4 REFERENCES

- 1. K. Ashbee, Fundamental Principle of fiber reinforced composites, 2cd edition, Technomic, pp. Xiii, 1993
- 2. R.F.Gibson, **Principle of Composite Material Mechanics**, McGraw-Hill, Inc., New York, pp8, 1994
- 3. W. D. Callister, Jr., Materials Science and Engineering An Introduction, 4th edition, John Wiley and sons, Inc., 1997
- 4. K. K. Chawla, Composite Materials Science and Engineering, 2nd Edition, Springer, New York, pp20, 1998
- 5. J. Kim and Y. Mai, Engineered Interfaces in Fiber Reinforced Composites, Elsevier, pp.183, 1998
- 6. L. T. Drzal and G. Hammer, "Graphite Fiber Surface Analysis Through XPS and Polar/Dispersion Free Energy Analysis", Appl. Surf. Sci., 4, 340-355, 1980
- 7. N. Sugiura, M. Kobuke, H. Asai and L. T. Drzal, "Topography of High Modulus PAN-based Carbon Fiber Surfaces", Proceedings of the 4th Japan-SAMPE, 1995
- 8. S. C. Bennett and D. J. Johnson, **Proc.** 5th London Carbon and Graphite Conference, Vol. 1, Society for Chemical Industry, London, pp377, 1978
- 9. L. T. Drzal, "The Epoxy Interphase in Composites", review chapter in Advances in Polymer Science II, 75, K. Dusek, ed., Spring-Verlag, pp. 16, 1985
- 10. L. Weitzsacker, M. Xie and L. T. Drzal, "Using XPS to Investigate Fiber/Matrix Chemical Interactions in Carbon Fiber Reinforced Composites", Surf. Interf. Anal. 25, 53-63, 1997
- 11. L. T. Drzal, "The Surface Composition and Energetics of Type A Graphite Fibers" Carbon, 15, 129-138, 1977
- 12. L. T. Drzal, J. Mescher and D. Hall, "The Surface Composition and Energetics of Type HM Graphite Fibers", **Carbon**, <u>17</u>, 375-382, 1979
- 13. L. T. Drzal, "The Surface Composition and Energetics of Graphite Fiber Surfaces", in **Treatise on Adhesion and Adhesives**, 5, R. Patrick, editor, 1981
- 14. L. T. Drzal, M. Madhukar and M. C. Waterbury, "Adhesion to Carbon Fiber Surfaces: Surface Chemical and Energetic Effects", Advances in Fiber Reinforced Composites Technology, Elsevier Science Publishers, Ltd., London, 1992

- 15. G. Fisher and L.T. Drzal, "The Effect of Surface Chemistry on Adhesion of Carbon Fibers to a Polyphenylene Sulfide (PPS) Resin", 4th International Conference on Composite Interfaces, Cleveland, OH, 1992
- 16. L. T. Drzal, M. Madhukar and M. C. Waterbury, "Surface Chemical and Surface Energetic Alteration of the IM6 Carbon Fiber Surface and Its Effect on Composite Properties", 14th Annual Meeting of the Adhesion Society, Hilton Head, SC, 1992
- 17. L. T. Drzal, M. Madhukar and M. C. Waterbury, "Adhesion to Carbon Fiber Surfaces: Surface Chemical and Energetic Effects", Composite Structures, 27, 65-72, 1993
- 18. C.L. Weitzsacker, and L.T. Drzal, "Analysis of the Fiber/Matrix Interface in Carbon Fiber Reinforced Polymer Composites by XPS", ANTEC '96: Proceedings of the 54th Annual Technical Conference of the Society of Plastics Engineers, 3, 3656-3660, 1996
- 19. J. B. Donnet, Carbon, Vol.6, pp161, 1968
- 20. H. P. Boehm, E. Diehl, W. Hech and R. Sappock, Agnew. Chem., Vol. 3, pp.669, 1964
- 21. F. Hopfgarten, Fiber Sci. Tech., Vol. 11, pp. 67, 1978
- 22. D. M. Brewis et al, Fiber Sci. Tech., Vol. 12, pp. 41, 1979
- 23. L. T. Drzal, "The Effect of Polymeric Matrix Mechanical Properties on Fiber-Matrix Interfacial Shear Strength", Mat. Sci. Engr., A126, 289-293, 1990
- 24. D. H. Kaelble, P. J. Dynes and E. H. Cirlin, J. Adhesion, Vol. 6, pp.23, 1974
- 25. L. T. Drzal, "The Role of the Fiber/Matrix Interphase on Composite Properties", Vacuum, 41, 1615-1618, 1990
- 26. G. Krekel, K. J. Huttinger, W. P. Hoffman, "The relevance of the surface structure and surface chemistry of carbon fibers in their adhesion to high temperature thermoplastics Part II Surface Chemistry", J. Mater. Sci., Vol. 29(13), pp.3461-3468, 1994
- 27. V. K. Raghavendran, *PhD Dissertation*, Department of Material Science and Mechanics, Michigan State University, 1998
- 28. L. T. Drzal, M. Richard and P. Lloyd, "Adhesion of Graphite Fibers to Epoxy Matrices. I. The Role of Fiber Surface Treatment", J. Adhesion, 16, 1-30, 1983

- 29. M. Desaeger, M. J. Reis and et al, "Surface characterization of poly(acrylonitrile) based intermediate modulus carbon fibers", J. Mater. Sci., Vol. 31(23), pp.6305-6315, 1996
- 30. K. E. Atkinson, G. J. Farrow and C. Jones, "Study of the interaction of carbon fiber surfaces with monofunctional epoxy resin", Composites Part A, Vol. 27(9), pp. 799-804, 1996
- 31. Composites—Engineered Materials Handbook. Vol. 1, ASM International, pp.122, 1987
- 32. L. T. Drzal, M. Rich, M. Koenigand and P. Lloyd, "Adhesion of Graphite Fibers to Epoxy Matrices. II. The Effect of Fiber Finish", J. Adhesion, 16, 133-152, 1983
- 33. DOW Plastics, DERAKANE Epoxy Vinyl Ester Resins_Chemical Resistance and Engineering Guide, Revised Edition, 1999
- 34. DOW Plastics, DERAKANE Resins Technical Product Information
- 35. DOW Plastics, Fabricating Tips__DERAKANE Epoxy Vinyl Ester Resins, Revised Edition, 1994
- 36. Brill, R. P. and Palmese, G. R., "An investigation of vinyl ester-styrene bulk copolymerization cure kinetics using Fourier Transform Infrared Spectroscopy", **J Appli. Polym Sci, Part B**, Vol. 76, No. 6, pp. 1572-1582, 2000
- 37. Ziaee, S. and Palmese, G. R., "Effect of temperature on cure kinetics and mechanical properties of Vinyl-Ester Resins", J Polym Sci, Part B: Polym Phys, Vol. 37, No. 7, pp. 725-744,1999
- 38. C. P. Hsu and L. J Lee, "Free-radical crosslinking copolymerization of styrene/unsaturated polyester resins: 1. Phase seperation and microgel formation" Polymer, Vol. 34, pp. 4496-4506, 1993
- 39. C. P. Hsu and L. J Lee, "Free-radical crosslinking copolymerization of styrene/unsaturated polyester resins: 2. Electronic spin resonance study"

 Polymer, Vol. 34, pp. 4507-4515, 1993
- 40. C. P. Hsu and L. J Lee, "Free-radical crosslinking copolymerization of styrene/unsaturated polyester resins: 3. Kinetics-gelation mechanism" Polymer, Vol. 34, pp. 4516-4523, 1993
- 41. R. P. Brill, R. L. McCullough, and G. R. Palmese, **Proc Am Soc Compos**, pp576-583, 1996

- 42. C. P. Hsu and L. J Lee, "Free-radical crosslinking copolymerization of styrene/unsaturated polyester resins: 1. Phase seperation and microgel formation" Polymer, Vol. 34, pp. 4496-4506, 1993
- 43. C. P. Hsu and L. J Lee, "Free-radical crosslinking copolymerization of styrene/unsaturated polyester resins: 2. Electronic spin resonance study" Polymer, Vol. 34, pp. 4507-4515, 1993
- 44. C. P. Hsu and L. J Lee, "Free-radical crosslinking copolymerization of styrene/unsaturated polyester resins: 3. Kinetics-gelation mechanism" Polymer, Vol. 34, pp. 4516-4523, 1993
- 45. Y. S. Yang and L. J. Lee, "Microstructure formation in the cure of unsaturated polyester resins", **Polymer**, Vol. 29, pp. 1793-1800, 1988
- 46. S. B. Liu, J. L Liu and T. L. Yu, "Microgelation in the curing of unsaturated polyester Resins", J Polym Sci, Part B: Polym Phys, Vol. 53, pp. 1165-1177, 1994
- 47. Y. J. Huang and C. J. Chen, "Curing of unsaturated polyester Resins: Effect of comonomer Composition. II High teperature reactions", J Polym Sci, Part B: Polym Phys, Vol. 47, pp. 1533-1549, 1993
- 48. M. B. Launikitis, "Vinyl Ester Resin", **Hand Book of Composite**, pp.38-49
- 49. L. S. Penn and T. T. Chiao, "Epoxy Resins", Hand Book of Composite, pp.57~88
- 50. A. ten Busschen, **Ph.D thesis**, Delft University of Thechnology, the Netherlands, 1996
- 51. S. M. Corbin, *M.S. Thesis*, Department of Chemical Engineering, Michigan State University, 1998
- 52. L. T. Drzal, "Composite Interphase Characterization", **SAMPE Journal**, <u>19</u>, 7-13, 1983
- 53. L. T. Drzal, M. Richand and P. Lloyd, "Adhesion of Graphite Fibers to Epoxy Matrices. I. The Role of Fiber Surface Treatment", **J. Adhesion**, <u>16</u>, 1-30, 1983
- 54. L. T. Drzal, M. Rich, M. Koenigand and P. Lloyd, "Adhesion of Graphite Fibers to Epoxy Matrices. II. The Effect of Fiber Finish", **J. Adhesion**, <u>16</u>, 133-152, 1983

- 55. L. T. Drzal, M. Richand and M. Koenig, "Moisture Induced Interfacial Effects on Graphite Fiber-Epoxy Interfacial Shear Strength", <u>Paper 4-G</u>, 38th Annual Technical Conference, Reinforced Plastic/Composites Institute, SPI, 1983
- 56. T. Chaudhry, H. Ho, L. T. Drzal, M. Harris and R. M. Laine, "Silicon Oxycarbide Coatings on Graphite Fibers. II. Adhesion, Processing, and Interfacial Properties", Matr. Sci. Engr., A195, 237-249, 1995
- 57. K. N. E. Verghese, N. S. Broyles, J. J. Lesko, R. M. Davis and J. S. Riffle, "Durability of polymer composites for infrastructure: the role of the interphase", Proceeding's of the 23rd Annual Meeting of the Adhesion Society, 2000
- 58. Teishev and G. Marow, "The effect of transcrystallinity on the transverse mechanical properties of single-polymer polyethylene composites", J. Applied Polymer Science, Vol. 56, pp. 959-966, 1995
- 59. Lustiger, "Morphological aspects of the interface in the PEEK-carbon fiber system", Polymer Composites, Vol. 13, No. 5, pp. 408-412, 1992
- 60. Moon, "The effect of interfacial microstructure on the interfacial strength of glass fiber/polypropylene resin composites", **J. Applied Polymer Science**, Vol. 54, pp. 73-82, 1994
- 61. E. Chen and B. Hsiao, "The effect of transcrystalline interface in advanced polymer composites", Polymer Engineering and Science, Vol. 32, No. 4, pp. 280-286
- 62. E. Jabbari and N. A. Peppas, "A model for interdiffusion at interfaces of polymer with dissimilar pysical properties", **Polymer**, Vol. 36, No. 3, pp.575-586, 1995
- E. Helfand, "Theory of unsymmetric polymer-polymer interfaces", J. Chemical Physics, Vol. 62, No. 4, pp.1327, 1975
- 64. P. G. Gennes, "Dynamics of fluctuation and spinodal decomposition in polymer blends", J. Chem. Phys. Vol. 72, No. 9, pp4756, 1980
- 65. P. Pincus, "Dynamics of fluctuation and spinodal decomposition in polymer blends. II", J. Chem. Phys. Vol. 75, No. 4, pp1996, 1980
- 66. D. K. Hadad, "Physical and chemical characterization of epoxy resins", **Epoxy**Resins_Chemistry and Technology, 2nd edition, edited by C. A. May, pp. 1089-1172, 1988
- 67. V. Rao and L. T. Drzal, "The Temperature Dependence of Interfacial Shear Strength for Various Polymeric Matrices Reinforced with Carbon Fibers", J. Adhesion, 37, 83-95, 1992

- 68. L. E. Nielen, Mechanical Properties of Polymers and Composites, Mercel Dekker, New York, 1974
- 69. V. K. Raghavendran, M. C. Waterbury, V. Rao and L. T. Drzal, "Influence of Matrix Molecular Weight and Processing Conditions on the Interfacial Adhesion in Bisphenol-A Polycarbonate/Carbon Fiber Composites", J. Adhes. Sci. Tech., 11, No.12, 1501-1512, 1997
- 70. A. Kelly and W. R. Tyson, "Tensile properties of fiber reinforced metals: Copper/Tungsten and Copper/Molybdenum", J. Mech. Phys. Of Solid, Vol. 13, pp.329-350, 1965
- 71. M. J. Pitkethly, J. P. Favre, U. Gaur, J. Jakubowski, S. F. Mudrich, D. L. Caldwell, L. T. Drzal, M. Nardin, H. D. Wagner and et al., "A Round-robin Program on Interfacial Test Methods", Compos. Sci. Technol., 48, 205-214, 1993
- 72. Yu. A. Gorbatkina, Adhesive Strength of Fiber-Polymer Systems, Ellis Horwood, New York, 1992
- 73. L. T. Drzal and M. Madhukar, "Fiber-Matrix Adhesion and Its Relationship to Composite Mechanical Properties" J. Matr. Sci., 28, 569-610, 1993
- 74. Hoecker, K. Friedrich, H. Blumberg and J. Karger-Kocsis, Comp. Sci. Tech., Vol.54, pp.317, 1995
- 75. H. D. Wagner, H. E. Gallis and E. Wiesel, J Mater. Sci., Vol.28, pp.2238, 1993
- 76. G. S. Sheu and S. S. Shyu, J. Adhesion Sci. Tech., Vol. 8, pp.1027, 1994
- 77. H. J. Jacobasch, K. Gruncke, P. Uhlmann, F. Simon and E. Mader, Composite Interfaces, Vol. 3, pp. 293, 1996
- 78. M. Nardin and J. Schultz, Composite Interfaces, Vol. 1, pp.177, 1993
- 79. P. Herrera-Franco and L. T. Drzal, "Comparison of Methods for the Measurement of Fiber-Matrix Adhesion in Composites", Composites, 23, 2-27, 1992
- 80. D. Hoyns, and L.T. Drzal, "Hydrothermomechanical Response and Surface Treated and Sized Carbon Fiber/Vinyl Ester Composites", ASTM Symposium on the Fiber Matrix and Interface Properties, 1994
- 81. V. Rao and L. T. Drzal, **Polym Compos**, Vol. 12, No. 48, 1991
- 82. L. H. Peebles, Carbon Fibers, CRC Press, Boca Raton, 1990

- 83. T.H. Yoon, H. M. Kang, M. Bump, and J. S. Riffle, "Effect of solubility and miscibility on the adhesion behavior of polymer-coated carbon fibers with vinyl esterresins", J. App. Poly. Sci. (USA), vol. 79, no. 6, pp. 1042-1053, 2001
- 84. Kim, I.C., Yoon, T.-H., "Enhanced interfacial adhesion of carbon fibers to vinyl ester resin using poly(arylene ether phosphine oxide) coatings as adhesion promoters", Journal of Adhesion Science and Technology (Netherlands), vol. 14, no. 4, pp. 545-559, Feb. 2000
- 85. Derakane 411-45 (Vinyl Ester Resin), Alloy Digest (USA), pp. 2, Aug. 1991
- 86. M. J. Reis, M. J., M. Botelho Do Rego, and J. D. Lopes Da Silva, J. Mater.Sci., Vol. 30, No. 118, 1995
- 87. M. J. Rich, S. Corbin, and L. T. Drzal, "Adhesion of carbon fibers to vinyl ester matrices", Proceedings of the 12th International Conference of Composite Materials, 1999
- 88. L. Weitzsacker, M. Xie and L. T. Drzal, "Using XPS to Investigate Fiber/Matrix Chemical Interactions in Carbon Fiber Reinforced Composites", Surf. Interf. Anal. Vol. 25, pp. 53-63, 1997
- 89. L. T. Drzal, N. Sugiura and D. Hook, "Effect of interfacial chemical bonding and surface topography on adhesion in carbon fiber/epoxy composites", Proceeding of the 1ith Annual Meeting of the American Society for Composites, 1994
- 90. L. T. Drzal, "The Epoxy Interphase in Composites", review chapter in Advances in Polymer Science II, 75, K. Dusek, ed., Spring-Verlag, pp. 16, 1985
- 91. L. Xu, Mater Thesis, School of Mechanics and Materials Science, Washington State University, 1998
- 92. J. M. Whitney and L. T. Drzal "Three Dimensional Stress Distribution Around An Isolated Fiber Fragment", ASTM STP 937, Toughened Composites, 179-196, 1987
- 93. L. Xu, L. T. Drzal, "Influence of interphase chemistry on the adhesion between vinyl ester resin and carbon fibers", **Proceedings of the 23rd Annual Meeting of "Adhesion Science for the 21st Century"**, 2000

CHAPTER 3

STATEMENT OF THE PROBLEM

The main objective of this study was to gain an understanding of the factors controlling interfacial adhesion between carbon fibers and vinyl ester resin; to model the contributions of the factors controlling the fiber/matrix adhesion; and furthermore to provide an engineered and optimized interface between carbon fiber and vinyl ester for tailoring a structurally efficient carbon fiber/vinyl ester composites. The adhesion was evaluated as interfacial shear strength (IFSS) measured by micro-indentation. Previous data has shown that the application of a lightly cross-linked amine-cured epoxy sizing to the carbon fiber surface creates a beneficial interphase between the carbon fiber and vinyl ester resin matrix resulting in a substantial increase in fiber-matrix adhesion and an improvement in the mechanical properties of carbon fiber/vinyl ester composites as well [14]. But the exact mechanism by which the use of this sizing improved adhesion is not known and the interaction between the epoxy sizing and the vinyl ester has to be optimized for compatibility and thickness. The first unknown to be investigated in this study is the influence of the thickness of the fiber epoxy sizing on the adhesion between carbon fiber and vinyl ester resin and find out the optimum thickness.

The vinyl ester utilized as a base system for this study was DERAKANE 411-C50 epoxy vinyl ester which contains 50% styrene as reactive diluents. The copolymerization between styrene and vinyl ester undergoes a heterogeneous, free radical, chain-growth,

crosslinking reaction. The polymerization catalysts of vinyl ester resin were found to be adsorbed on the carbon fiber surface. Cobalt was detected at 2.6% at the surface of the carbon fiber exposed to cobalt naphthenate (CoNap) and a minor change was also noted in the surface chemistry of the fiber exposed to dimethyl aniline (DMA), which are the promoters and accelerators for the free radical copolymerization respectively [5]. Considering the "controlled and designed" epoxy sizing of optimum thickness as the engineered interphase between carbon fiber and vinyl ester resin, it should isolate the carbon fibers from contact with the vinyl ester resin and hence eliminate the adsorption of the catalysts onto the carbon fibers surface. Comparing the micro-indentation data of the composites with an engineered interphase to that of the composites made with "asreceived" carbon fibers, the influence of the adsorbed catalysts on the adhesion between carbon fibers and vinyl ester resins can be found. On the other hand, compared to the pure epoxy vinyl ester resin, the pure styrene monomer has a much lower surface energy. As a result of the surface energy forces, there is a potential to create a styrene rich layer on the surface of reinforced carbon fiber in the composites.

Vinyl ester resin can undergo as much as 9% volume shrinkage with cure while a typical epoxy system undergoes only 3-4% shrinkage during cure ^[6,7]. This shrinkage can induce significant stresses in the composite even before loading. A new type of vinyl ester resin having lower cure volume shrinkage was found ^[8]. One of the investigations of this part of the research is to use the low shrinkage DGEBA-T403 carbon fiber sizing, the "controlled and designed" interphase, to isolate the fibers from the vinyl ester resin and then to observe the influence of the cure volume shrinkage on the IFSS values measured by micro-indentation. The other strategy is to find of the influence of matrix

resin cure volume shrinkage on the fiber/matrix adhesion by comparing the IFSS data of vinyl ester matrices of different volume shrinkage.

Once the physics and chemistry of the interphase and the interaction of the epoxy sizing with the vinyl ester matrix is known, finite element model would be used to understand the experimental results. Using IDEAS for the pre-processing and ABAQUS for processing and post-processing, a set of non-linear contact finite element models were set up to determine the influence of the thickness of the sizing material and the results were compared with the experimental data. LS-DYNA, one of the most powerful non-linear finite element analysis methods, was used for the simulation of the cure volume shrinkage and the stress brought by the shrinkage in the third part of the research.

The completed research has been organized into three major sections as described above. Section 1: Use of a controlled and designed interphase to improve the adhesion between carbon fiber and vinyl ester matrix which focused on the influences of the sizing thickness and sizing property gradient on the interfacial shear stress. Section 2: The influence of the component chemistry on the adhesion between carbon fiber and vinyl ester matrix was investigated. This section focused on the effect of the constituents of the vinyl ester resin system on the interfacial shear stress, the effects of the catalysts, the effects of the styrene monomers and the DGEBA vinyl ester monomers. Section 3. Thermal characterization of the interphase between carbon fiber and vinyl ester matrix which focused on effects of the cure volume shrinkage of vinyl ester and the interfacial thermal residual stress on adhesion between carbon fiber and vinyl ester resin.

REFERENCES:

- 1. S. M. Corbin, **M.S. Thesis**, Department of Chemical Engineering, Michigan State University, 1998
- 2. D. Hoyns, and L.T. Drzal, "Hydrothermomechanical Response and Surface Treated and Sized Carbon Fiber/Vinyl Ester Composites", ASTM Symposium on the Fiber Matrix and Interface Properties, 1994
- 3. M. J. Rich, S. Corbin, and L. T. Drzal, "Adhesion of carbon fibers to vinyl ester matrices", Proceedings of the 12th International Conference of Composite Materials, 1999
- 4. L. Xu, L. T. Drzal, "Influence of interphase chemistry on the adhesion between vinyl ester resin and carbon fibers", **Proceedings of the 23rd Annual Meeting of "Adhesion Science for the 21st Century"**, 2000
- 5. L. Weitzsacker, M. Xie and L. T. Drzal, "Using XPS to Investigate Fiber/Matrix Chemical Interactions in Carbon Fiber Reinforced Composites", Surf. Interf. Anal. 25, 53-63, 1997
- 6. M. B. Launikitis, "Vinyl Ester Resin", Hand Book of Composite, pp.38-49
- 7. L. S. Penn and T. T. Chiao, "Epoxy Resins", **Hand Book of Composite**, pp.57~88
- **8.** <u>WWW.FUCHEM.COM</u>

CHAPTER 4

EXPERIMENTAL METHODS

4.1 FIBER SIZING

4.1.1 Sizing Materials

Diglycidyl Ether of Bisphenol A (DGEBA) and an aliphatic Polyether Triamine (Jeffamine T-403) were used as a carbon fiber sizing and curing agent respectively. Diglycidyl Ether of Bisphenol A (DGEBA) was widely used as an organic sizing material. The molecular structure of DGEBA and Jeffamine T-403 are shown as Figure 4.1. DGEBA can be formulated to accommodate most of limitations presented by specific curing requirements. Jeffamine T-403 was selected to be the curing agent for DGEBA considering its aliphatic amine nature, amine functional group and molecular structure. Aliphatic amine—cured epoxy is room temperature cured which can keep the thermal stresses to a minimum [1-4]. This system cannot be used at high temperature. Table 4.1 presents the selected properties of DGEBA cured with Jeffamine T-403.

In a mixture of epoxy resin and curing agent, competitive adsorption may take place.

The amines have a surface free energy higher than epoxy. The epoxy may be adsorbed on the basal plane of carbon fibers ^[5-7]. The adsorbed epoxy may be displaced by a

$$\begin{array}{c} O \\ CH_2-CH-CH_2 \\ +R-CH_2-CH-CH_2 \\ -R-CH_2-CH-CH_2 \\ -R-CH_2-CH-CH_2-CH-CH_2 \\ -R-CH_2-CH-CH_2 \\ -R-CH_2-CH-CH_$$

Diglycidy Ether Bisphenol A (DGEBA)

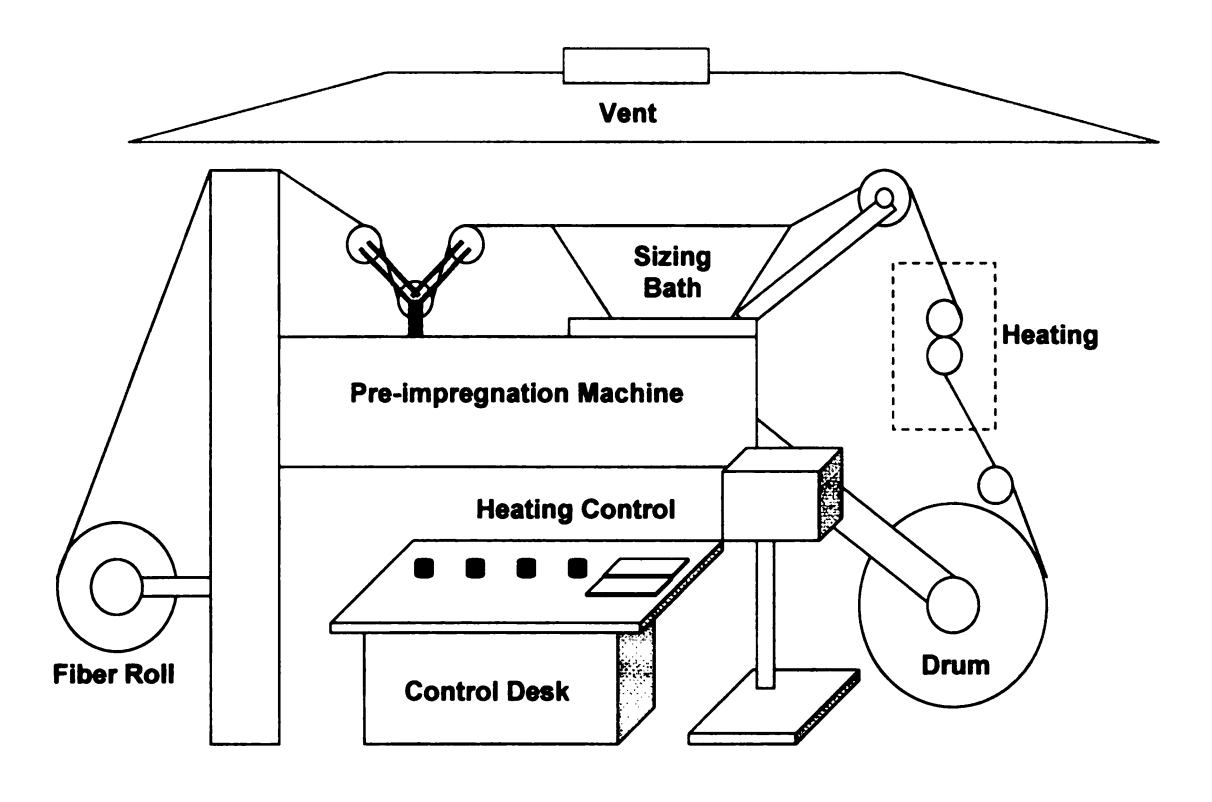
where, $x+y+z \sim 5.3$

Aliphatic Polyether Triamine (JEFFAMINE T-403)

Figure 4.1 Molecular of Diglycidy Ether of Bisphenol A (DGEBA) and Jeffamine T 403

Properties	DGEBA-T403
Tension Modulus, E, GPa (Msi)	3.24 (0.47)
Poisson Ratio, v ₁₂	0.354
Shear Modulus, G, GPa (Msi)	1.27 (0.184)
Coefficient of Thermal Expansion (CTE), α, (10 ⁻⁶ /°C)	60
Heat Distortion Temperature (°C)	62
Density, ρ, (g/m³)	1.16
Surface Energy, γ, (mJ/m²)	40 ^[5]

Table 4.1 Selected Properties of DGEBA-T403 [2]



• Tension 0.6 • Drum Carriage 25 • Rotation 15rpm

Figure 4.2 Schematic of the pre-impregnation machine to apply sizing to the carbon fibers

curing agent molecule resulting a region where the local composition at the interface is different from the bulk ^[7].

4.1.2 Sizing Process

A stoichiometric mixture of DGEBA and T-403 was mixed and let cure for 30 minutes, then added to acetone to form the sizing solution for the carbon fiber. Fibers were sized with a Pre-impregnation machine, Figure 4.2. AS4 carbon fibers were allowed to go through the bath filled with sizing solution and left to dry for 24 hours. The fibers were cut into 6 in length and kept in tubes sealed with tube caps. The Pre-impregnation machine was set to Tension at 0.6, Drum carriage at 25 and Rotation at 15.

4.1.3 Sizing Thickness Measurement (TGA)

Thermal Gravimetric Analysis (TGA) measures changes of mass of a sample as a function of time isothermally, or as a function of temperature, from ambient to 1000°C in a controlled gaseous environment. It can provide the percentage of weight loss after coated fibers have been heated up to 400°C for 3 hours to burn off the organic materials. Assuming all the fibers are evenly coated, the sizing thickness can be calculated based on the densities of both the organic materials and the fiber. A typical TGA data was shown in Figure 4.3. A 2950 TGA HR instrument of Mode: TGA 1000°C was used. The typical experimental parameters were set up as following:

Method Segments:

- 1. Ramp 20.00°C/min res 4.0°C to 400 °C
- 2. Isothermal for 120 mins
- 3. Ramp 10.00°C/min to 600°C

Sample Flow 40

Reference Flow 60

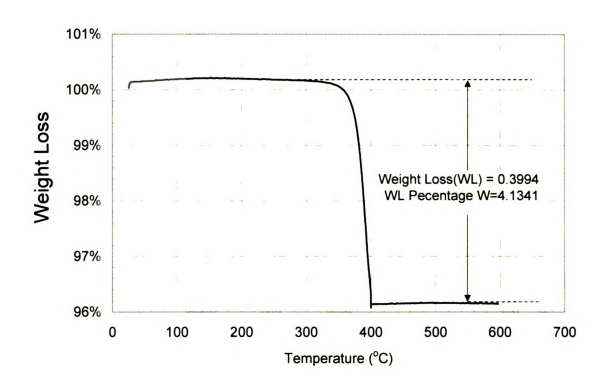
Advanced Parameters:

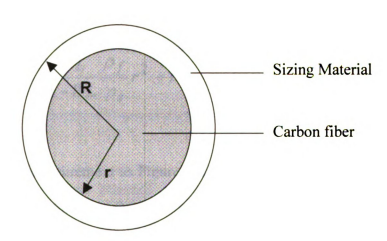
Data Sampling interval: 2.0sec/pt Data Compression Threshold Values Temperature: 0.05 °C

Signal A: 0.0000mg

Post Test Parameters:

Futnace: Open And Unlosd Air Cool for 6.00min.





Carbon fiber and the sizing materials

Figure 4.3 Using TGA to measure the sizing thickness

59

As shown in Figure 4.3, assume the total weight loss percentage is WL, known the density of carbon fiber is ρ_f and the density of the sizing material is ρ_s , then,

$$WL = \frac{\pi (R^2 - r^2)\rho_s}{\pi [(R^2 - r^2)\rho_s + r^2\rho_f]}$$
4.1

The sizing thickness t=R-r, then

$$R = \sqrt{\frac{WL}{1 - WL} \frac{\rho_f}{\rho_s} r^2 + r^2}$$
 4.2

So,

$$t = R - r = \sqrt{\frac{WL}{1 - WL} \frac{\rho_f}{\rho_s} r^2 + r^2} - r$$
 4.3

For a TGA measurement as Figure 4.3, refer to Table 2.1 and Table 4.1, the density of the AS4 carbon fiber and DGEBA-T403 were 1.77gcm^{-3} and 1.16gcm^{-3} . According to equation 4.3, t=113.3 nm for AS4 carbon fiber with a diameter of $7 \mu \text{m}$. With this calculation, the sizing has been assumed to be even through out the whole fiber tow. Therefore, the thickness of sizing calculated from the weight loss measured by TGA is an average number.

4.1.4 Environmental Scanning Electron Microscope (ESEM)

Environmental Scanning Electron Microscope (ESEM) is a new technique in scanning electron microscopy specifically designed to study insulating materials. Polymers, biological cells, bacteria, concrete, etc can be observed in the ESEM without prior specimen preparation or conductive coatings which are necessary for a traditional Scanning Electron Microscope. Environmental SEM provides information regarding the topography, morphology, and microstructure of a specimen by the gaseous detection device which utilizes the ionization of the water vapor for the detection of secondary electrons from the specimen surface. The real sizing topographies on the coated fiber surface were observed by ESEM. A model 2020 ElectroScan ESEM was used to observe fiber sizing.

4.2 Measurements of Mechanical Properties of Materials

4.2.1 Dynamic Mechanical Thermal Analysis (DMTA)

Dynamic Mechanical Thermal Analysis (DMTA) is an analytical technique, which measures the modulus (stiffness) and damping (energy dissipation) properties of materials as those materials are deformed under periodic (oscillatory) stress as a function of temperature.

In DMTA, a sample is subject to a low-strain sinusoidal deformation, and its response to the deformation is measured. The resultant measurements obtained are the storage modulus E', which is related to the stiffness of the material, and the loss modulus E",

which determines the viscous loss properties. A third parameter, tan δ , is calculated by

dividing E" by E'. As the temperature is increased from subambient to the melt-state the

tan δ curve exhibits a series of peaks. The most significant peak is found in the region of

the glass transition temperature (Tg). Previous studies revealed not only the glass

transition temperature of the matrix material, but also a peak in the tan δ curve where the

Tg of the coating material was detected [8]. This indicates that the DMTA is not only a

good technique for the measurement of mechanical properties of materials but also a

useful tool for characterization of the composite interphase. A typical DMTA plot is

shown in Figure 4.4.

A 2980 DMTA instrument and Multi-Frequency-Single Cantilever was used. From

the curves in Figure 4.4 storage modulus at certain temperature such as 30°C was

measured and glass transformation temperature was measured from the tan δ curve. The

typical experimental parameters were set up as following:

Method Segments: 1.Ramp 3.00 °C/min to 170°

Amplitude: 50µm

Frequency Table (Hz): 1.000

Advanced Parameters: Data sampling interval: 4.0sec/pt

Post Test Parameters

Return to temperature range: 25.00 °C to 30.00 °C

Furnace: Open

Clamp: Lock

62

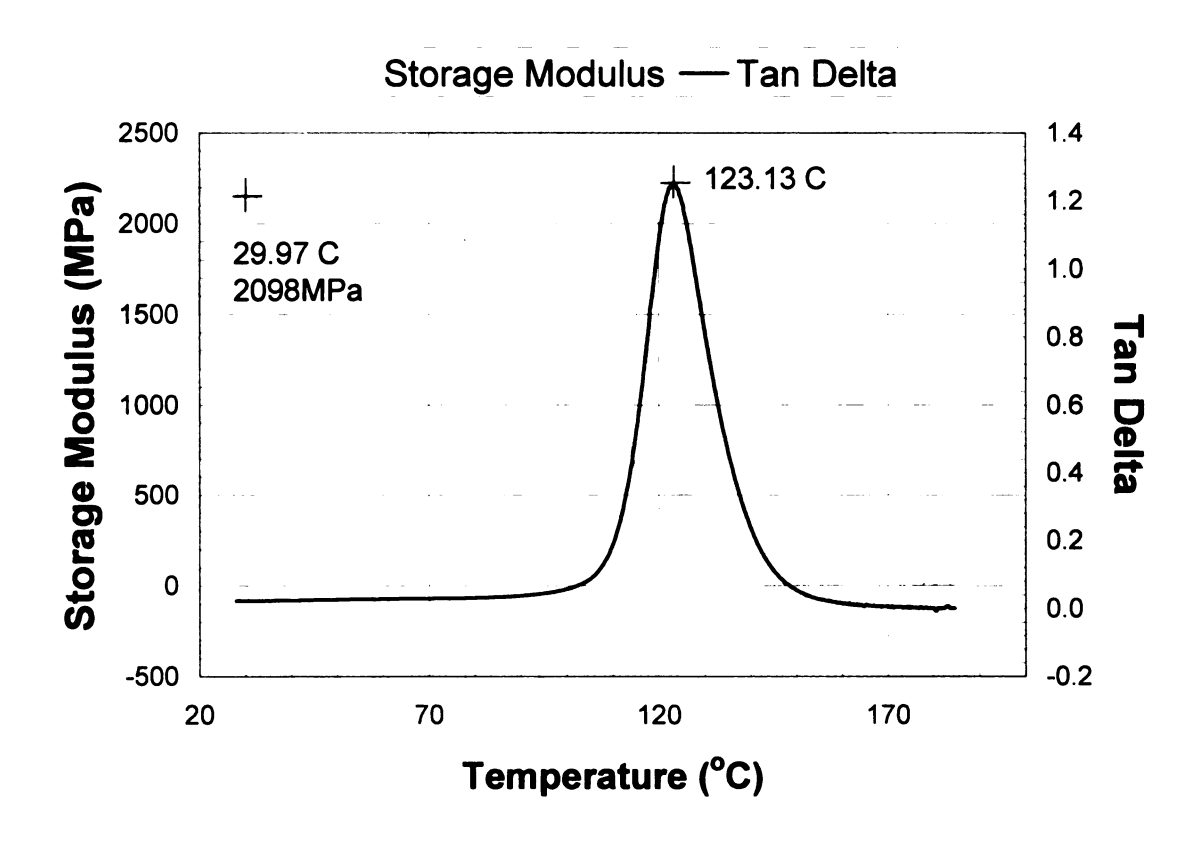


Figure 4.4 Using DMTA to measure the storage modulus at certain temperature and the glass transformation temperature

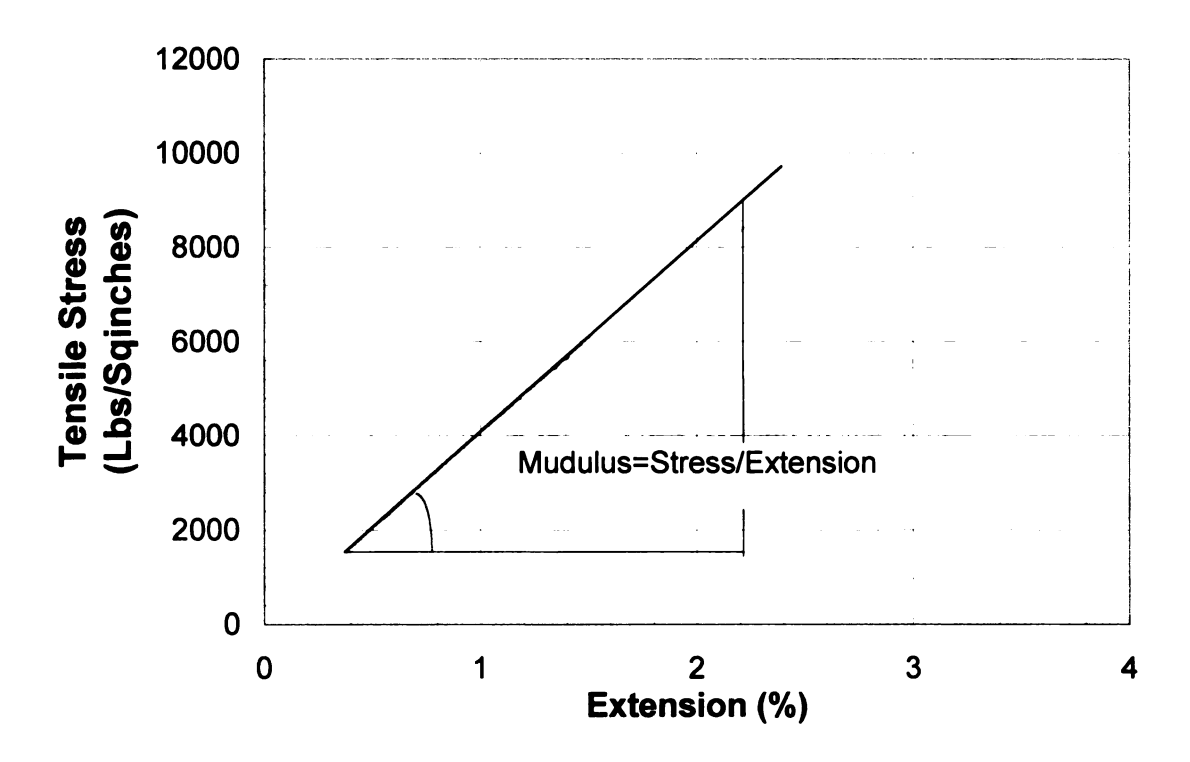


Figure 4.5 Use UTS to measure the tensile modulus

4.2.2 United Testing System (UTS)

Standard Test Method for Tensile Properties of Plastic— Test Method D683 was

carried out by a United Testing System to measure the elastic modulus of the vinyl ester.

This test method covers the determination of the tensile properties of unreinforced and

reinforced plastics in the form of standard dumbbell-shaped test specimens when tested

under defined conditions of pretreatment, temperature, humidity, and machine speed.

The typical experimental parameters were set up as following:

Load Cell Capacity (Lbs): 1000

Cross Head Speed (in/min): 0.1

Preload Value (Lbs): 5

One typical load-extension curve given by UTS is as Figure 4.5. The modulus of

elasticity is calculated by extending the initial linear portion of the load-extension curve

and dividing the difference in stress corresponding to any segment of section on this

straight line by the corresponding difference strain.

4.2.3. MTS Nano-indentation and Nano-scratch Test

The nano-indentation method was originally designed to for the purpose of probing

the mechanical properties of very small volumes of materials. It is ideal for mechanically

characterizing thin films, coatings and surface layers including those modified by ion

implantation, because the layers does not have to be removed from its substrate [9]. Most

recently, it was found that the nano-scratch test could be successfully employed in the

65

investigation of composite interphases ^[10]. A MTS nanoindentation machine was used to investigate both the mechanical properties of the bulk material and the properties of the interphases between materials. The resolution and ranges of the instrument is listed in Table 4.2.

Table 4.2 The resolution and the ranges of MTS nano-scrach XP head and nano-indentation DCM Head

	Resolutions XP Head	DCM Head
Loading Resolution	1nN	1nN
Displacement Resolution	0.4nm	0.0002nm
Indenter Range	1mm	20μm
Load Range	500mN	10mN

4.2.3.1 Nano-Indentation Test

Generally the indentation process is described as three steps. 1. As the indenter is driven into the material, both elastic and plastic deformation cause the formation of a hardness impression conforming to the shape of the indenter to some contact depth, h_c . 2. Then the machine holds position for a short time at a constant load in the indenter. 3. As the indenter is withdrawn, only the elastic portion of the displacement is recovered. It is the recovery in the third step which allows one to determine the elastic properties of a material.

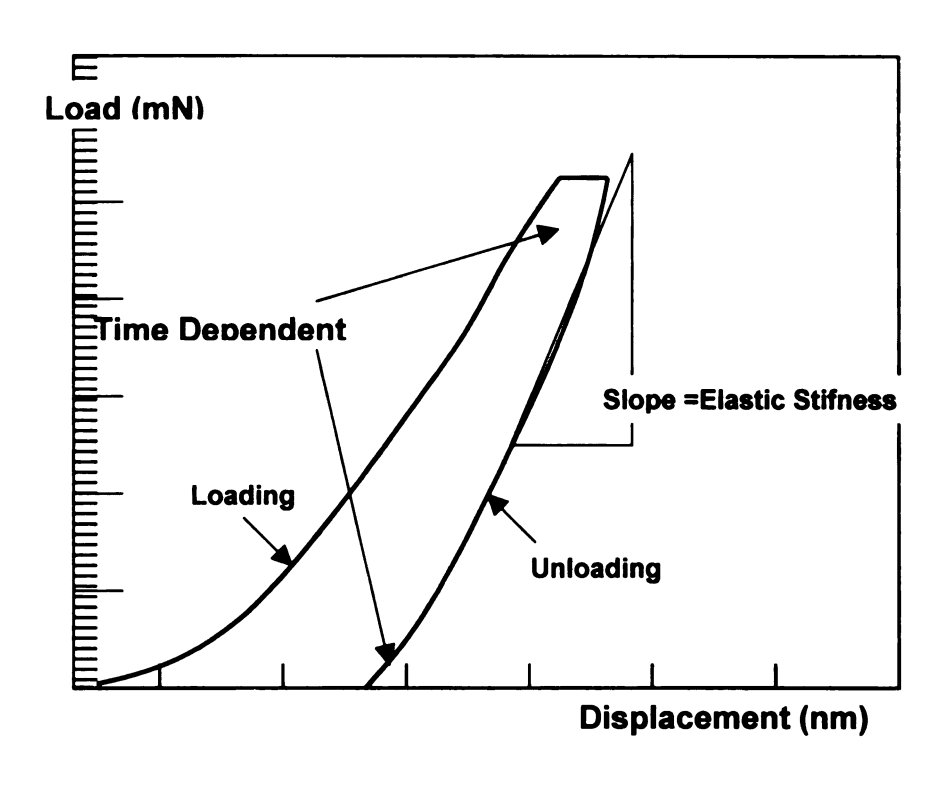


Figure 4.6 A hypothetical set of continuous load-displacement data collected during the Nano-Indentation experiment^[9]

The indenter tip is a DCM type with a Berkovich pyramid shape. A hydrothetical set of continuous load-displacement data is present in Figure 4.6. ^[9] Note that the slope has dimensions of force per unit distance, and it is also known as elastic stiffness, S, of the contact. The reduced elastic modulus, E_r, accounts for bi-directional displacements in both the indenter and the sample which is related to S as:

$$E_r = \frac{1}{\gamma \beta} \frac{\sqrt{\pi}}{2} \frac{S}{\sqrt{A}}$$
 4.4

where A is a factor related to contact area, for a conical tip with contact radius, a, $a \approx (\pi/A)^{1/2}$; The factor γ corrects for these approximations and depends on the strain imposed by the indenter and the Poisson's ratio pf the test material; β =1 for any tip that creates a circular contact, β =1.012 for a Vickers pyramid, β =1.034 for a Berkovich pyramid, and

$$\frac{1}{E_r} = \frac{1 - v_s^2}{E_L} + \frac{1 - v_t^2}{E_L}$$

where E_s and v_s are the elastic modulus and Poisson's ration for the sample. E_i and v_i are the same properties for the indenter. For diamond, E_i =1141 GPa and v_i =0.07. For most engineering material have a Poisson's ratio between 0.15 and 0.35, always less than 0.5. With an input number of v_s , the machine can calculate the E_s .

4.2.3.2 Nano-Scratch Test

The nano- scratch test involves moving the diamond indentor tip across a sample surface at a fixed depth. The tip used in this scrapping experiment is also Berkovich pyramid shape but is of XP type. The scratch tip was oriented with the sharp edge into the direction of motion. The normal force is maintained at a constant value and the lateral force is measured from the deflection of the shaft and the lateral displacement. The ratio of these two forces is the coefficient of friction (COF) between the material of the indenter and that of the scratched material which is different from the one in physics concept, see Figure 4.7. The depth of the indenter is also recorded, thus indicating the hardness of the surface being scratched.

The interphase transition information can be influenced by two factors. One is the stress field and corresponding plastic zone, the other is the tip size. When the indenter is pressed into the sample material it creates a corresponding stress field and associated zone of plastic [11-13]. Thermosetting polymers are materials for which the coefficient of work hardening is very small. The stress and plasticity interaction effect should be negligibly small when a scratch is created in the regions of polymer materials. However, when the indenter tip is in close proximity to the interface near a carbon fiber where the elastic modulus is at least two orders of magnitude above that of the polymer, the effect could be significant. Therefore, a scratch extending from the stiffer carbon fiber to the softer polymer is more preferred than a scratch from polymer to carbon fiber.

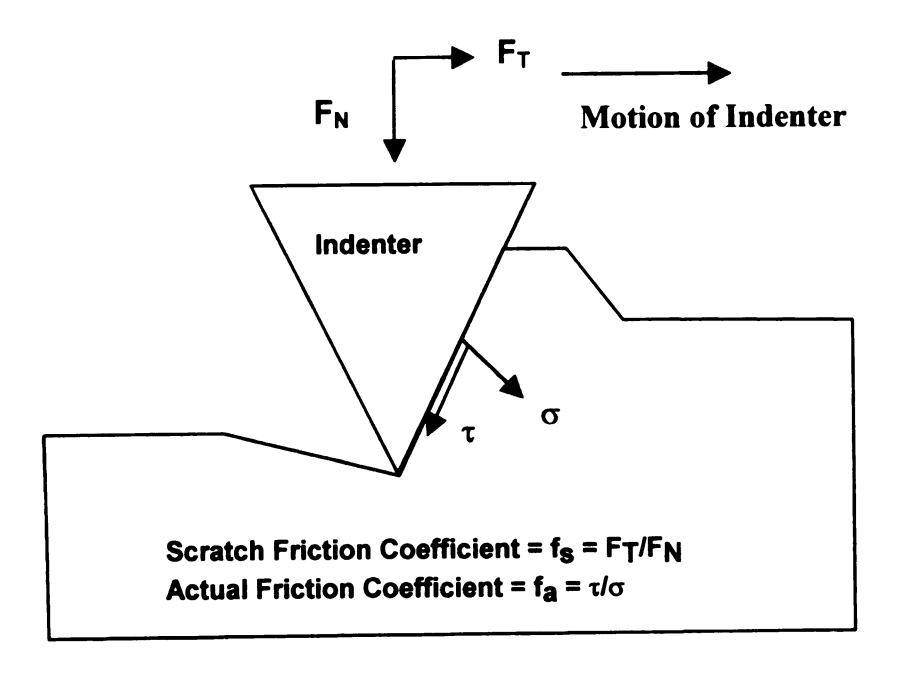
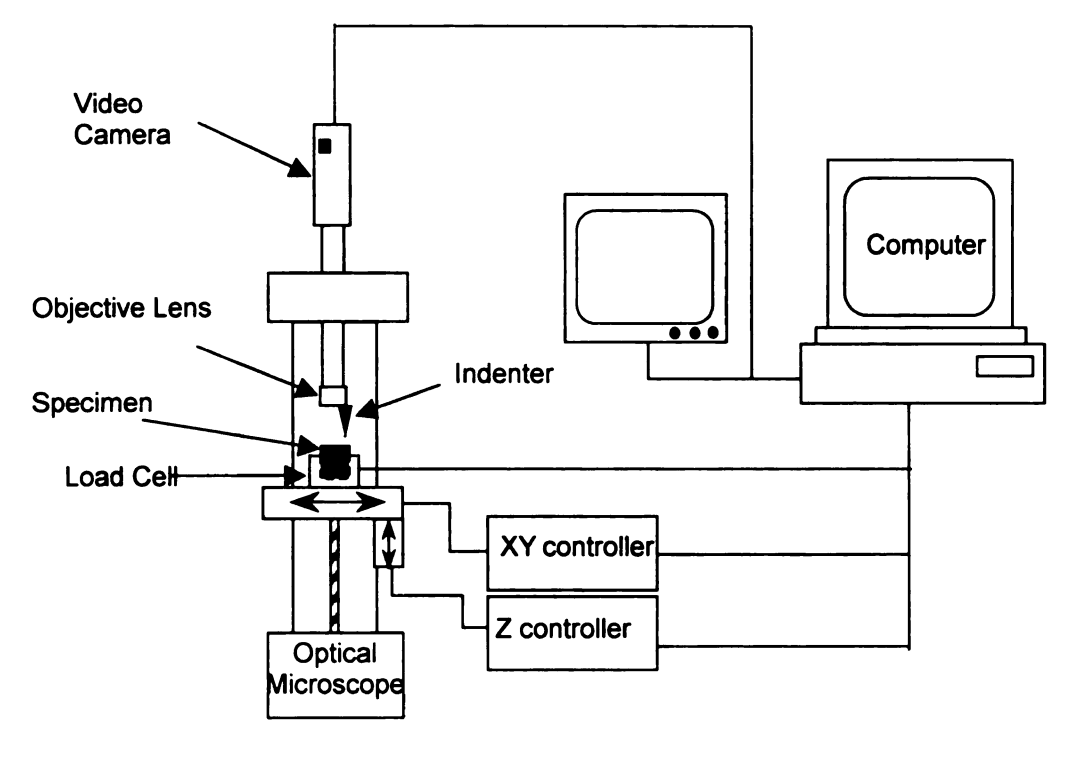


Figure 4.7 Coefficient of friction (COF)^[9]

The depth of the scratch depends on the indenter size. The indenter size could enlarge an infinitesimally small interface into a much wider region creating an artifact in the data. As mentioned before, materials of different hardness will have different depth of scratch. This scratch tip size and depth influence is compensated by a C++ program which includes calculations based on some reasonable assumptions, see Appendix II.

4.3 Measurement of the Adhesion between Carbon Fiber and Vinyl Ester Resin

The Interfacial Testing System (ITS) apparatus was used to conduct microindentation measurements to determine the interfacial shear stress (IFSS) [15]. The
measured interfacial strength is given by a generalized empirical equation (ITS shear
equation) which is embedded in the data reduction software of the apparatus. The ITS
apparatus indentation test is an in situ interface test for real composites and has the
advantage of reflecting actual process conditions. It can determine the interphase
strength due to fatigue or environmental exposure, or possibly monitor the interphase
properties of parts in service. In this method a sample of actual composite is tested.
Selected single fibers perpendicular to a cut and polished surface are compressively
loaded to produce debonding or fiber slippage. Interphase bonding is monitored
microscopically between steps, until debonding is observed, see Figure 4.8 and Figure
4.9. ITS micro-indentation tests were performed until 10-15 good failures were observed
for each fiber/matrix system. The standard deviation of measured IFSS values for each
system could be very large. Normally a standard deviation of 10~15% of IFSS would be



$$IFSS = 181100 \frac{f_g}{d_f^2} \left\{ 0.875696 \sqrt{\frac{G_m}{E_f}} - 0.018626 \ln(\frac{d_n}{d_f}) - 0.026496 \right\}$$
 4.6

 $f_g = Load on Fiber$

G_m= Shear Modulus of Matrix

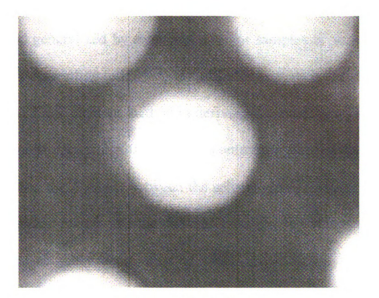
 E_f = Tensile Modulus of Fiber

d_n= Distance between the Nearest Fiber

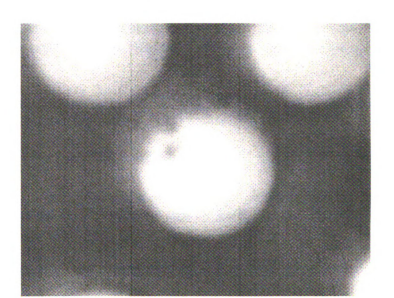
 d_f = Diameter of the Fiber

A= Conversion Factor

Figure 4.8 Interfacial Testing Systems (ITS) used for performing micro-indentation tests on fiber reinforced composites [14]



Fiber before test



Fiber after test

Figure 4.9 ITS images for fiber before and after test

acceptable. It is important to point out that the fiber selection for the ITS test was critical to obtaining reproducible results. The ITS shear equation is derived based on a maximum shear stress criterion using the results of a linear axi-symmetric finite element analysis ^[15,16] and generalized by empirical data for samples of various fiber and matrix combinations ^[15]. According to Ho ^[17], the ITS shear equation, equation 4.6, agrees well with the nonlinear finite element method in deriving the maximum interfacial shear stress when the fiber volume fraction=30~50%. To control the fiber volume fraction condition for the testing fiber, the distance between the selected test fiber and its nearest neighbor must exceed 2 micron meters and the distance between the selected test fiber and the at least three nearest neighbor fibers must be within a distance of half of diameter of the selected test fiber. In addition, the selected test fiber and the fibers near it must be free of defects such as voids, scratched, chips, and cracks.

4.4 REFERENCES

- 1. S. M. Corbin, M.S. Thesis, Department of Chemical Engineering, Michigan State University, 1998
- 2. L. S. Penn and T. T. Chiao, "Epoxy Resins", Hand Book of Composite, pp.57~88
- 3. M. A. F. Robertson, M. B. Bump, K. E. Verghese, S. R. McCartney, J. J. Lesko, and J. S. Riffle, "Designed Interphase Regions in Carbon Fiber Reinforced Vinyl Ester Matrix Composites", **J. Adhesion**, mg7802, SAS98Vol. 74, 1999
- 4. Bergeret, N. Bina and A. Crespy, "Epoxy resins as surface treatments for mica flakes in propylene/ethylene copolymer composite" Composite Interfaces, Vol.5 No. 6 pp. 529-542, 1998
- 5. L. T. Drzal, "The Epoxy Interphase in Composites", review chapter in Advances in Polymer Science II, 75, K. Dusek, ed., Spring-Verlag, pp. 16, 1985
- 6. K. Horie, H. Murai and I. Mita, Fiber Sci. Tech., Vol 9, pp253, 1976
- 7. J. L. Racich, and J. A. Koutsky, **Boundary Layers in Thermosets, Chemistry and properties of Crosslinked Polymers**, ed. S. Labana, pp 303, Academic Press, 1977
- 8. "Advanced Techniques for Polymer Characterization" Beijing University of Aeronautics and Astronautics (BUAA), 1990
- 9. J, Hay, "Mechanical testing by indentation", Applied Nano Metrix, Inc, 1999
- 10. Hodzic, Z. H. Stachurski, J. K. Kim, "Nano-indentation of polymer-glass interfaces Part I. Experimental and mechanical analysis", **Polymer**, Vol. 41, pp. 6895-6905, 2000
- 11. K. L. Johnston, Contact Mechanics, Cambridge University Press, 1987
- 12. B. D. Beake and G. J. Leggett, "Nanoindentation and nanoscratch testing of uniaxially and biaxially drawn poly(ethylene terephthaslate film", **Polymer**, Vol. 43, pp. 319-327, 2001
- 13. S. Gao and E. Mader, "Characterization of interphase nanoscale property variation in glass fiber reinforced polypropylene and epoxy resin composites", Composites, 2001

- 14. V. K. Raghavendran, *PhD Dissertation*, Department of Material Science and Mechanics, Michigan State University, 1998
- 15. The Interfacial Testing System (ITS), **The Dow Chemical Company, Freeport**, Texas
- 16. J. F. Mandell, D. H. Grande, T. H. Tsiang and F. J. McGarry, "Modified microdebonding test for direct in situ fiber/matrix bond strength determination in fiber composites", Composite Materials: Testing and Design, ASTM STP893, American Society for Testing and Materials, pp. 87-108, 1986
- 17. H. Ho and L. T. Drzal, "Evaluation of Interfacial Mechanical Properties of Fiber Reinforced Composites Using the Microindentation Method", accepted for publication in Composites, Part A, 1998

CHAPTER 5

IMPROVEMENT OF ADHESION BETWEEN CARBON FIBERS AND VINYL ESTER RESIN WITH EPOXY SIZING

Vinyl ester resins have been extensively used for the manufacture of low cost high performance composites. Carbon fibers are important reinforcement materials for the production of high stiffness and strength composites. However when carbon fibers are combined with vinyl ester, the mechanical properties of the resulting composites are lower than desirable because of widely reported low adhesion between carbon fiber and vinyl ester [1-9]. Previous data has shown that the application of a lightly cross-linked epoxy polymer onto the carbon fiber surface provides a beneficial interphase between the carbon fibers and vinyl ester resin matrices in promoting the interfacial shear strength (IFSS) and the mechanical properties of carbon fiber reinforced vinyl ester matrix composites [2,9,10]. The interaction between the epoxy sizing and the vinyl ester resin has to be optimized not only for compatibility but also sizing thickness if further improvements are to be realized. This chapter focuses on the understanding the adhesion dependence on epoxy sizing thickness between carbon fibers and vinyl ester resin; determination of the optimized fiber sizing thickness; and investigation of the mechanism by which an epoxy sizing influences carbon fiber/vinyl ester adhesion. The fiber/matrix adhesion was evaluated as interfacial shear strength measured with micro-indentation. The compatibility between the epoxy sizing and the vinyl ester matrix resin was

investigated with nano-indentation and nano-scratch characterization experiments as well. A set of non-linear contact finite element models was also set up to simulate the micro-indentation process. It was found that the epoxy sizing resulted in an increase in fiber/matrix adhesion of about 30%. Apparently a stronger interphase was formed when the epoxy sizing forms chemical bonds with the carbon fibers and an interpenetrating network with the vinyl ester resin. It was concluded that the sizing thickness has an optimum value around 90nm for the best adhesion. The finite element analysis agrees with these results.

5.1 INTRODUCTION

Vinyl ester resins are now widely used in large-volume and low-cost applications primarily with glass fiber as reinforcement. The manufacture and availability of heavy tow (i.e. large number of carbon fiber filaments in each tow) carbon fibers has lead to price reductions without a loss in strength or stiffness [11]. Because of their superior specific strength and stiffness, the low price carbon fibers could be economically competitive with glass fibers for use in markets previously deemed too expensive, such as infrastructure, automobiles and etc. Additional economic advantage would be enjoyed if carbon fibers could be substituted for glass fibers used in existing composite manufacturing methods, such as resin transfer molding with vinyl ester matrices. However, composites of carbon fibers in vinyl ester polymers possess unacceptably low mechanical properties [1,2]. It is well known that fiber/matrix adhesion can be a significant reason for lowering the mechanical properties of a composite material. Low

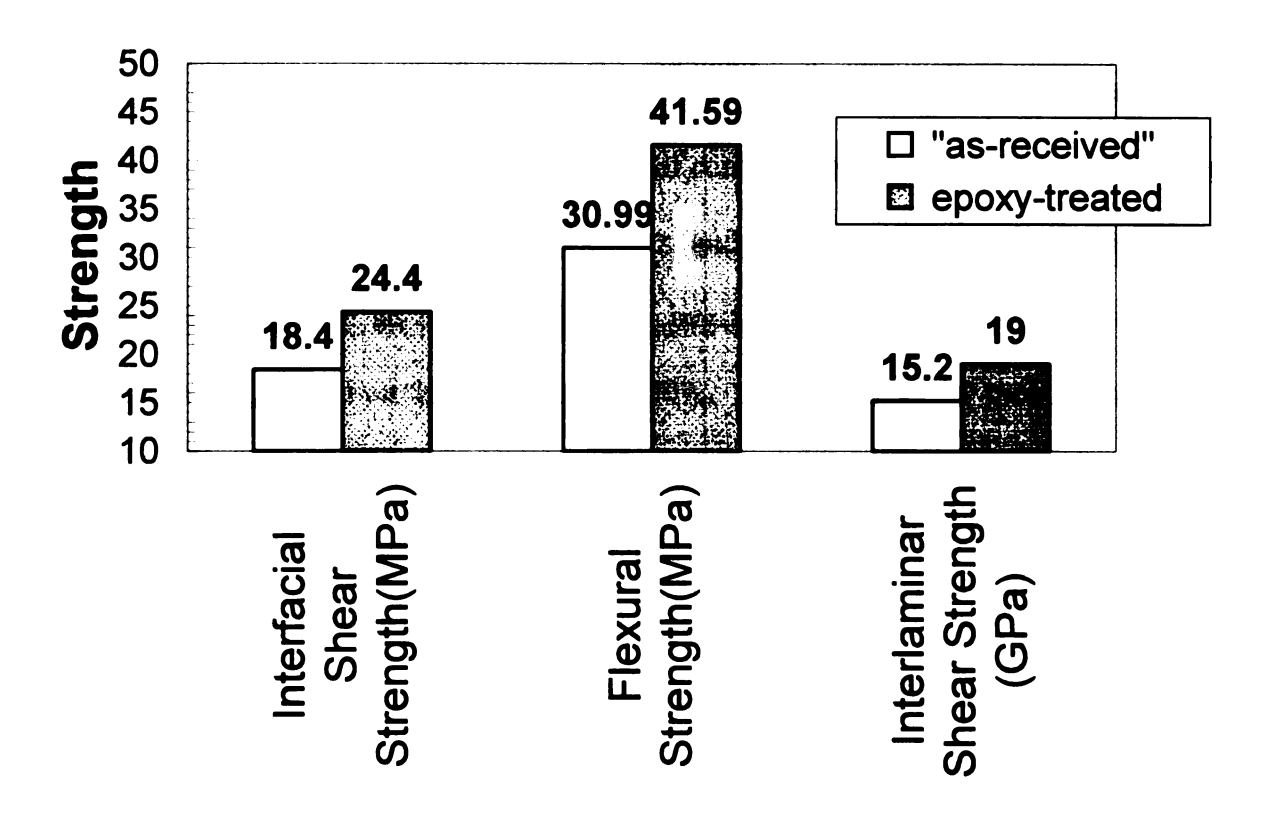


Figure 5.1 Effect of fiber sizing on the interfacial shear strength and composite mechanical properties [2]

adhesion was extensively reported between vinyl ester and carbon fiber ^[1-9]. The interfacial shear strength of a common carbon fiber/vinyl ester system possessed only 50% of that of a carbon fiber/epoxy system ^[1,2,9]. The use of vinyl ester matrices reinforced with carbon fibers requires an improvement in fiber-matrix adhesion levels.

DGEBA Epoxy (Epon 828) cured with Jeffamine T403 (T403) was applied as a sizing for Panex 157% carbon fibers ^[2]. Panex 157% carbon fibers are PAN-based carbon fibers with an electrochemical surface treatment. A toughened fiber/matrix interphase region was achieved and properties of composite were recorded by single fiber fragmentation (SFFT), three points flex tests and Iosipescu out-of-plane shear test. Corbin found that with an epoxy sizing, the interfacial shear strength measured with single fiber fragmentation increased about 30%. The mechanical properties of the composite material, flexural strength and interlaminate shear strength, also increased 34% and 25% respectively, as shown in Figure 5.1^[2]. This chapter focuses on the understanding the influences of epoxy sizing thickness on the adhesion between carbon fibers and vinyl ester resin; finding out the optimized fiber sizing thickness, and investigating the mechanism of the carbon fiber/vinyl ester adhesion improvement with epoxy sizing on the fiber surface.

5.2 EXPERIMENTAL MATERIALS AND METHODS

Experimental Materials: The fiber was an AS4 carbon fiber from Hexcel, Inc. It is a type A, electrochemical surface treated (S), about 7-micron diameter, PAN based carbon fiber. The fiber tow size is 12,000 filaments. The matrix resin was Derakane 411-C50 vinyl ester resin from Dow Chemical which contain 50wt% of Epoxy-based vinyl ester

and 50wt% of styrene monomer. The catalysts of D411-C50 were CHP-5 (diluted cumene hydroperoxide) from Witco Chemical used as the initiator and CoNap and DMA were both from Aldrich Chemicals used as promoters and accelerators respectively. Diglycidyl Ether of Bisphenol A (DGEBA) and Aliphatic Polyether Triamine (Jeffamine T403) were from Shell and Huntsman respectively. Figure 5.2 shows the molecular structures of all the chemicals used in these experiments.

Experimental Methods: A stoichiometric mixture of Diglycidyl Ether of Bisphenol A (DGEBA) and Aliphatic Polyether Triamine (Jeffamine T-403) was prepared and held for one half hour before dilution in acetone to form a sizing solution. Fiber sizing was carried out using a pre-impregnation machine. An ElectroScan Environmental Scanning Electronic Microscopy (ESEM) was used to investigate the uniformity of the sizing. Thermal Gravimetric Analysis (TGA) was used to measure the thickness of the sizing. A digitally controlled, programmable oven is used for specimen curing to make sure all the samples were processed in the same way. Figure 5.3 is the catalyst formulation and the time-temperature schedule for the cure process used in this chapter. Adhesion was evaluated as an interfacial shear stress (IFSS) measured with a micro-indentation system, Interfacial Testing System (ITS). Nano-indentation and nano-scratch techniques were used to profile the gradient of the sizing/matrix interphase.

Figure 5.2 Molecular Structures for the chemicals used in this chapter

D411-C50 CURE FORMULATION

CATALYSTS	D411-C50	
CHP-5	2.00%	
CoNap	0.30%	
DMA	0.10%	

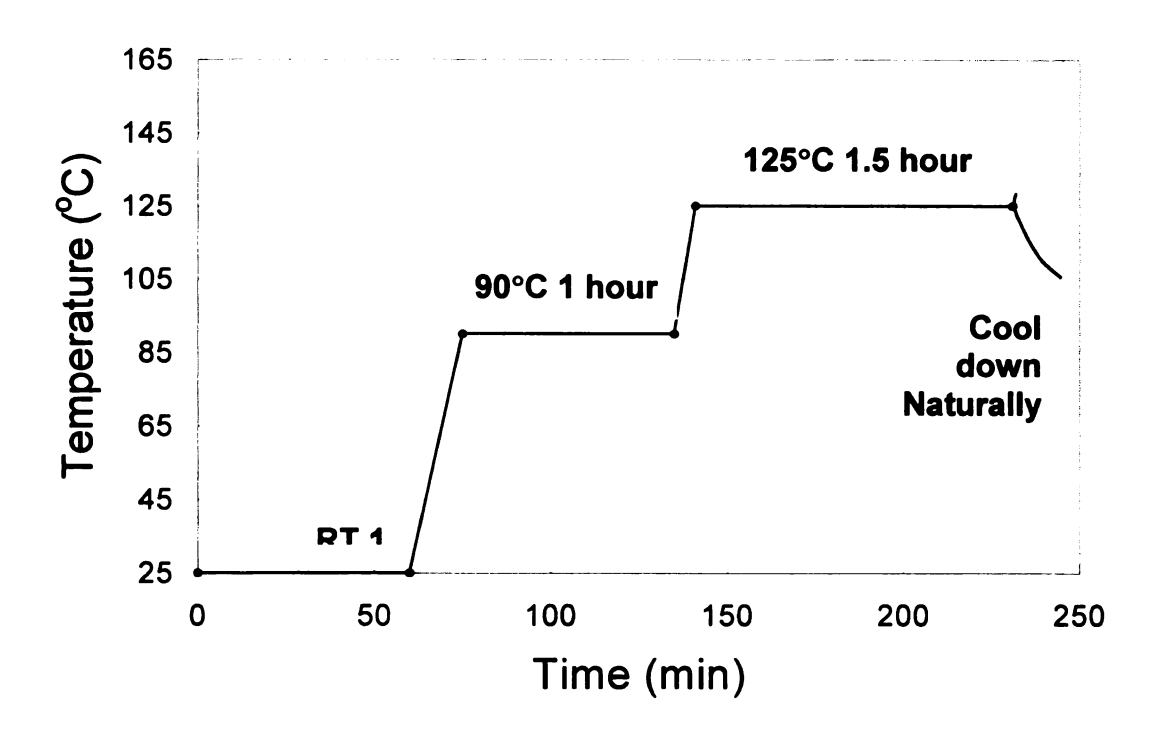


Figure 5.3 Cure formulation and cure process

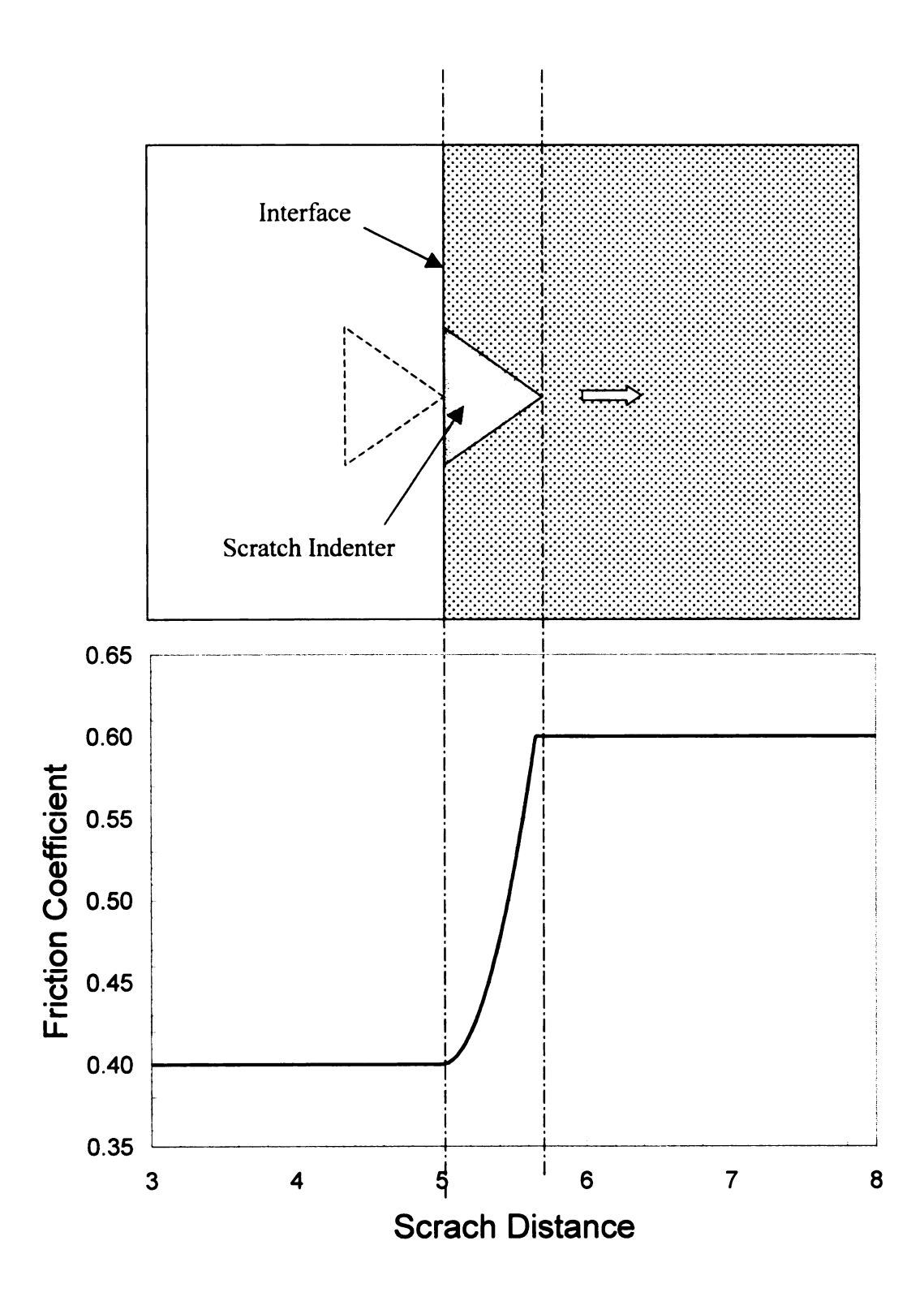


Figure 5.4 The effect of the tip size to an interface with infinitesimal wideness

Effect of Indentation Tip Size of the Nano-Indentation Scratch Test: As shown in Figure 5.4, the indenter size can create an artifact by enlarging an infinitesimally small interface formed when the sizing meets the vinyl ester matrix. The interface line will be a region in the measured value of the coefficient of friction in the scratch test. As shown in the figure, the region can be identified when the indenter begins to make contact with the interface and ends when the indenter is totally out of the interface. The indenter size depends on the depth of the scratch. The depth is determined by the hardness of the test material and the vertical load applied during the scratch experiment. The role of the scratch tip size and depth was compensated through the use of a C++ program simulation, refer Appendix II. The calculation was based on some reasonable assumptions and allowed for a more quantifiable determination of the interphase region compensating for the shape of the indenter.

Finite element analysis: A two-dimensional axisymmetric finite element model which utilizes a two-dimensional scheme was set up based on a four phase cylinder model as shown in Figure 5.5. The boundary condition between the fiber and the indenter is contact which brought nonlinearities to this model. Other boundaries such as the boundary between fiber and interphase, the boundary between interphase and matrix, and the boundary between matrix and composite were all set to be continuous which assumed perfect bonds between the two neighbor materials.

All the materials used in the model were assumed to be homogeneous isotropic, linear elastic material which is rarely the real case. No residual stresses were considered. The width and length of the 2-dimensional model is $20\mu m$ and $100\mu m$ respectively. Fiber diameter, d_f , was an input number measured from the ITS test. The interphase was divided into 8 layers. The thickness of the interphase is $8\times0.02\mu m=0.16\mu m$. For

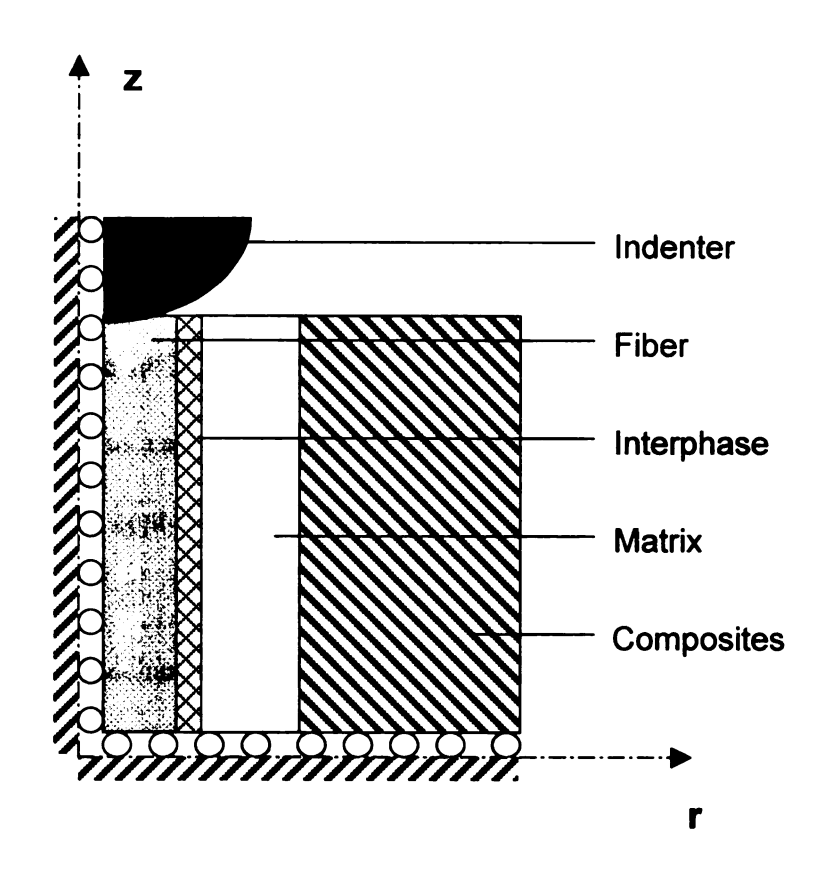


Figure 5.5 Four-phase model (drawing not to the scale) for finite element analysis

interphase thickness equals to 0.02 µm, one layer of the interphase materials properties were set to be the same as DGEBA epoxy. The other seven layers were set to be the same properties as vinyl ester. A similar set of boundary conditions was also used for interphase thicknesses equal to 0.1 µm, five layers of the interphase materials properties were set to be the same as DGEBA epoxy while the other three layers were set to be the same properties as vinyl ester.

According to Ho and Drzal^[12-14], the ITS empirical equation agrees well with the nonlinear finite element method in deriving the maximum interfacial shear stress as the interfacial shear strength when the fiber volume fraction=30~50%. The best agreement can be obtained V_f =36%. Neglect the interphase, Figure 5.3, $\pi a^2 / \pi (a+b)^2$ =0.36, then a/(a+b)=0.6, because a=7/2, then a+b=11.667/2. Thickness of the matrix=b=2.33 μ m. Matrix thickness also can be determined by the fiber arrangement type and volume fraction of the fiber content of the composite. The width of the composite is (20-2.33-0.16- d_f)/2.

The material mechanical properties used in the models are listed in Table 1. Composite properties were calculated base on the "rule of mixture" of a transversely isotropic composite from Chamis ^[15]. The models were meshed using IDEAS. Axisymmetric four-node elements were used. The boundary conditions were set up using IDEAS. Contact loading and calculation were carried out using ABAQUS.

	Fiber	Interphase	Matrix	Composite
Tensile Modulus, E, (GPa)	241	2.1	3.38	85
Shear Modulus, G, (GPa)	96.5	0.92	1.24	32
Poisson Ratio, v	0.250	0.356	0.356	0.318

Table 5.1 Materials Mechanical Properties for Finite Element Model

5.3 RESULTS AND DISCUSSIONS

5.3.1 The Thickness of Sizing can be Controlled by the Concentration of Sizing Solution

Fibers were sized with a pre-impregnation machine. The machine was set to Tension at 0.6, Drum carriage at 25 and Rotation at 15. A stoichiometric mixture of Diglycidyl Ether of Bisphenol A (DGEBA) and Aliphatic Polyether Triamine (Jeffamine T403) was mixed and left standing for 30 minutes, before adding acetone to form the sizing solution. Fiber tows were immersed and pulled through a bath containing the sizing solution and then dried at room temperature for 24hours. The fiber tows with totally dried DGEBA-T403 sizing materials were cut into 6 inch pieces and sealed in glass tube to keep the sizing from deteriorating with storage. The thickness of fiber sizing was calculated from the weight loss measured by TGA which was an average value of the sizing thickness. The sizing thickness was linearly related to the concentration of the DGEBA-T403/Actone sizing solution as shown in Figure 5.6. The thickness of sizing can also be influenced by the tension of the fiber tow during process and the rotation speed and the carriage speed of the drum as well.

The uniformity of the sizing was investigated by Environmental Scanning Electron Microscope (ESEM). ESEM examination of the sized fibers shows that the sizing material was distributed unevenly as shown in Figure 5.7. From the ESEM observation, the 5% sizing solution sized fiber gives the most uniform coating. For the 1% sizing

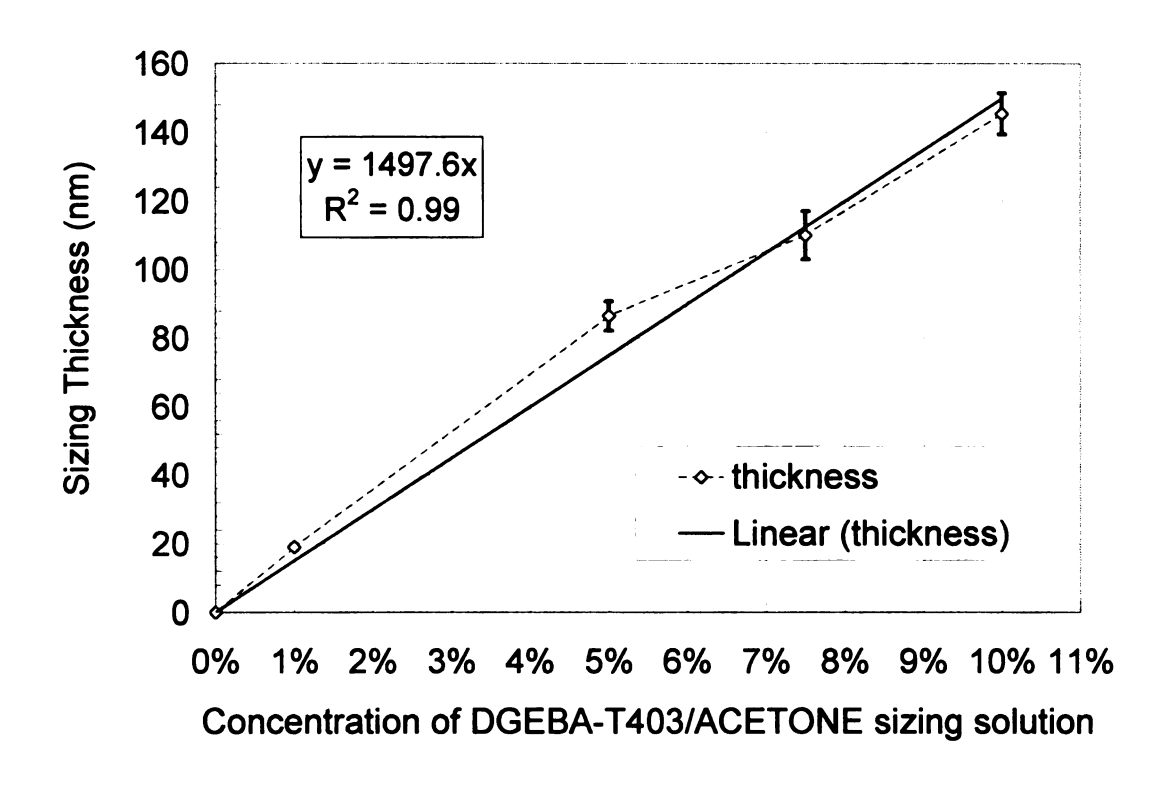


Figure 5.6 The sizing thickness versus the concentration of sizing solution

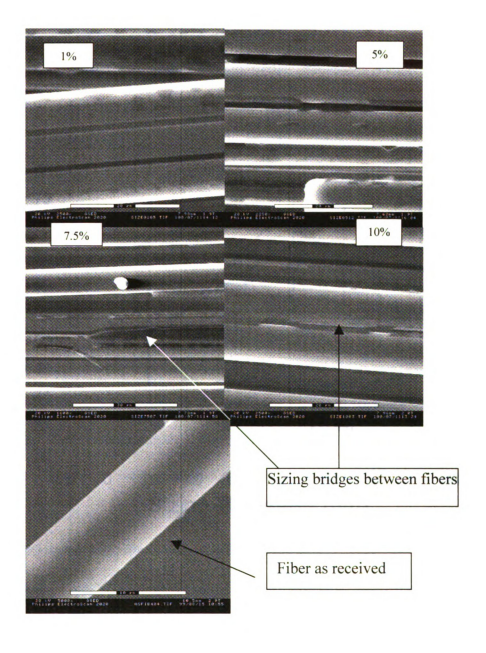


Figure 5.7 Sizing Quality Assessed with Environmental Scanning Electron Microscope (ESEM)

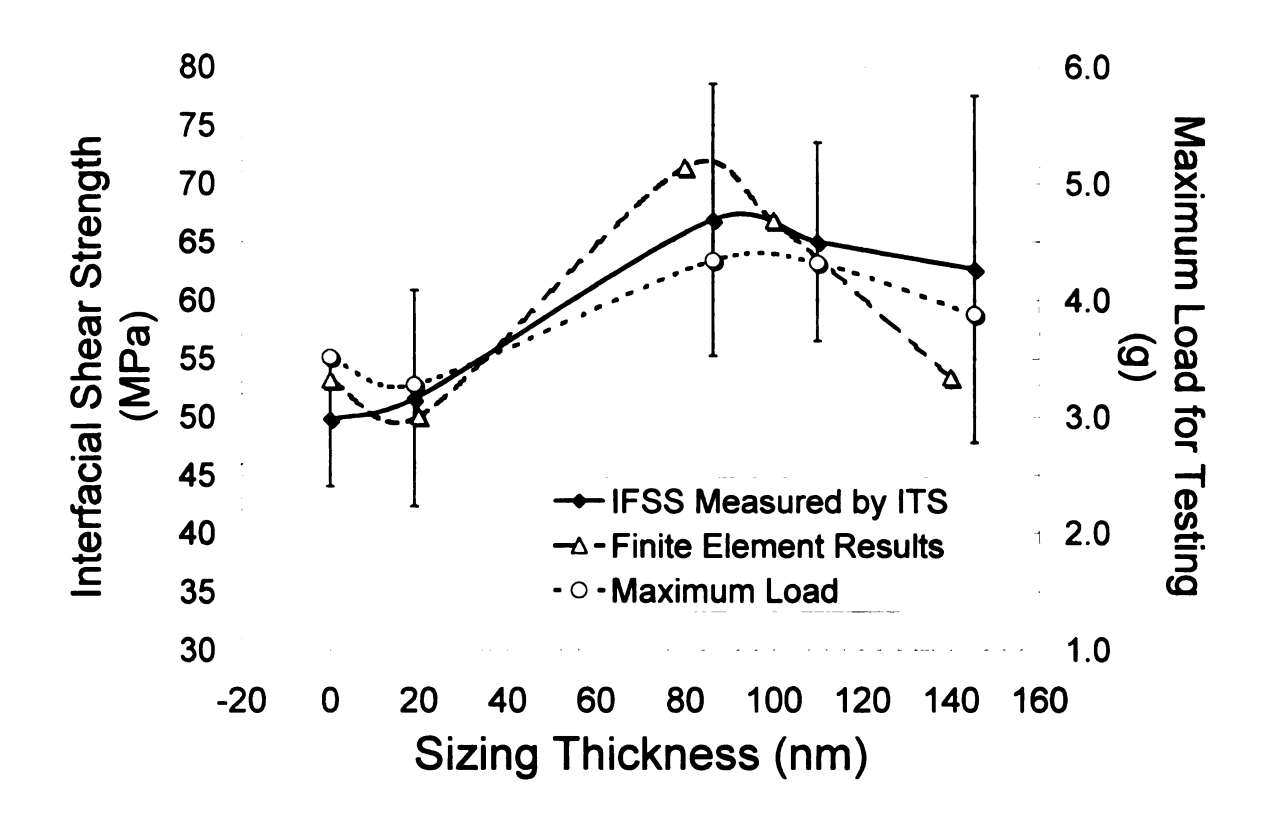


Figure 5.8 The interfacial shear strength (IFSS) related to the sizing thickness

solution sized fibers, the fiber surface was not totally covered by the sizing material even through the calculation based on TGA data tells that the sizing thickness is 20nm. The sizing could not be sufficient when sized with a sizing solution of 1% concentration. This might indicate that the sizing material, which is slightly cross-linked, stays at the fiber surface with a thickness of more than 20nm after drying. The sizing applied from the 7.5% and 10% sizing solution created fibers which have "sizing bridges" between them. There is no other detectable topographic phenomenon between the different sizing solution sized fibers except the so-called "sizing bridges".

5.3.2 Improvement of carbon fiber/vinyl ester adhesion with DGEBA sizing and the optimum sizing thickness for the best Interfacial Shear Strength (IFSS)

Test data form Interfacial Testing System (ITS) showed that with Diglycidyl Ether of Bisphenol A (DGEBA)/ Aliphatic Polyether Triamine (Jeffamine T403) epoxy sizing, the Interfacial Shear Strengths (IFSS) increased up to 34.3%, Figure 5.8. ITS tests also showed that fibers with sizing thickness around 90nm give the maximum value of IFSS. The IFSS of fiber with 90nm sizing thickness increased 30% when compared with that of fibers without sizing. The IFSS value had little increase after the sizing thickness greater than 100nm considering the error bars. The finite element model was a simulation of the real ITS test. The load was applied on the fiber as a point contact as the indenter did in the real test. The load was the maximum shown in Figure 5.8 with respect to the thickness of sizing. The results of the finite element model was compatible to the results of the ITS tests for maximum IFSS. The IFSS decreases when the sizing thickness is

greater than 100nm. This is because the input moduli of the pure epoxy sizing material layers are only 2.1GPa. Comparing with modulus of 3.38GPa of vinyl ester matrices, the epoxy interphase in the model by itself is softer than the matrix material. Therefore, it is reasonable that as the sizing becomes thicker, its influence increases. Too much sizing makes the IFSS decrease in the finite element analysis which neglects inter-diffusion between the fiber sizing and matrix resin. In the real case, the interphase formed with vinyl ester inter-diffusing with the epoxy sizing is stronger than the pure epoxy sizing material itself. The experimental data indicate that a 5% sizing solution can provide sufficient sizing material on the fiber surface to form strong bonding between the fibers and sizing material.

5.3.3 The Role Of DGEBA Sizing Material Between Carbon Fiber And Vinyl Ester

The previous discussions show that the fiber sizing creates a beneficial interphase between the carbon fiber and vinyl ester resin matrix resulting in a substantial increase in fiber-matrix adhesion regardless of the magnitude of the matrix cure shrinkage. As discussed in chapter 2.1, the AS-type carbon fibers receive an electrochemical oxidation surface treatment during production which has been reported to promote adhesion to epoxy matrix materials through a two-step mechanism [16.17]. Firstly, the treatments remove a weak out fiber layer initially present on the fiber. Secondly, surface chemical groups are added which increase the interaction with the epoxy. XPS investigation was carried out by Weitzsacker and etc. which monitored the oxygen/carbon and nitrogen/carbon ratio [16.17]. The changes in the O/C and N/C ratio indicated that

The reaction groups are joined by the same kind of lines. The respective products of the reactions are shoed at the end of the respective kind of arrows

Figure 5.9 Potential chemical reactions between carbon fiber surface and epoxy/amine system

reactions between the epoxy and carbon fiber surface had occurred. As mentioned in chapter 2.1, the carbon fiber surface chemistry includes hydroxyl, carbonyl and carboxyl functional groups; however not all of these functional groups react with either the epoxy or the amine. Figure 5.9 illustrates possible reactions between carbon fiber surface and epoxy/amine compounds. Comparing the chemistry of vinyl ester with amine-cured epoxy, the amine-cured epoxy sizing material has a greater possibility of forming a chemical bond with the carbon fiber surface. Previous studies have found that as little as 3% of chemical bonding accounts for a 25% increase in the Interfacial Shear Stress (IFSS) [18]

Derekane 411 vinyl ester is made from Diglycidyl Ether of Bisphenol A (DGEBA) epoxy. According to the rule of miscibility, two materials with similar chemistry should be compatible. Investigations had been carried out to profile the interphase between DGEBA and D411-C50 [19,20] and determine the extent of miscibility. An interphase specimen was made by fabricating a 2 layered specimen consisting of a DGEBA-T403 layer made from sizing solution coupled to a layer of D411-C50 resin mixed with its catalysts. The specimen was cured after both components were brought into contact, and then cured according to standard process. In Figure 5.10, nanoindentation tests were conducted from the DGEBA-T403 side to the D411-C50 side of the interphase. For test #1, 40 indents, tilt 25°, spacing 20μm and test #2 was 30 indents, tilt 45°, spacing 10μm. Elastic moduli calculated from the indentation release curve are shown in Fig.14, where. Distance 0 is about the location of the interphase. It was interesting to see that the value of the moduli in the interphase region was a value between those of the DGEBA and D411 bulk materials. Test #1 gave very consist moduli for both the DGEBA and the

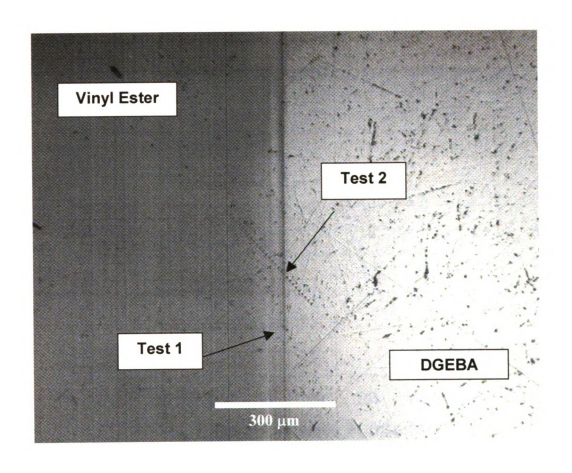


Figure 5.10 Nano-indentation test

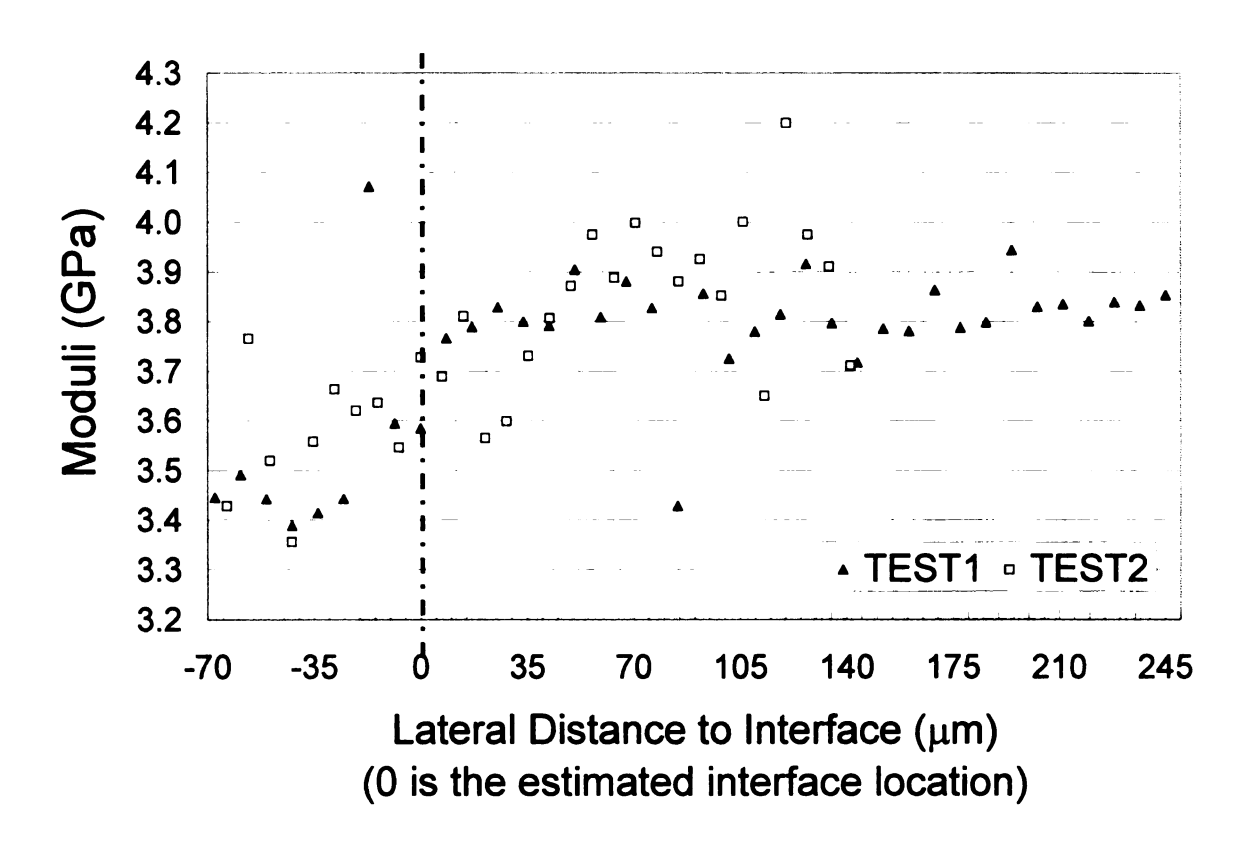


Figure 5.11 Nano-indentation results for the DGEBA/Vinyl ester interphase

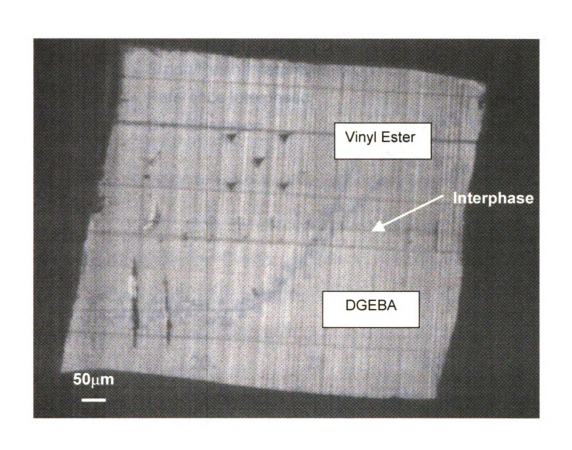


Figure 5.12 Nano-scratch test traces for vinyl ester/DGEBA interphase

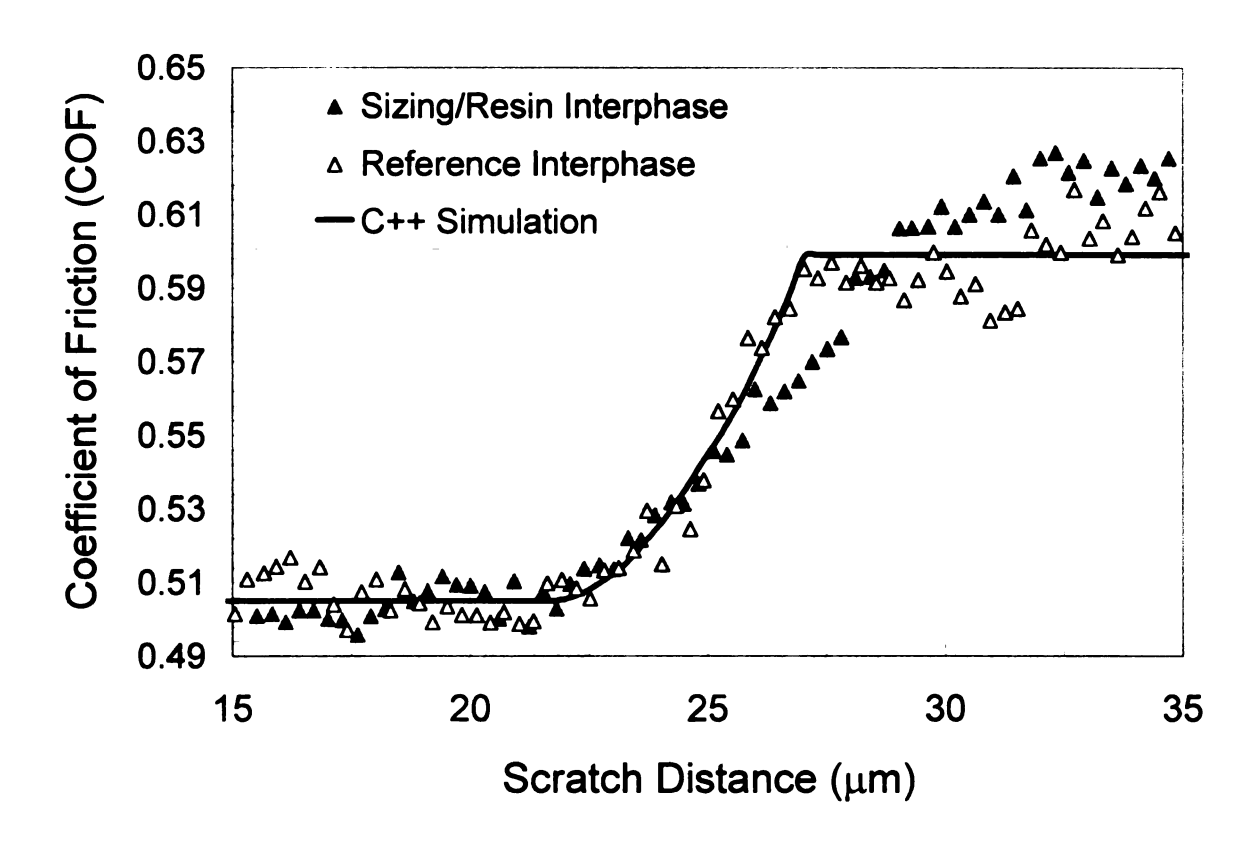


Figure 5.13 Comparison of the nano-scratch data between DGEBA sizing/vinyl ester interphase and reference interphase

D411 side, about 3.45GPa and 3.8GPa respectively. The scatter in measured values of test #2 was greater because of the stress field overlap caused by the plastic deformations of the resins after indentation. This was because the spaces between each indentation were too small compared with the tip size of the indenter in test #2. To avoid the overlap of the stress field during the nanoindentation test, the nano-scratch technique was used.

Unlike the nano-indentation test, the nano-scratch test gives continuous information using an index called the coefficient of friction (COF) between the material of the indenter and that of the scratched materials. According to the published literature for nano-scratch experiments conducted with polymers, when the same diamond scratch tip is used, the harder substrate material produces a lower COF. A reference interphase sample with no inter-diffusion was fabricated from the sizing solution after complete oven drying. The vinyl ester resin was poured on this hardened layer and cured. The scratch trace and scratch data were shown in Figure 12 and Figure 13. The sample surfaces were microtoned with a diamond knife to avoid the introduction of artifacts as a result of polishing. The scratch distance is 50 µm, the scratch depth is around 700nm. The scratch data were related to the tip size as mentioned in the Experimental Methods Section and the tip size is related to the depth of scratch. For Figure 5.13, the line is the representation of the effect of the tip size, the open triangles are the COF for the reference interphase which was assumed to be quite narrow. The solid triangles are the COF of the sizing /matrix interphase. The COF of the reference interphase was consistent with the simulation line. It was very clear that the width of sizing/matrix interphase was much larger than that of the reference interphase, with additional data showing that the width could be $0.5\sim1.5 \mu m$.

Summarizing the discussion presented above, it could be concluded that the epoxy sizing material provided both more chemical bonding opportunities to the fiber surface as well as becoming a suitable interphase allowing inter-diffusion of the monomers in vinyl ester resin. Comparing the IFSS value from micro-indentation and finite element simulation of the micro-indentation process, a stronger interphase has been formed with the inter-diffusion between epoxy sizing and vinyl ester matrix resin in the real composites. This situation could be described as illustrated in Figure 5.14. Let, t=0 be the time the fiber emerged in the resin and $t=\infty$ represent the final composite material. The interphase formed between the carbon fiber and vinyl ester with epoxy fiber sizing would form chemical bonds between carbon fiber and epoxy sizing and interpenetrating networks between the epoxy sizing and vinyl ester matrix resin.

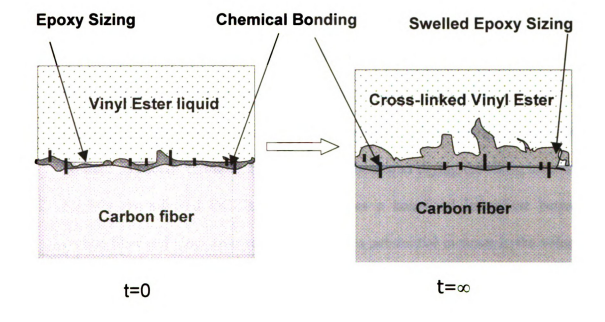


Figure 5.14 Model for the interphase between carbon fiber and vinyl ester resin with epoxy sizing

5.4 CONCLUSIONS

The application of a slightly cross-linked epoxy-amine polymer as a sizing on the carbon fiber surface has been found to be an effective way to increase the adhesion between carbon fiber and vinyl ester resin. The interfacial shear stress measured by microindentation increases up to 34%. From this study the following conclusions can be made:

- 1. The sizing thickness on the carbon fiber surface can be controlled by the concentration of sizing solution. The sizing material was unevenly distributed on the fiber surface after dry. 5wt% of DGEBA-T403 could provide sufficient sizing material on the AS4 carbon fiber surface to form strong bonding between the fibers and sizing material, in this case when the fiber diameter is 7~8 μm. Too much sizing material or to high of a concentration of the sizing solution could produce so called "sizing bridges" between fibers after drying the sizing material.
- Slightly cross-linked DGEBA-T403 provides a beneficial interphase between carbon fiber and vinyl ester resin resulting in a substantial increase in the value of interfacial shear strength, more than 30%. The optimum sizing thickness is 90~100nm.
- 3. Finite element analysis results are compatible with the micro-indentation result. The maximum value of IFSS is attained when the sizing thickness is about 90~100nm. When the thickness is larger than this value, the modulus of the pure epoxy sizing material is lower than the vinyl ester matrix material. The IFSS

decreases as the modulus of the matrix I the interphase decreases. The interdiffusion between DGEBA sizing material and vinyl ester could bring an interphase which is stronger than the epoxy sizing material itself.

4. DGEBA epoxy sizing provides a beneficial interphase between the carbon fiber and vinyl ester resin. First of all it provides more possibilities to form chemical bonds between the composite matrix resin and the surface of the carbon fiber reinforcement. Second, the epoxy vinyl ester was made from DGEBA epoxy which should be compatible with the DGEBA sizing material. Third styrene monomers are very small which could penetrate the slightly cross-linked epoxy sizing material. Nano-scratch measurement found that the inter-diffusion distance could be up to 1.5 microns. The optimum sizing thickness is 90~100nm. Nano-indentation and nano-indentation scratch tests have been helpful in determining the interphase profile.

5.5 REFERENCES

- 1. D. Hoyns, and L.T. Drzal, "Hydrothermomechanical Response and Surface Treated and Sized Carbon Fiber/Vinyl Ester Composites", ASTM Symposium on the Fiber Matrix and Interface Properties, 1994
- 2. S. M. Corbin, M.S. Thesis, Department of Chemical Engineering, Michigan State University, 1998
- 3. V. Rao and L. T. Drzal, **Polym Compos**, Vol. 12, No. 48, 1991
- 4. L. H. Peebles, Carbon Fibers, CRC Press, Boca Raton, 1990
- 5. T.H. Yoon, H. M. Kang, M. Bump, and J. S. Riffle, "Effect of solubility and miscibility on the adhesion behavior of polymer-coated carbon fibers with vinyl esterresins", J. App. Poly. Sci. (USA), vol. 79, no. 6, pp. 1042-1053, 2001
- 6. Kim, I.C., Yoon, T.-H., "Enhanced interfacial adhesion of carbon fibers to vinyl ester resin using poly(arylene ether phosphine oxide) coatings as adhesion promoters", Journal of Adhesion Science and Technology (Netherlands), vol. 14, no. 4, pp. 545-559, Feb. 2000
- 7. Derakane 411-45 (Vinyl Ester Resin), Alloy Digest (USA), pp. 2, Aug. 1991
- 8. M. J. Reis, M. J., M. Botelho Do Rego, and J. D. Lopes Da Silva, **J. Mater.Sci.**, Vol. 30, No. 118, 1995
- 9. M. J. Rich, S. Corbin, and L. T. Drzal, "Adhesion of carbon fibers to vinyl ester matrices", Proceedings of the 12th International Conference of Composite Materials, 1999
- 10. L. Xu, L. T. Drzal, "Influence of interphase chemistry on the adhesion between vinyl ester resin and carbon fibers", Proceedings of the 23rd Annual Meeting of "Adhesion Science for the 21st Century", 2000
- 11. Zoltek Corp., St. Louis MO.
- 12. H. Ho and L. T. Drzal, "Non-linear Numerical Study of the Single-Fiber Fragmentation Test, Part I: Test Mechanics", Composites Engineering, 5, No. 10-11, 1231-1244, 1995
- 13. H. Ho and L. T. Drzal, "Non-linear Numerical Study of the Single-Fiber Fragmentation Test, Part II: A Parametric Study", Composites Engineering, 5, No. 10-11, 1245-1259, 1995

- 14. H. Ho and L. T. Drzal, "Evaluation of Interfacial Mechanical Properties of Fiber Reinforced Composites Using the Microindentation Method", accepted for publication in Composites, Part A, 1998
- 15. C. C. Chamis, **NASA Tech. Memo. 83320**, 1983
- 16. L. T. Drzal, M. Rich, M. Koenigand and P. Lloyd, "Adhesion of Graphite Fibers to Epoxy Matrices. II. The Effect of Fiber Finish", J. Adhesion, 16, 133-152, 1983
- 17. L. T. Drzal, M. Richard and M. Koenig, "Moisture Induced Interfacial Effects on Graphite Fiber-Epoxy Interfacial Shear Strength", Paper 4-G, 38th Annual Technical Conference, Reinforced Plastic/Composites Institute, SPI, 1983
- 18. L. T. Drzal, N. Sugiura and D. Hook, "Effect of interfacial chemical bonding and surface topography on adhesion in carbon fiber/epoxy composites", Proceedings of the 10th Annual Meeting of the American Society for Composites, 1994
- 19. L. Xu, L. T. Drzal, A. Al-Ostas, , and R. Schalek, "Improvement Of Adhesion Between Vinyl Ester Resin and Carbon Fibers by A Controlled and Designed Interphase", Proceeding of the 2002 Adhesion Society/WCARP-II Meeting, 2002
- 20. L. Xu, T. Mase, and L. T. Drzal, "Influence Of Matrix Cure Volume Shrinkage on the Adhesion between Vinyl Ester and Cardon Fiber", Proceedings of the 14th International Conference for Composite Materials, 2003

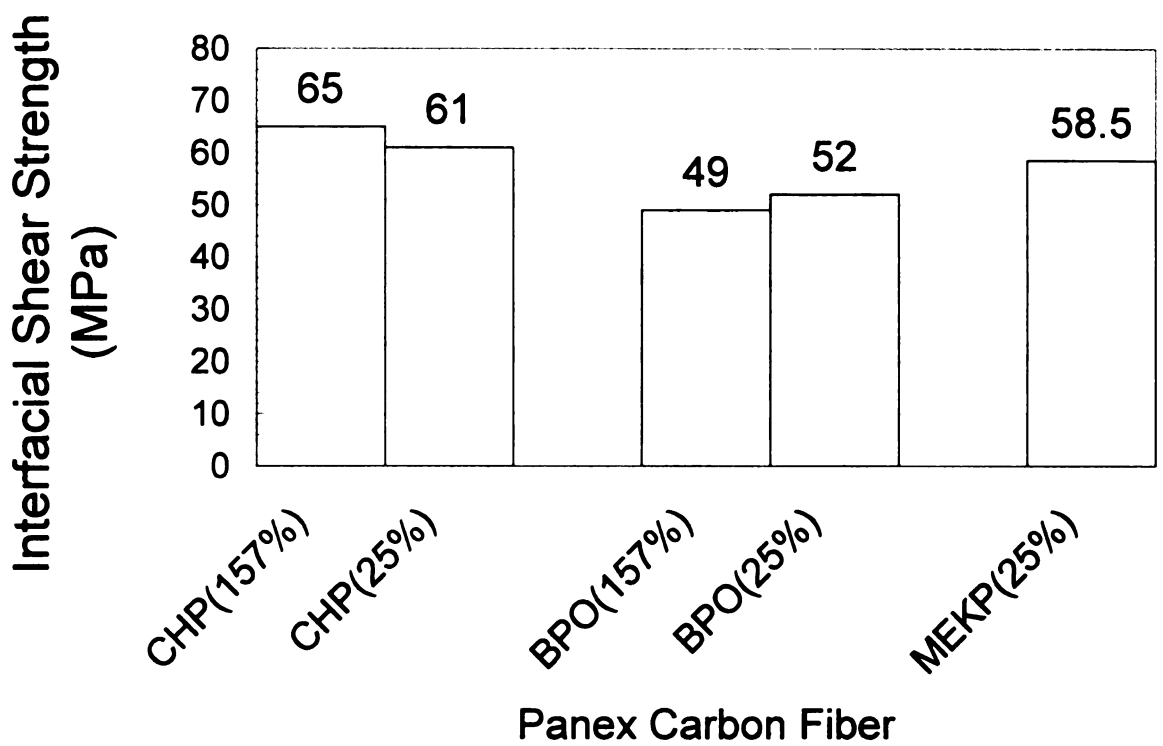
CHAPTER 6

INFLUENCE OF THE COMPONENT CHEMISTRY ON THE ADHESION BETWEEN VINYL ESTER AND CARBON FIBER

Understanding the mechanism of adhesion between carbon fiber and vinyl ester is critical important to tailoring structurally efficient composites. Typical vinyl ester resins contain 35-50% styrene as reactive diluents which could potentially be separated from the matrix resin at the fiber/matrix interphase [1-4]. Cure catalysts of vinyl ester system were found to be adsorbed on the carbon fiber surface [5] which could significantly change both the chemistry and the mechanical properties of the fiber/matrix interphase. As discussed in CHAPER 5, slightly cross-linked epoxy sizing, Diglycidyl Ether of Bisphenol A (DGEBA) epoxy cured with Aliphatic Polyether Triamine (Jeffamine T403) amine, provides a benefit interphase between carbon fiber and vinyl ester resin and the optimum sizing thickness is 90~100nm. Using epoxy fiber sizing to isolate the carbon fiber surface from the vinyl eater resin, the effect of the vinyl ester, styrene and catalysts on the adhesion between AS4 carbon fiber and DERAKANE 411-C50 vinyl ester was investigated in this chapter. It was found that that the adsorption of the promoter and accelerator on the carbon fiber surface does not substantially affect the fiber/matrix adhesion. Optimum fiber-matrix adhesion can be obtained by properly selecting initiator and adjusting the amount of initiator. It was also concluded that application of a lightly cross-linked amine-cured epoxy polymer to the carbon fiber surface creates a beneficial interphase between the carbon fiber and vinyl ester resin matrix resulting in a substantial increase in fiber-matrix adhesion. The vinyl ester and styrene components interact differently with the DGEBA-T403 sizing at the carbon fiber and vinyl ester interphase.

6.1 INTRODUCTION

Typical vinyl ester resins contain 35-50% styrene as reactive diluents. The copolymerization between styrene and vinyl ester is a heterogeneous, free radical, chaingrowth, and cross-linking reactions. Corbin found that among the three initiators, methyl ethyl ketone peroxide (MEKP), cumene hydroperoxide (CHP), and benzoyl peroxide (BPO), CHP provided the best result for the Panex carbon fiber/Derekane 411-C50 vinyl ester adhesion ^[6], shown in Figure 6.1. Previous research by Weitzsacker, Drzal et al. ^[5] have investigated the reactions of the catalyst and/or promoters to determine if they were competing with the vinyl ester matrix resin for reactive sites at the carbon fiber surface. Cobalt was detected at 2.6% at the surface of the AS4 carbon fiber exposed to cobalt naphthenate (CoNap) and a minor change was also noted in the surface chemistry of the fiber exposed to dimethyl aniline (DMA) which are the promoters and accelerators for the free radical copolymerization respectively. The adsorption of catalysts on the carbon fiber surface could induce two conditions: 1). The matrix material could be offstoichiometric that could affect the mechanical properties of the material; further more affect the strength of the interphase. Because different amount of initiators, promoters and accelerators produce different heats of reaction, crosslink density and degrees of microgel formation and/or phase separation [1-4] as well as a different interphase microstructure between the fibers and the matrix. 2). The adsorption of the catalysts ions on the carbon fiber surface normally would occupy the reactive sites of the carbon fiber surface; carbon fiber surface would be less reactive site after adsorption which could reduce the amount of chemical bonding between carbon fiber and vinyl ester resin. It was reported that even as little as 3% of chemical bonding accounts for a 25% increase in the Interfacial Shear Stress (IFSS) [7] Since removal of even a small amount of the initiator or promoter from the vinyl ester to the carbon fiber surface has the potential to greatly affect the polymerization reaction, one strategy is to prevent these constituents from getting to the fiber surface by applying a 'coating' or 'sizing' to isolate the fiber surface from the vinyl ester and cure catalysts. As discussed in CHAPTER 5, it was found that that the application of a lightly cross-linked epoxy polymer, Diglycidyl Ether of Bisphenol A (DGEBA) epoxy cured with Aliphatic Polyether Triamine (Jeffamine T403) onto the carbon fiber surface provides a beneficial interphase between the carbon fiber and vinyl ester resin matrix resulting in an increase in fiber-matrix adhesion while at the same time preventing the fiber from adsorbing the initiator and catalyst [6, 8-10]. The optimum sizing thickness was found to be 90~100nm when 5% DGEBA-T403/Acetone sizing solution was used for the sizing process [9]. Another issue in this study is the wetting condition of the vinyl ester at the carbon fiber surface. As mentioned above, typical vinyl esters use styrene as the reactive dilute. Compared with pure vinyl ester resin, pure styrene monomer has a lower surface energy that would be preferred by the carbon fiber surface. A rich styrene layer potentially formed on the carbon fiber surface



Panex Carbon Fiber (the percentages are the levels of surface treatment)

Figure 6.1 Comparison of the interfacial shear strength between Panex carbon fiber/Derekane 411-C50 vinyl ester adhesion with different initiator

of a cured composite could be one of the reasons that lower the fiber/matrix adhesion. Using DGEBA-T403 epoxy fiber sizing to isolate the fibers from the matrices, the effect of the reaction catalyst and the vinyl ester and styrene, have been investigated and are reported in this research.

6.2 EXPERIEMTAL MATERIALS AND METHODS

Materials: the fiber is an AS4 carbon fiber from Hexcel, Inc. It is a type A, surface treated (S), PAN based carbon fiber. The fiber tow size is 12K filaments. The matrix resin is Derakane 411-C50 vinyl ester resin from Dow Chemical which contain 50wt% of Bisphenol A Epoxy-based Vinyl Ester and 50wt% of Styrene. CHP-5 (diluted cumene hydroperoxide (CHP)) from Witco Chemical is used as the initiator because it provided the best IFSS among the three initiators, CHP, MEKP (methyl ethyl ketone peroxide) and BPO (butanone peroxide). Both CoNap and DMA are from Aldrich Chemicals which are used as promoters and accelerators respectively. Diglycidyl ether of bisphenol A (DGEBA or Epon828) and Aliphatic Polyether Triamine (JEFFAMINE T403) are from Shell and Huntsman respectively. Pure styrene monomer and pure bisphenol A epoxy based vinyl ester were kindly donated by Huntsman and Reichhold respectively.

Methods: a digitally controlled, programmable oven was used for specimen curing to make sure all the samples were processed in the same way, refer Figure 5.3 for the time-temperature schedule. Dynamic Mechanical Thermal Analysis (DMTA), DMA 2980 from TA Instruments, and physical testing, United Testing System (UTS), of the

composite samples was conducted to measure the mechanical properties of the matrix resin formulations. Adhesion was evaluated as an interfacial shear stress (IFSS) measured with a microindentation system. Interfacial Testing System (ITS) apparatus was used for microindentation measurement to measure the interfacial shear stress (IFSS). A thorough discussion of the apparatus and the empirical equations for calculation of IFSS are included in CHAPTER 4. The nanoindentation technique was used to test the mechanical property of materials.

Controlled and Designed Interphase: as discussed previously, a lightly crosslinked DGEBA epoxy sizing provides a beneficial interphase between the carbon fiber and vinyl ester resin. The optimum sizing thickness is 90~100nm corresponding to the thickness obtained when using a 5% concentration sizing solution. This 90~100nm thick of epoxy sizing on the fiber surface should completely coat the fiber surface with this slightly cross-linked epoxy. This epoxy coating would isolate the functional groups on the carbon fiber surface from contacting the vinyl ester matrix resin and its catalysts. It is also known that the epoxy sizing material provided more opportunities to form chemical bonds to the fiber surface. Furthermore, since the epoxy is only lightly crosslinked, the monomers in the vinyl ester resin can diffusion into the sizing material to form a stronger fiber/matrix interphase in the real composite material. The thickness of this interphase can be controlled by the properly selecting the concentration of sizing solution and the parameters of sizing processing pre-impregnation machines.

Sample Preparation: two kinds and three sets of each sample were made. The two kinds of samples refer to two kinds of fibers, one made from AS4 carbon fiber "as-received", named as "AS4", the other were made from a 5% sizing solution sized AS4 carbon fiber, named as "CAS4". The three sets refer to three sets of vinyl ester matrix cure recipes. Since it was shown that adsorption of the catalysts of the D411-C50 resin could take place on the carbon fiber surfaces, it was expected that the vinyl ester in the interphase region would not have the same stoichiometry as the bulk. Therefore, several offstoichiometric compositions were prepared and their physical properties were measured. The curing recipes are listed in Table 6.1. Data Set 1 refers to those samples cured with recipe 1-I, 1-II and 1-III which refers to a reduction in the concentration of CHP-5. Data Set 2, 2-I, 2-II and 2-III is a composition with a reduction in the amount of CoNap and Data set 3, 3-I, 3-II and 3-III with a reduction of DMA respectively. The IFSS between carbon fiber and D411-C50 with depletion of cure catalysts, corresponding to the recipe listed in Table 1 2-III (without CoNap, the promoter) and 3-III (without DMA, the accelerator), were also measured.

	I	II	III
	2.0%CHP-5	1.5%CHP-5	1.0%CHP-5
1	0.3%CoNap	0.3%CoNap	0.3%CoNap
	0.1%D M A	0.1%D M A	0.1%DMA
	2.0%CHP-5	2.0%CHP-5	2.0%CHP-5
2	0.2%CoNap	0.1%CoNap	
	0.1%D M A	0.1%DMA	0.1%DMA
	2.0%CHP-5	2.0%CHP-5	2.0%CHP-5
3	0.3%CoNap	0.3%CoNap	0.3%CoNap
	0.075%D M A	0.5%DMA	

Table 6.1 Cure formulations

6.3 RESULTS AND DISCUSSIONS

6.3.1 Influence Of The Catalyst Concentration On The Properties Of The Matrix

Material

The data plotted as vertical bars in Figure 6.2, Figure 6.3 and Figure 6.4 were the amounts of CHP-5, CoNap and DMA respectively, indicated by percentages, used in the various formulations. For an isotropic material, $G_m=E_m/[2(1+v)]$, where E_m is the Young's modulus and v is the Poisson ratio of the matrix material respectively. The Poisson ratio of each formulation was assumed to be 0.36 (refer to reference 6) and insensitive to the amount change of the CHP-5. The shear modulus and the Young's modulus then are related through the relationship $G_m=E_m/2.7$. Figure 6.2, Figure 6.3 and Figure 6.4 show that a small change of the catalyst could result in a detectable change in the glass transition temperature, but the change of the mechanical properties such as tensile modulus and storage modulus from DMTA measurement are rather small even in two extreme situations (no CoNap and no DMA), especially for the calculated shear modulus which is about 1/3 of the tensile modulus. Also the change of glass transition temperature is not proportional to the change of the mechanical properties. Equation 6.1 is the empirical equation for the calculation of the interfacial shear strength (IFSS) from Equation 6.1 was based on a finite element analysis and adjusted by the ITS. experimental data [11-12]. The change in the shear moduli, G_m, of the vinyl ester cured with different formulation was so small that it is assumed that the depletion of catalyst from the matrix material near the carbon fiber surface does not affect the mechanical

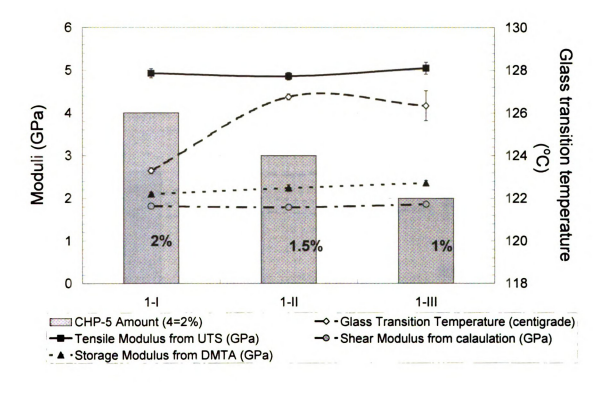


Figure 6.2 Influence of the amount of CHP-5 to the properties of cured D411-C50 resin

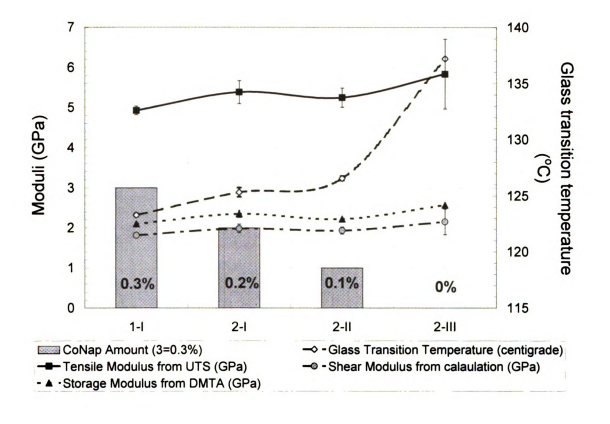


Figure 6.3 Influence of the amount of CoNap to the properties of cured D411-C50 resin

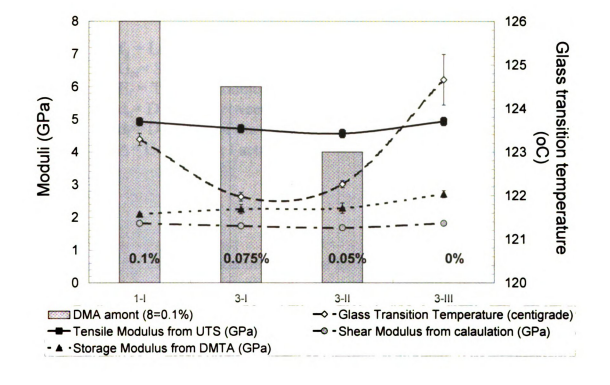


Figure 6.4 Influence of the amount of DMA to the properties of cured D411-C50 resin

property of the material. Any changes of the Interfacial Shear Strength (IFSS) are the result of change of the chemical or physical bonding between the fiber and the matrix, not the mechanical properties of the matrix resin.

$$IFSS = A \frac{f_g}{d_f^2} \left\{ 0.875696 \sqrt{\frac{G_m}{E_f}} - 0.018626 \ln(\frac{d_n}{d_f}) - 0.026496 \right\}$$

$$6.1^{[11-12]}$$

where,

 $f_g = Load$ on Fiber

G_m= Shear Modulus of Matrix

 E_f = Tensile Modulus of Fiber

d_n= Distance between the Nearest Fiber

d_f = Diameter of the Fiber

A= Conversion Factor

6.3.2 The effect of catalyst concentration on the Interfacial Shear Strength (IFSS)

As adsorption of catalysts on the carbon fiber surface was found. The adsorbed catalyst ions could compete for the reactive sites of the carbon fiber surface with the matrix polymer to reduce the amount of chemical bonding which could lower down the adhesion between fiber and matrix. It was found and previously reported that that 3% increase of chemical bonding could account for a 25% of increase of adhesion [7.13]. Since the sizing provided by 5wt% of DGEBA-T403/ACETONE sizing solution was effective at isolating the carbon fibers from contacting

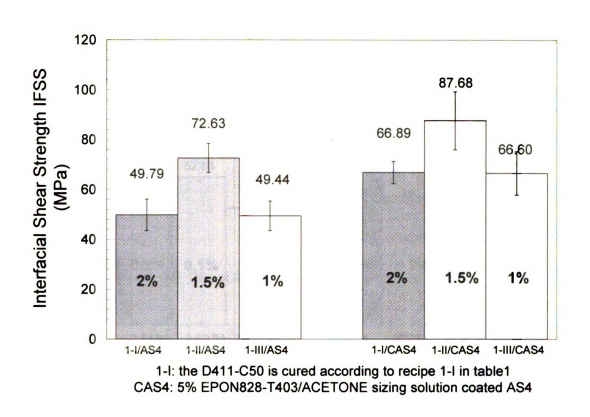
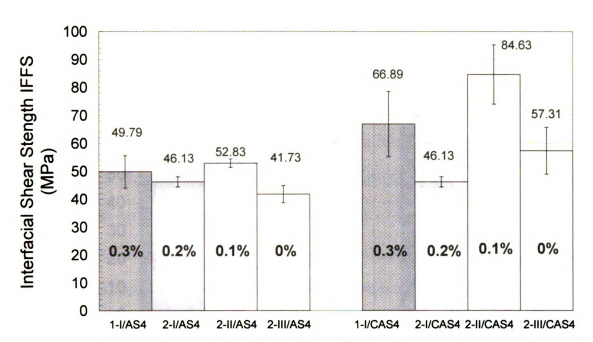
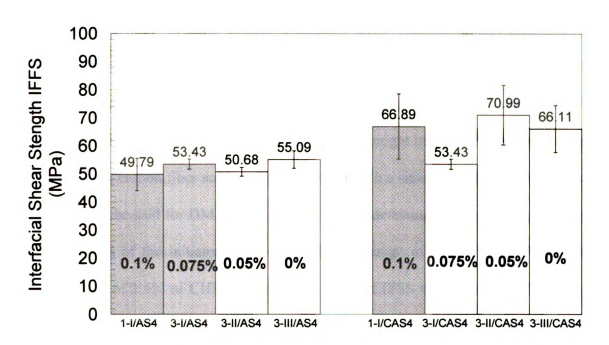


Figure 6.5 The influence of the amount of CHP-5 to the IFSS between D411-C50 and AS4/Coated AS4 fibers



CAS4: 5%EPON-T403/ACETONE sizing solution coated AS4 2-III: the D411-C50 is cure according to recipe 2-III in table 1

Figure 6.6 The influence of the amount of CoNap to the IFSS between D411-C50 and AS4/Coated AS4 fibers



CAS4: 5%EPON-T403/ACETONE sizing solution coated AS4 3-III: the D411-C50 is cured accroding to recipe 3-III in table 1

Figure 6.7 The influence of the amount of DMA to the IFSS between D411-C50 and AS4/Coated AS4 fibers

the vinyl ester and the catalysts. The sizing would prevent the carbon fiber from interacting chemically with the constituents of the vinyl ester matrix. The set of bars on the left side in these figures correspond to the samples made of 'as-received' fibers, indicated as AS4, and the data on the right side refer to fibers 'with epoxy sizing', indicated as CAS4, which were sized with the 5wt% of DGEBA-T403/ACETONE sizing solution. The percent numbers in Figure 6.5, Figure 6.6 and Figure 6.7 are the amounts of CHP-5, CoNap and DMA in each vinyl ester formulation respectively. The fibers with epoxy sizing overall produce greater interfacial shear strength (IFSS) than the 'asreceived' fibers. For 'as received' fibers, it is clear that the IFSS of the samples with different amount of CoNap and DMA are almost the same, even for those without CoNap and DMA, see Figure 6.6 and Figure 6.7. Figure 6.6 might indicate that although cobalt adsorbs on the carbon fiber surface, it does not result in a significant change in adhesion. The same can be said for DMA in Figure 6.7. It is interesting to see that slight changes in the amount of the initiator cause a significant change of IFSS (Figure 6.5). At a concentration of 1.5% of CHP-5, the greatest value of IFSS was measured. Changes in the initiator concentration are responsible for a change in the number of reactive species in the vinyl ester system. It appears that at a certain concentration, the vinyl ester copolymer has a microstructure (phase separation or micro-gel formation) which produces good adhesion.

6.3.3 The Contribution of Pure Vinyl Ester and Styrene Monomer of the D411-C50 Vinyl Ester Resin to the Adhesion

Further investigation has been carried out to find the roles that pure styrene and pure vinyl ester play in forming the interphase between AS4 carbon fiber and D411-C50 vinyl ester resin. New composite specimens were prepared with the AS4 carbon fibers in either pure vinyl ester or pure styrene where the catalyst concentration was adjusted to maintain the same double bond concentration based on the standard recipe, recipe 1-I, in table 1. As an input parameter for the ITS test, as shown in Equation 6.1, the shear moduli of both pure materials are critical to get the value number of interfacial shear strength (IFSS). Pure bisphenol A epoxy-based vinyl ester is a solid and styrene monomer has a very high vapor pressure which makes neither one very easy to process at room temperature. To obtain the in-situ mechanical properties, a nano-indentation test was used with the corresponding ITS sample. The nanoindentation testing area is far away from the fiber area to avoid other affects. Literature citations of mechanical properties (D411-C50 vinyl ester was provided by the manufacturer) are also used as references, Figure 6.8.

The ITS test results are very interesting, (Figure 6.9). The data on the left side in Fig.12 corresponds to samples made with 'as-received' fibers and the data on the right side are for fibers sized with DGEBA-T403/ACETONE sizing solution. Again, for 'as-received' fibers, there are slight IFSS differences between vinyl ester (~+20%), and styrene (~-10%) compared to the D411-C50 vinyl ester. Styrene gives the lowest IFSS

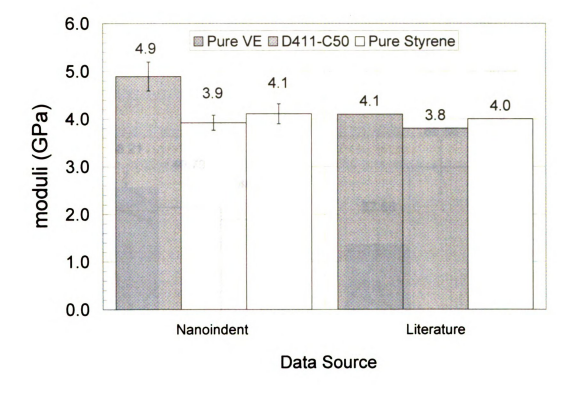


Figure 6.8 Moduli comparison between vinyl ester, D411-C50 and styrene

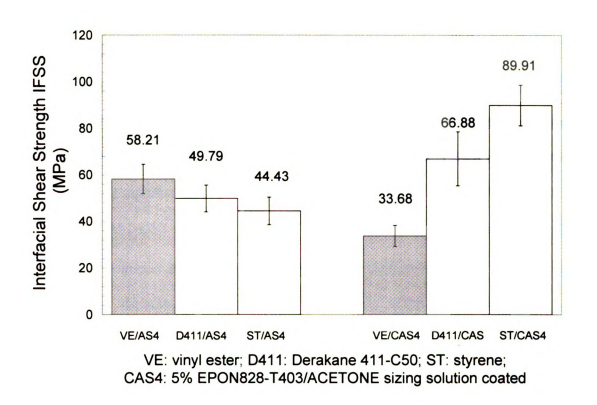


Figure 6.9 The IFSS of vinyl ester, D411-C50 and styrene with AS4 and coated AS4 fibers

because it is the softest material among these three. D411-C50 gives an IFSS value in between. As pure styrene resin has lower surface energy (compare with the surface energy of Benzene: 26.7mJ/m^{2[14]}) than pure bisphenol A epoxy-based vinyl ester (compare with the surface energy of epoxy resin: 40mJ/m^{2[15]}). Theoretically the carbon fiber surface would prefer styrene rather than bisphenol A epoxy-based vinyl ester. But the IFSS number above does not indicate that there is a styrene rich layer at the interphase between fiber and D411-C50 mixture. In contrast, the carbon fiber with the lightly cross-linked sizing has the highest adhesion in the pure styrene matrix. According to Rouse model ^[16] the overall mobility and diffusion coefficient D is proportional to M⁻¹ and the overall mobility and diffusion coefficient D is proportional to M⁻² according to Reptation Model ^[17]. This suggests that the styrene monomers (monomer molecular weight, M, is 104g/mole while vinyl ester is about 900g/mole) diffuse into lightly cross-linked DGEBA-T403 sizing and bring about a big change to the fiber/matrix interphase. It might create a stronger material; smoother gradient at the interphase compared to pure bisphenol A epoxy-based vinyl ester resin.

6.4 CONCLUSIONS

Derakane 411-C50 vinyl ester resin is a mixture of vinyl ester and styrene monomer, crosslinked by a free radical polymerization. The interface between this resin and AS4 carbon fiber is much more complex than that between epoxy and AS4 carbon fiber. From this study, several conclusions can be made.

- Slight change of catalyst concentration does not make a major difference in the
 mechanical properties of the cured D411-C50 resin. The glass transition
 temperatures of the cured resin appear to be influenced by the catalyst
 concentration. The glass transition temperature is not necessarily related to the
 mechanical properties of the materials for this system.
- 2. The adsorption of the catalysts, neither the promoter (CoNap) nor the accelerator (DMA) significantly influences the level of adhesion between AS4 carbon fiber and D411-C50 vinyl ester resin. Changes in the initiator (CHP-5) concentration cause changes in the polymerization of the vinyl ester system. Optimum fiber-matrix adhesion could be obtained by properly select the initiator and adjusting the amount of initiator.
- 3. A sizing selected for isolating the carbon fiber surface from the reacting polymer appears to be useful in improving adhesion. With DGEBA-T403 sizing, the interfacial shear strength between D411-C50 and AS4 carbon fiber can be increased indicating a strong interphase formed.
- 4. The contributions of styrene and vinyl ester in D411-C50 to the adhesion between the fiber and matrix are different especially for fibers with the lightly cross-linked

DGEBA-T403 sizing. The styrene monomers diffuse into the DGEBA-T403 sizing material and provide a much smoother interphase than only pure vinyl ester.

5. Neither the adsorption of catalysts on the carbon fiber surface nor the potential of phase separation between styrene monomers and vinyl ester molecules are the reasons of lower adhesion between carbon fiber and vinyl ester resin. Other factors such as resin cure shrinkage should also be considered.

6.5 REFERENCES

- 1. Y. S. Yang and L. J. Lee, "Microstructure formation in the cure of unsaturated polyester resins", Polymer, Vol. 29, pp. 1793-1800, 1988
- 2. S. B. Liu, J. L Liu and T. L. Yu, "Microgelation in the curing of unsaturated polyester Resins", J Polym Sci, Part B: Polym Phys, Vol. 53, pp. 1165-1177, 1994
- 3. Y. J. Huang and C. J. Chen, "Curing of unsaturated polyester Resins: Effect of comonomer Composition. II High teperature reactions", J Polym Sci, Part B: Polym Phys, Vol. 47, pp. 1533-1549, 1993
- 4. R. P. Brill and G. R. Palmese, "An investigation of vinyl-ester—styrene copolymerization cure kinetics using Fourier Transform Infrared Spectroscopy", J. App. Poly. Sci., Vol. 76, pp1573-1582, 2000
- 5. L. Weitzsacker, M. Xie and L. T. Drzal, "Using XPS to Investigate Fiber/Matrix Chemical Interactions in Carbon Fiber Reinforced Composites", Surf. Interf. Anal. 25, 53-63 1997
- 6. S. M. Corbin, M.S. Thesis, Department of Chemical Engineering, Michigan State University, 1998
- 7. L. T. Drzal, N. Sugiura and D. Hook, "Effect of interfacial chemical bonding and surface topography on adhesion in carbon fiber/epoxy composites", Proceedings of the 10th Annual Meeting of the American Society for Composites, 1994
- 8. L. Xu, L. T. Drzal, "Influence of interphase chemistry on the adhesion between vinyl ester resin and carbon fibers", Proceedings of the 23rd Annual Meeting of "Adhesion Science for the 21st Century", 2000
- 9. L. Xu, L. T. Drzal, A. Al-Ostas, , and R. Schalek, "Improvement Of Adhesion Between Vinyl Ester Resin and Carbon Fibers by A Controlled and Designed Interphase", Proceeding of the 2002 Adhesion Society/WCARP-II Meeting, 2002
- L. Xu, T. Mase, and L. T. Drzal, "Influence Of Matrix Cure Volume Shrinkage on the Adhesion between Vinyl Ester and Cardon Fiber", Proceedings of the 14th International Conference for Composite Materials, 2003
- 11. The Interfacial Testing System (ITS), The Dow Chemical Company, Freeport, Texas
- 12. J. F. Mandell, D. H. Grande, T. H. Tsiang and F. J. McGarry, "Modified microdebonding test for direct in situ fiber/matrix bond strength determination in fiber composites", Composite Materials: Testing and Design, ASTM STP893, American Society for Testing and Materials, pp. 87-108, 1986

- 13. K. J. Hook, R. K. Agrawal and L. T. Drzal, "Effects of microwave processing on fiber-matrix adhesion. II. Enhanced chemical bonding of epoxy to carbon fibers", J. Adhesion, Vol. 32, pp. 157-170, 1990
- 14. L. Xu, **Mater Thesis**, School of Mechanics and Materials Science, Washington State University, 1998
- 15. L. T. Drzal, "The Epoxy Interphase in Composites", review chapter in Advances in Polymer Science II, 75, K. Dusek, ed., Spring-Verlag, pp. 16, 1985
- 16. P. C. Hiemenz, **Polymer Chemistry: The Basic Concept**, Dekker, New York, pp. 185-190, 1984
- 17. J, Esmaiel and P.A. Nikolaos, "Polymer-polymer interdiffusion and adhesion" J.M.S.-RREV. MACROMOL.CHEM. PHYS., C34(2), pp.205-241,1994

CHAPTER 7

CURE VOLUME SHRINKAGE OF VINYL ESTER RESINS AND THEIR INFLUENCE ON ADHESION BETWEEN CARBON FIBERS AND VINYL ESTER MARIX RESINS

Composites of carbon fibers and vinyl ester polymers possess unexpected low mechanical properties due to low fiber-matrix adhesion [1-3]. Vinyl ester resin can undergo as much as 10% volume shrinkage with cure while typical epoxy system undergoes only 3-4% shrinkage during cure [4-6]. The cure volume shrinkage could have induced significant stresses in the fiber/matrix interphase already before composite loading. This could also be an important factor that lowers the adhesion between carbon fiber and vinyl ester resin. In this study, the influence of the matrix cure volume shrinkage on the adhesion between carbon fiber and vinyl ester resin was investigated. Cure volume shrinkage of vinyl ester resins were measured with a dilatometer. Adhesion was evaluated as interfacial shear strength (IFSS) measured with micro-indentation experiments. Finite element analyses were used to simulate the stress at the interphase and matrix and how it would change with matrix shrinkage. It was found that cure volume shrinkage of vinyl ester could introduce a residual interfacial radial tensile stress which would decrease the adhesion between fiber and matrix. The greater the shrinkage the more significant the reduction in adhesion. The cure volume shrinkage was determined by the molecular weight of the vinyl ester monomer and styrene content and also is related to the cure process and catalysts for polymerization. It was also found that an epoxy sizing applied to the fiber, which swelled as a result of exposure to styrene could counteract the cure volume shrinkage of the matrix. The results from finite element analyses were consistent with the experimental results that larger shrinkage produced a higher von Mises effective stress.

7.1 INTRODUCTION

Free radical cured thermosetting vinyl ester resins, typically containing 35~50% of styrene monomer as reactive diluents, have superior toughness and chemical resistance compared to unsaturated polyester. But composites of carbon fibers and vinyl ester polymers possess unexpected low mechanical properties due to low fiber-matrix adhesion [1-3]. Upon cure, the volume shrinkage of vinyl ester resin is generally lower than that of unsaturated polyester resin but higher than that of epoxy resin. Vinyl ester resin can undergo as much as 5-10% volume shrinkage with cure depending on the molecular weight of the vinyl ester monomer and the content of styrene (see Table 2.3). The cure volume shrinkage can induce significant residual stresses in the fiber/matrix interphase before loading. This could be the one of the most important factors that lowers the adhesion between carbon fiber and vinyl ester resin. As discussed in CHAPTER 5, the application of a lightly cross-linked Diglycidyl Ether of Bisphenol A (DGEBA) cured with Aliphatic Polyether Triamine (Jeffamine T-403) epoxy sizing to the carbon fiber surface creates a beneficial interphase between the carbon fiber and vinyl ester resin matrix resulting in a substantial increase in fiber-matrix adhesion and the sizing has a optimum thickness ^[2,3,7,8]. Vinyl ester resin can undergo as much as 10% volume shrinkage with cure while typical epoxy systems undergo only 3-4% shrinkage during cure ^[4-6]. One of the strategies of this research is to use the low shrinkage DGEBA-T403 carbon fiber sizing to isolate the carbon fibers from the vinyl ester resin to observe the influence of the cure volume shrinkage on the IFSS values measured by microindentation. The other strategy is to find of the influence of matrix resin cure volume shrinkage on the fiber/matrix adhesion by comparing the IFSS data of different vinyl ester matrices of different volume shrinkage. Most recently, Shanghai Fuchem Chemical Company has developed a new-type epoxy vinyl ester resin which was claimed "free" of cure volume shrinkage ^[9]. In summary, the goal of this study is to gain an understanding of the matrix cure volume shrinkage on the adhesion between carbon fiber and vinyl ester matrix resin.

7.2 EXPERIMENTAL MATERIALS AND METHODS

Experimental Materials: the fibers used in this study are AS4 carbon fibers from Hexcel, Inc. The matrix resins are Derakane 411-C50 epoxy vinyl ester resin (D411-C50) from Dow Chemical and Fuchem 891 epoxy vinyl ester resin (Fuchem891) from Shanghai Fuchem Chemicals Co. respectively. CHP-5 (diluted cumene hydroperoxide) from Witco Chemical and MEKP (methyl ethylketone peroxide) from Aldrich chemicals was used as the initiator. Both CoNap and DMA from Aldrich Chemicals were used as promoters and accelerators respectively. Diglycidyl ether of bisphenol A (DGEBA epoxy) and Aliphatic Polyether Triamine (JEFFAMINE T403) were from Shell and Huntsman

respectively. Refer Figure 2.6, Figure 2.7 and Figure 5.2 for the molecular structures of the epoxy vinyl ester resins, the sizing epoxy material and the cure catalysts. Molecular structure of D411-C50 and Fuchem 891 are both bisphenol A epoxy based vinyl ester but different molecular weights, about 900g/mol for D411-C50 and 1500~2000g/mol for Fuchem 891 respectively. Both resin use styrene as a reactive diluent. The styrene content of D411-C50 and Fuchem891 are 50% and 35% respectively.

Fuchem 891 vinyl ester resin was developed by Shanghai Fuchen Chemicals Co as a new-type of epoxy vinyl ester resin featuring low shrinkage together with an improved elongation rate & impact resistance performance. Fuchem 891 vinyl ester resin is also a mixture of DGEBA epoxy vinyl ester (refer Figure 2.7) and styrene. The styrene content is about 35%. It was claimed that the result from tests shows that the pure vinyl ester resin has a 0.015% linear shrinkage after curing in ambient temperature, 0.160% after 2 hours of post-curing at 80°C. Refer Appendix III for the relationship between linear shrinkage and volumetric shrinkage. Considering D411-C50 vinyl ester resin has large volume shrinkage with cure, Fuchem 891 was use in this research to quantify the influence of the cure volume shrinkage to the adhesion between carbon fiber and vinyl ester resin. The property comparison of the D411-C50 and Fuchem 891 are listed in Table 7.1.

Properties	D411-C50	Fuchem 891	
DGEBA Vinyl Ester Molecular Weight (g/mol)	907	1500-2000	
Styrene Content	50%	35%	
Tension Modulus, E, (GPa)_	3.38	3.12	
Tension Strength, (MPa)	79.3	75	
Elongation, %	5~6	4.0	
Barcol Hardness	35	33	
Density, ρ, (g/m³)	1.12		
Heat Distortion Temp.	99~105°C	92±2°C	

Table 7.1 Property comparison of D411-C50 to Fuchem 891 vinyl ester

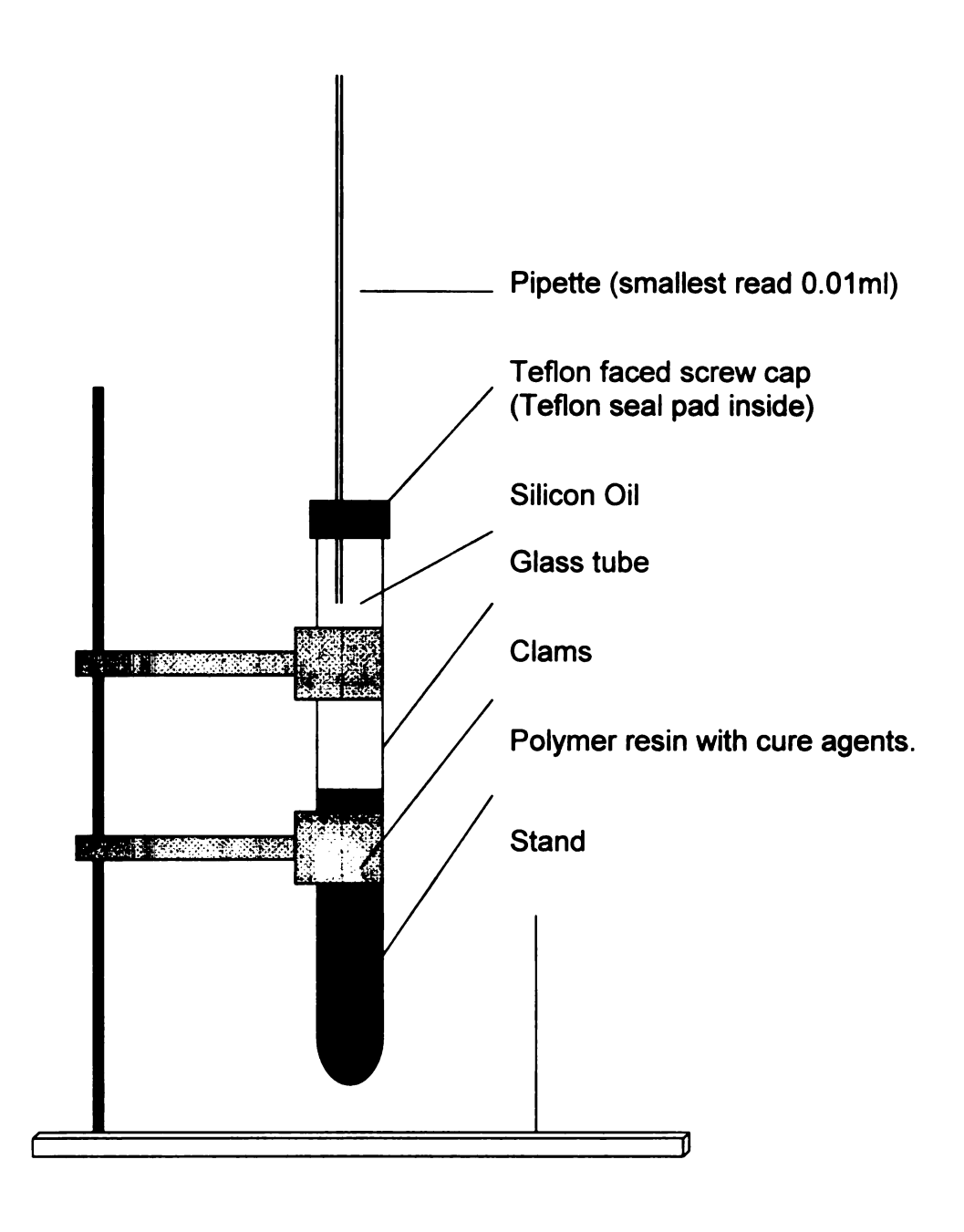


Figure 7.1 The dilatometer apparatus used to measure the volumetric change with cure

Experimental Methods: a lab-made dilatometer was used to measure cure volume shrinkage of vinyl ester resin from liquid resin to full cure. Dilatometry is a technique that uses the volume decrease (density increase) that occurs upon polymerization to follow that conversion time. Figure 7.1 depicts the simple dilatometer used in this study. The design depends mainly on the expected volume change after resin curing. This is a glass culture tube with a Teflon-faced screw cap equipped with a 2-ml pipette in which the liquid (silicone oil) level can be read, the smallest read was 0.01ml. The screw cap was drilled through, the hole diameter is almost the same as that of the pipette. A Teflon sealant pad whose diameter is that same as the screw cap was drilled through with a much small diameter so that it can vacuum seal the gap between the pipette and the screw cap. Silicone oil which is very stable under 120°C is used as the indicator liquid.

A digitally controlled, programmable oven was used for specimen curing to make sure all the samples were processed in the same way. The cure processes were the same for all samples: room temperature for 1 hour, 90°C for 1 hour and 125°C for 1.5 hours. Two types of recipe systems were used for the samples for the investigation of influence of cure shrinkage on the adhesion between carbon fiber and vinyl ester resin. Two different systems were used with different initiators. One is CHP-5 and the other one is MEKP. See Figure 2.6 for the molecular structures. The CHP-5 cure system was based on the cure recipe for D411-C50 recommended by the manufacturer and the MEKP cure system is based on the cure recipe for Fuchem 891 recommended by the manufacturer, shown in the gray columns of Table 8.2. For the same initiator, the corresponding recipes, the white columns of Table 8.2, were calculated from the recommended recipes, the gray columns, based on the concentration of the carbon-carbon double bond, C=C.

The mixture of DGEBA and JEFAMINE T-403 was prepared and held for one half hour then added to acetone to form a 5wt% sizing solution. Fiber sizing was carried out by using a pre-impregnation machine. Dynamic Mechanical Thermal Analysis (DMTA), DMA 2980 from TA Instruments, and physical testing, was conducted to measure the mechanical properties of the matrix resin. A MTS nano-indentation instrument was used to measure the bulk moduli of the vinyl ester resins. Nano-scratch was also carried out by the MTS nano-indentation machine to quantify the gradient of the modulus between the sizing and the DGEBA epoxy and D411-C50 vinyl ester resin matrices. A RMC MT-7 ultramicrotome was used for preparing the nano-scratch sample surface with a diamond knife. Adhesion was evaluated as interfacial shear strength (IFSS) measured with a micro-indentation system, Interfacial Testing System (ITS). Finite element analyses were used to simulate the stress distribution around the fiber-sizing-matrix interphases during volume shrinking of the matrix resin and the micro-indentation process as well.

Finite Element Analysis: consider the composite as an orthotropic material with regularly spaced fibers as shown in Figure 7.2. A single fiber is singled out for simulation, and furthermore, only a quarter of this fiber is modeled because of symmetry. The dashed line indicated the representative volume element (RVE) that is simulated and is considered the fiber the micro-indenter would contact. This RVE is extended downward a length of 20 times the fiber diameter in the Z direction to form a 3-dimensional RVE. The two sides of this dashed line intersecting at the fiber center represent symmetry planes for this repeating cell Figure 7.2. Also shown in this figure is an interphase region between the fiber and matrix shown as a gray ring around the fiber.

Initiator		Fuchem 891	D411-C50	
	CHP-5	1.40%	2.00%	
CHP-5	CoNap	0.21%	0.30%	
MEKP	MEKP	2.00%	2.85%	
	CoNap	0.10%	0.14%	

Table 7.2 The catalyst recipe for the investigation of the cure volume shrinkage in vinyl ester matrices

A commercial finite element code, LS-DYNA [10], was used to model the matrix/interphase shrinkage and indenter contact. The explicit aspect of the code was used to model the matrix/interphase shrinkage followed by contact with the indenter. A thermal excursion was used to model the matrix/interphase shrinkage. A linear elastic, orthotropic, temperature dependent material was used. This material model is timeindependent. Standard orthotropic elastic constants are E_a , E_b , E_c , v_{ba} , v_{ca} , v_{cb} , G_{ab} , G_{bc} , The thermoelastic constitutive behavior is defined by three, orthotropic coefficients of thermal expansion, α_a , α_b , α_c , that produce normal strain components defined by $\varepsilon_i = \alpha_i \Delta T$, where T is the temperature. All of the thermoelastic parameters used are given in Table 7.3. Note the coefficient of thermal expansion in the fiber directions (b-direction) are set to zero. This was done so the surface the tup impacted remained planar. When these coefficients were not zero the matrix and interphase contracted considerably relative to the fiber making a domed surface for indenting. For the interphase two values are listed that represent the CTE for the 7.18% and 1.73% shrinkage respectively. The higher CTE value is for the lower volume shrinkage because the temperature excursion was less in this case.

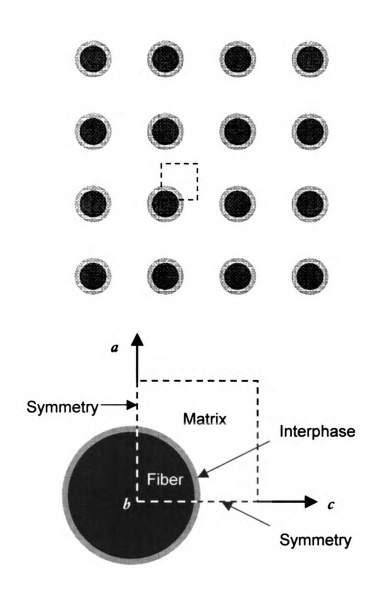


Figure 7.2 A transversely isotropic array of composite fibers with the representative volume element indicated by a dashed line $^{\rm I\!I}$.

Fiber	(GPa)				(GPa)		(°K · 10 ⁻⁶)
E_a	21	v_{ba}	0.256	G_{ab}	10.0	α_a	8.5
E_b	241	V_{ca}	0.33	G_{bc}	10.0	α_b	0
E_c	21	V_{cb}	0.256	G_{ca}	8.3	α_c	8.5
Interphase							
E_a	3.24	V_{ba}	0.356	G_{ab}	1.195	α_a	8.26/34.3
E_b	3.24	v_{ca}	0.356	G_{bc}	1.195	α_b	0
E_c	3.24	V_{cb}	0.356	G_{ca}	1.195	α_c	8.26/34.3
Matrix							
E_a	3.38	v_{ba}	0.356	G_{ab}	1.246	α_a	80
E_b	3.38	V_{ca}	0.356	G_{bc}	1.246	α_b	0
E_c	3.38	v_{cb}	0.356	G_{ca}	1.246	α_c	80

Table 7.3 Themomechanical properties for finite element model

7.3 RESULTS AND DISCUSIONS

7.3.1 Cure Shrinkage of Vinyl Ester Matrices

The effectiveness of the lab-made dilatometer could be confirmed by the data shown in Figure 7.3. There were three of the lab-made dilatometers were set up at the same time for the sample measurements. The Y-axis was the reading of the silicone oil level directly obtained from the lab-made dilatometer. The X-axis was the time. Time 0 was the time of completion of the adding of the curing agents to the liquid resin. The mixing took about 2 minutes after the cure agents added in. The initial silicone oil levels of the three lab-made dilatometers were different though those of the measurement 1 and measurement 2 were very close. Since the difference in readings was the important factor, the initial differences did not matter.

The results of the cure volume shrinkage measured by the lab-made dilatometer are shown in Figure 7.4. The data shows that D411-C50 produces a volume shrinkage of 7~8% upon curing. Whereas the Fuchem 891 vinyl ester resin cured with the recommended recipe, 2% of MEKP and 0.1% of CoNap, produced a very small cure volume shrinkage, only 1.73%. (It is interesting that when Fuchem 891 vinyl ester resins were cured with CHP-5 as initiator using a concentration the same as that of D411-C50 recommended by the manufacturer, the cure volume shrinkage is 5.85%, not a small number!)

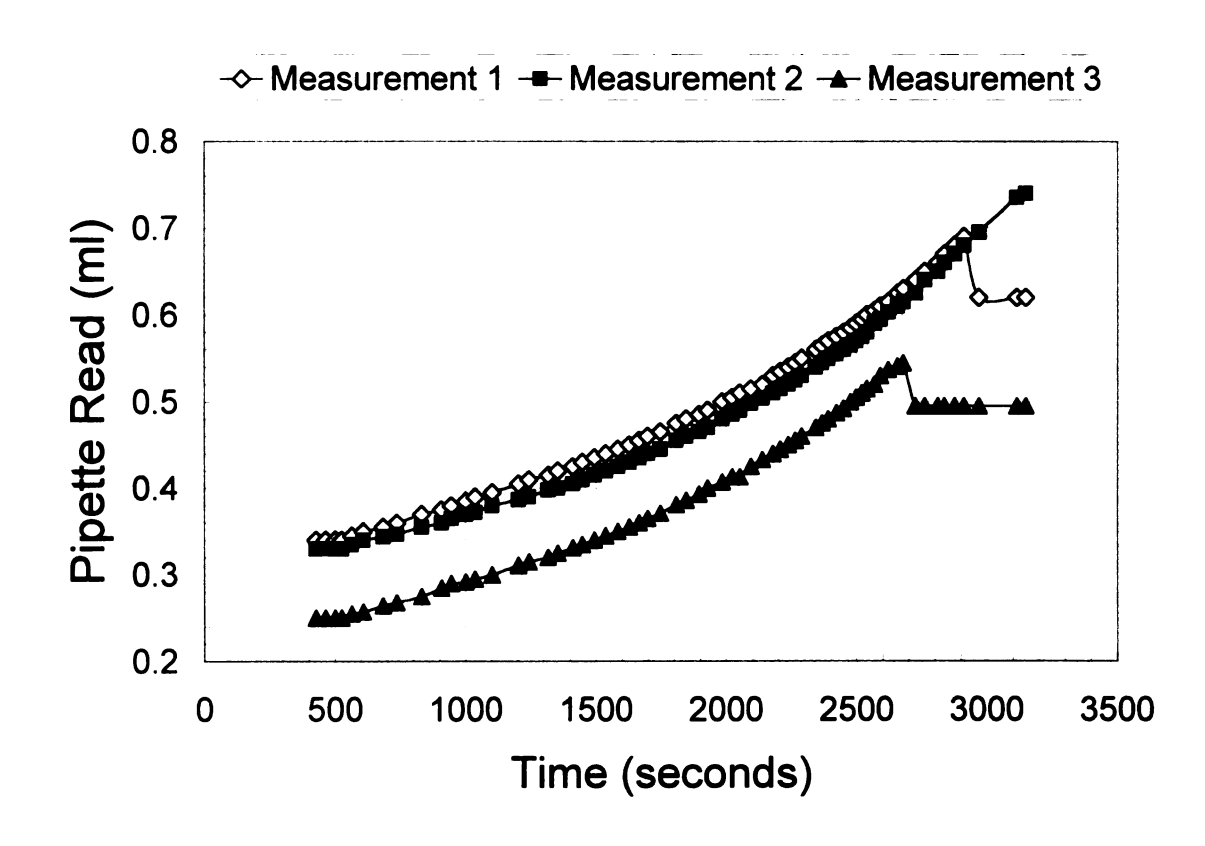


Figure 7.3 The silicone oil level in the pipette of the lab-mad dilatometer versus time

Figure 7.4 The volume shrinkage observed from the lab-made dilatometer according to time

Fuchem 891 DGEBA epoxy vinyl ester resin was claimed by the manufacturer as having a 0.015% linear shrinkage after curing in ambient temperature, 0.160% after 2 hours of post-curing. The relationship between linear shrinkage to volumetric shrinkage can be described as following Equation 7.1 refer Appendix III.

$$\frac{\Delta V}{V_0} = 3\frac{\Delta l}{l_0}$$
 7.1

where $\Delta V/V_0$ is the volumetric shrinkage and $\Delta L/L_0$ is the linear shrinkage. 1.73% of volumetric shrinkage equals to 0.54% of linear shrinkage which is much bigger than 0.015%, which was claimed by the manufacturer. The linear shrinkage was measured with a stainless steel mold which was a semi-circle of 2.22cm of internal diameter and 2.86cm of external diameter and 25cm in length. The measurement technique was close to ASTM D2566. Refer to A. T. Busschen^[11] in chapter 2, this kind of measurements has shown an anisotropic cure shrinkage even for isotropic material depending on the surroundings. Another set of tests was carried out by the manufacturer which the same method was used but the samples were post cure at 125°C for 2hour. The result was reported as: "0.35% linear shrinkage, and the volume shrinkage rate is 1%".

This differences are most probably due to the test method used. The method using semi-circle stainless steel mold measured the linear direction which is the most constrained direction, in another word, the smallest shrinkage shown direction but most significant residual stress direction. While the lab-made dilatometer used in this study measured the three dimensional shrinkage even through the tube still provides constraint to the vinyl ester.

The cure volume shrinkage of vinyl ester could be changed not only depending on the catalysts but also the cure process. Figure 7.5 shows that room temperature cured vinyl esters resulted in lower cure volume shrinkages. But DMTA tests found that room temperature cured vinyl ester was not fully cured. Figure 7.6 illustrates a typical DMTA measurement. A room temperature cured Fuchem 891 sample was cured with a temperature cycle from room temperature to 160°C twice at the ramp of 6°C/minute (cure recipe was recommended by the manufacturer, see Table2). In the second run of the DMTA test, a much higher storage modulus and high glass transition temperature (Tg) was detected indicating that full cure was not achieved in the first DMTA run. Room temperature cure is not sufficient for this free radical polymerization.

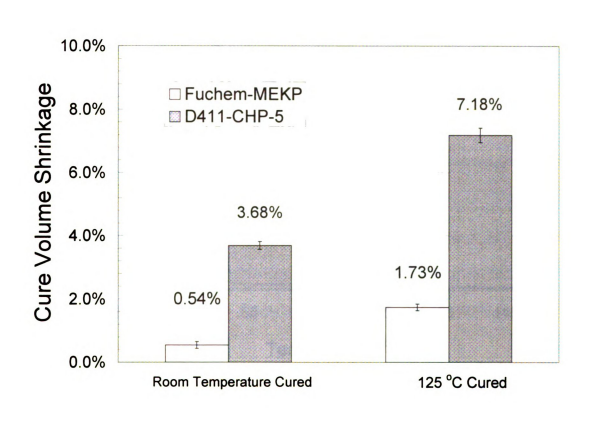


Figure 7.5 Influence of Cure Process to the Cure Volume Shrinkage of Vinyl Ester

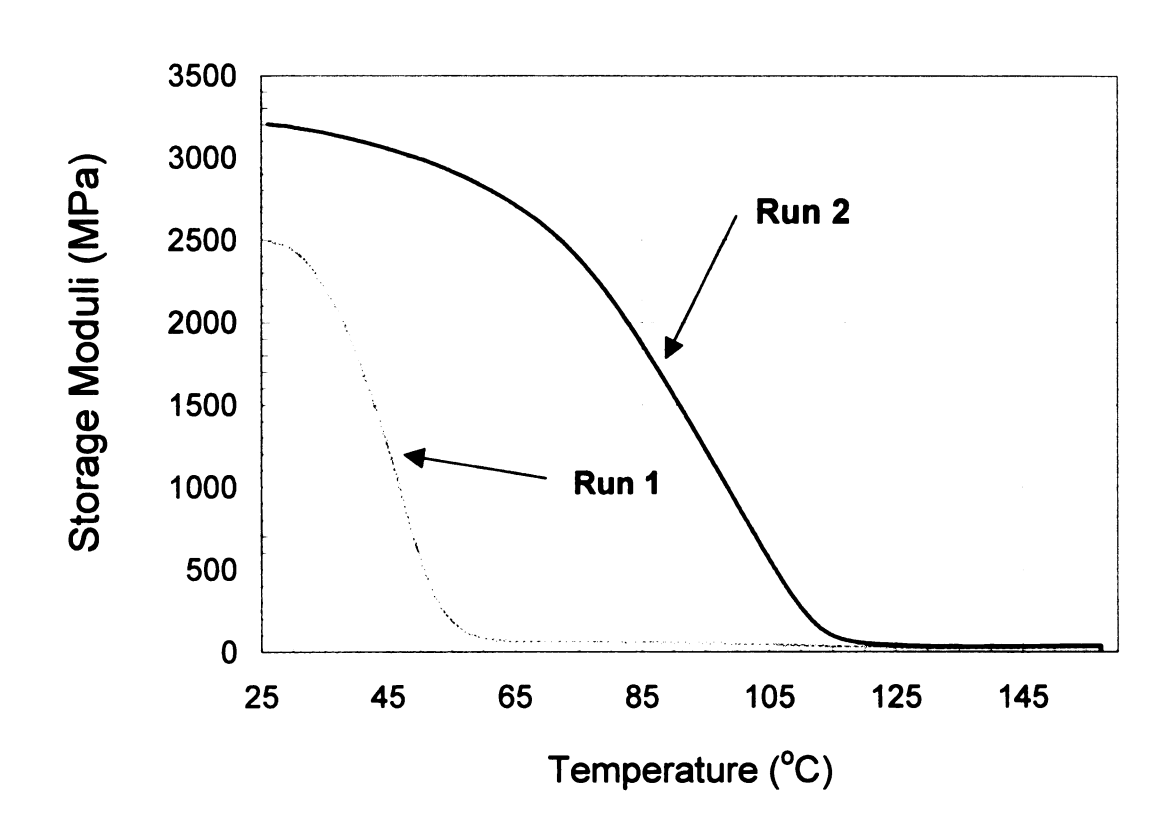


Figure 7.6 One of the DMTA Measurement for Room Temperature Cured Fuchem 891

7.3.2 Influence of Cure Volume Shrinkage of Matrix Resin on the Adhesion between Carbon Fiber and Vinyl Ester

The mechanical properties of matrix, which are very important for ITS interfacial shear strength measurements, were measured by nano-indentation. During the cure process, it was found that styrene vaporization was significant. The vaporization would be different for samples made with open sample molds from those sample whichs were made with less open molds and significantly different from the samples made with the totally closed lab-made dilatometer. To avoid the influence of styrene vaporization, nano-indentation was used to measure the bulk mechanical properties of the material. It was also found that the bulk elastic moduli measured by nano-indentation were compatible to the tensile moduli measured. The influence of the cure volume shrinkage of the vinyl ester materials on their bulk moduli were shown in Figure 7.7. The bulk moduli of the vinyl ester materials increased with the increase of the cure volume shrinkage of the materials. It might indicate that the larger the cure shrinkage the more compact morphology the polymer chains achieve resulting in an increase of the material mechanical property.

Two sets of composite samples were tested by the ITS to find out the influence of the cure volume shrinkage of the matrix material on the adhesion between fiber and matrix. One set of composite samples was the vinyl esters having different cure volume shrinkage reinforced by AS4 carbon fiber 'as received' and the other set was the vinyl esters having different cure volume shrinkage reinforced by AS4 carbon fiber with 5% of DGEBA-Jeffamine T-403/Acetone sizing solution. The test results are shown in

Cure Volume Shrinkage

Figure 7.7 Influence of vinyl ester cure volume shrinkage on the bulk moduli

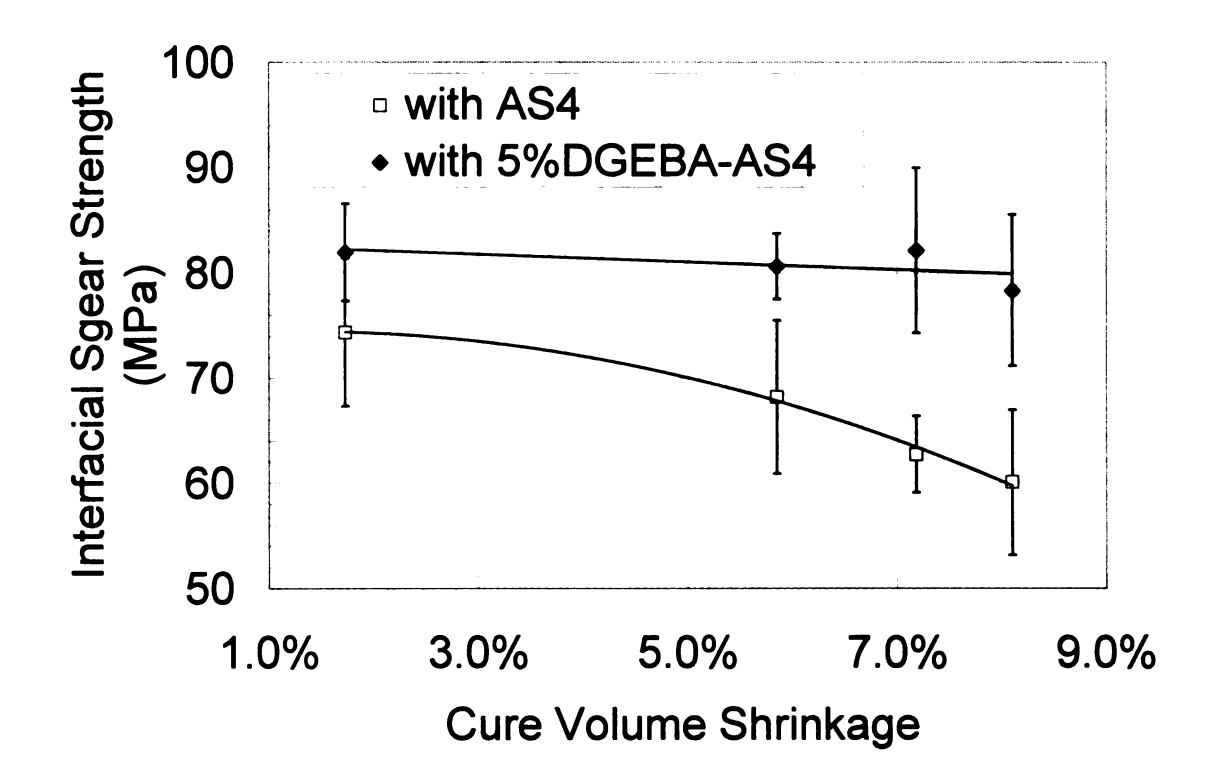


Figure 7.8 Influence of vinyl ester cure volume shrinkage on the Interfacial shear strength

Figure 7.8. The ITS test results are very interesting, for the samples made with AS4 carbon fiber as received, the interfacial shear strength showed a progressive decrease with the cure volume shrinkage of the matrix material, the larger the cure volume shrinkage --- the more significant the decrease of the interfacial shear strength. In contrast, for the samples made with carbon fiber with DGEBA-T403 sizing, the value of the interfacial shear strength underwent little change even for big cure volume shrinkage of 8.2%. This suggested that the cure volume shrinkage would produce a residual stress which had a negative effect on the adhesion between carbon fiber and vinyl ester resin. And it was also suggested that the sizing material plays a very important role in elimination of the residual stresses caused by the cure volume shrinkage.

7.3.3 Interphase between DGEBA Epoxy Sizing and Vinyl Ester of Different Volume Shrinkage

Further investigation was carried out to find the influence of the vinyl ester cure volume shrinkage on the interphase between the DGEBA epoxy sizing. Figure 7.9 is the nano-scratch trace. The scratch data which was averaged by scratch distance of 300nm is shown in Figure 7.10 where for Sizing/D411-CHP interphase the D411-CHP vinyl ester had a volumetric shrinkage of 7.18% and for Sizing/Fuchem-MEKP interphase the Fuchem-MEKP had a volumetric shrinkage of 1.73%. Both data of Sizing/D411-CHP interphase and Sizing/Fuchem-MEKP interphase are off from the reference interphase which is consisting to the C++ simulation. But the scratch data between Sizing/D411-CHP interphase and Sizing/Fuchem-MEKP interphase are barely observable.

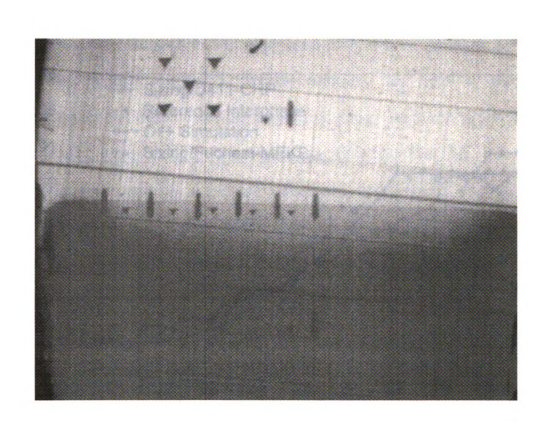


Figure 7.9 Nano-scratch trace for the interphase of DGEBA epoxy sizing/Fuchem 891-MEKP

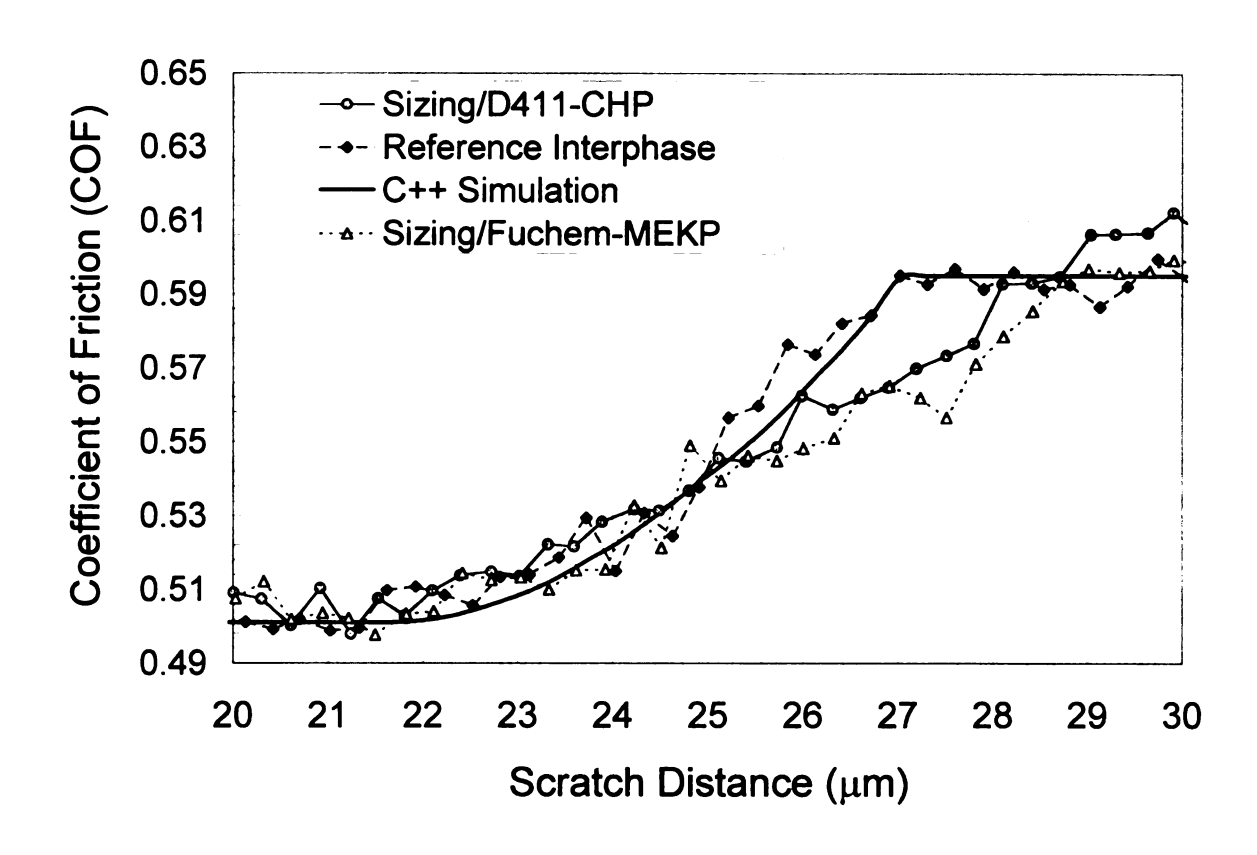


Figure 7.10 Comparison of nano-scratch data for the interphase of DGEBA epoxy sizing/Fuchem 891-MEKP and the interphase of DGEBA epoxy sizing/D411-CHP

7.3.4 Finite Element Analysis of the Residual Stress Caused by Cure Volume Shrinkage

The residual stress caused by cure volume shrinkage was studied with finite element analysis. Two situations were selected for this study. One was the Derakane 411-C50 vinyl ester cured with CHP-5 which undergoes a volume shrinkage of 7.18% upon cure and the other was Fuchem 891 vinyl ester cured with MEKP. As mentioned in the experimental methods section, a thermal excursion was used to model the matrix/interphase shrinkage. Once the temperature change associated with 1.73% and 7.18% matrix shrinkage was determined the indenter loading of the fiber was modeled. The indenter was modeled by a spherical contact entity (*CONTACT_ENTITY) which was given a prescribed displacement. A displacement function defined in three, piecewise linear portions was prescribed. Initially, while the temperature was decreasing the indenter remains fixed. Once the temperature has lowered to the required value, the indenter moved in a bi-linear fashion. The indenter rate for the first half of the loading is reduced to avoid impacting the fiber too harshly.

The nature of the indenter displacement function may be seen by examining the indenter force (Figure 7.11). Notice the difference between these two plots between times 0.01 and 0.025 ms where the 7.18% case is loading. What is happening is the contraction of the matrix, interphase and fiber is lengthening the RVE enough to contact the tup before it starts to move. Ultimately, the two cases match up during the loading phase of the fiber, so the early difference was ignored.

A good measure of the distortional strain energy (shearing energy) is the von Mises effective stress. Figure 7.12 shows the von Mises stress for a matrix element adjacent to

Figure 7.11 Indenter force time history

Figure 7.12 Von Mises stress for a point in the matrix at the interphase-matrix boundary located approximately 18 μm from the free surface.

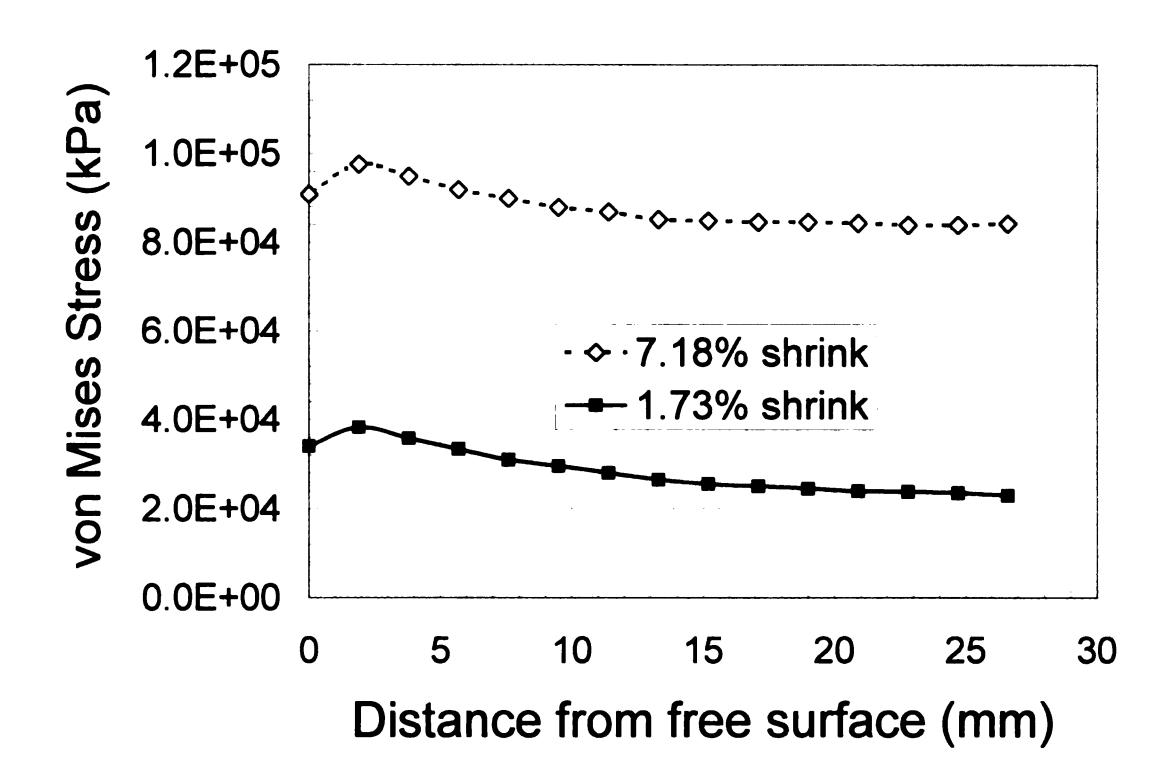


Figure 7.13 von Mises Stress Distribution at 5 g Indenter Load

the interphase and approximately 18 μm from the free surface in the cases of 1.73% and 7.18% volume shrinkage. (The maximum stress occurs in this vicinity.) Again the nature of the prescribed tup displacement is apparent in the von Mises stress curves. The stress evolutions from the tup loading are similar, but the volume shrinkage has these starting at different value. Thus, the matrix shrinkage has a considerable influence on the matrix stress.

7.4 MODELLING INTERPHASE STRENGTH

During this work, the fiber/matrix adhesion was evaluated as interfacial shear strength (IFSS) measured by Interfacial Testing System (ITS) micro-indentation apparatus given by a generalized empirical equation (ITS shear equation, equation 7.2), which is embedded in the data reduction software of the apparatus.

$$IFSS = A \frac{P}{D^2} \left[B \left(\frac{G_m}{E_f} \right)^{\frac{1}{2}} - CLn \left(\frac{d}{D} \right) - E \right]$$
 7.2

Where:

IFSS=Interfacial Shear Strength (psi)

P=Maximum Load (g)

D=Fiber Diameter (um)

 G_m =Matrix Shear Modulus (psi)

 E_f =Fiber Tensile Modulus (*psi*)

d=Distance to Nearest Neighbor (um)

A, B, C, E = Constants;

A=1,81100 B=0.875696 C=0.018626 E=0.026496

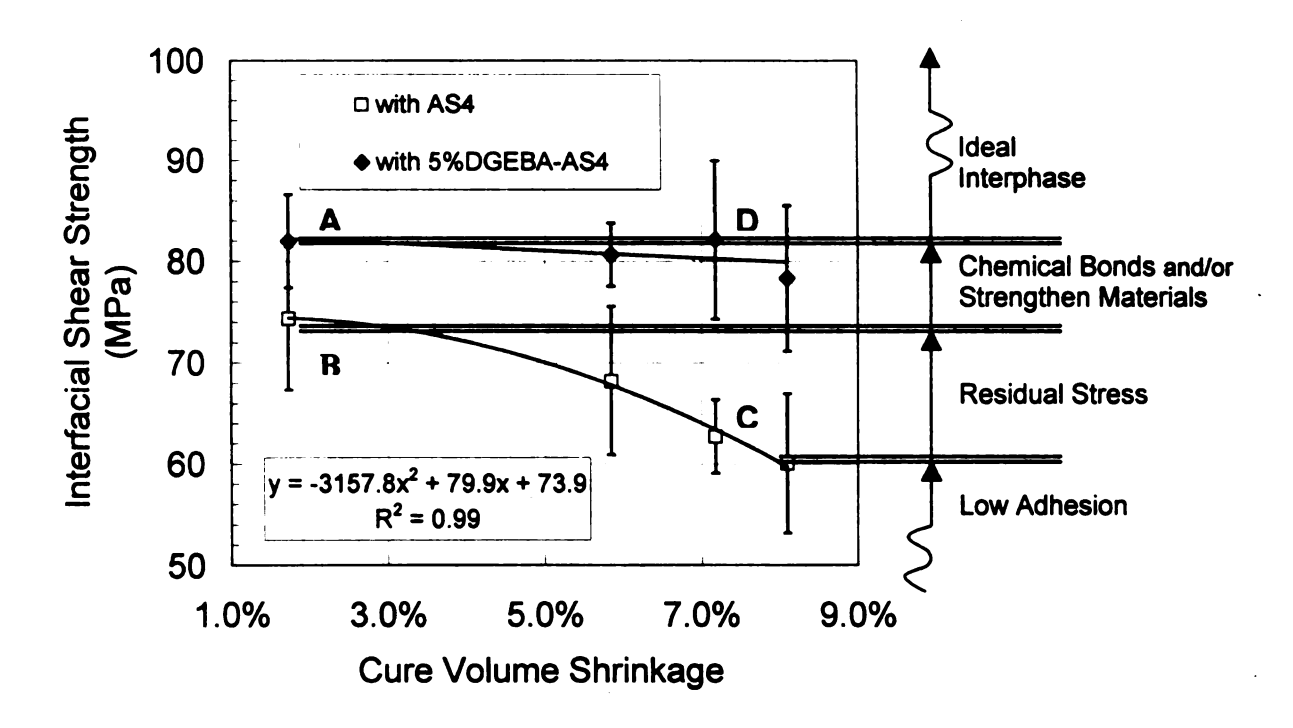


Figure 7.14 The interphase property presented by interfacial shear strength(IFSS) plot

for details. Accounting for the fiber E_f , matrix G_m , morphology of the in situ composites d_n/d_f , this equation ignores the fiber/matrix interphase. Actually the interphase property was tested by the Load on Fiber for Debonding, f_g and presented as part of the IFSS value. See Figure 7.14, sample A, B, C, and D were all made from the AS4 carbon fibers and vinyl ester matrices of almost the same shear modulus. Because a very stringent fiber selection criterion was applied to all the tests, differences between d_n/d_f were very small. The differences between the IFSS values should represent the differences of the interphases. For example, comparing the IFSS of sample A to that of the sample B, sample A has a stronger interphase which could be the result of the change in chemical bonding and/or the material at the interphase; Comparing Sample D to sample C, sample D has the stronger interphase which could be because of the change in chemical bonding plus the relaxation of the residual stress; and sample A and sample D could have interphase of same strength even they have different vinyl ester matrices.

Based on data in Figure 7.14, prediction of the interfacial shear strength of a fiber/matrix system could be accomplished through use of equation 7.3:

IFSS
$$\propto (\alpha - v\%)^2 * \left[\beta \left(\frac{G_m}{E_f} \right)^{\frac{1}{2}} - \lambda Ln \left(\frac{d}{D} \right) - \delta \right] + \sigma_{CB}$$
 7.3

Where:

IFSS=Interfacial Shear Strength

 α =adjust parameter related to cure volume shrinkage

v%=percentage of cure volume shrinkage

 G_m =Matrix Shear Modulus

 E_f =Fiber Tensile Modulus

D=Fiber Diameter

d=Distance to Nearest Neighbor

 $\sigma_{\rm CB}$ =Strength provided by additional chemical bonding

 β , λ , and δ are Constants;

7.5 CONCLUSIONS

- Cure volume shrinkage of vinyl ester resins are generally determined by the average molecular weight of the vinyl ester monomer and the content of styrene monomer. Normally larger average molecular weight of the vinyl ester monomer and lower the content of styrene monomer result in small cure volume shrinkage as noted in the literature^[4]. The shrinkages were also related to the catalyst of the free radical polymerization and time-temperature schedule of the process. Different cure temperature and catalysts produce different heats of reaction, cross-link density and degrees of micro-gel formation and/or micro-phase-separation ^[12-14]
- 2. The cure volume shrinkage of vinyl ester could introduce residual interfacial tensile stress which would decrease interfacial shear strength (IFSS) values suggesting a negative effect on the adhesion between fiber and matrix. The greater the shrinkage the more the adhesion is reduced. The bulk moduli of the vinyl ester resin measured by nano-indentation increase as the cure volume shrinkages increase resulting in an increase of the material mechanical properties.
- 3. The epoxy sizing on the fiber surface is very important for the relaxation of thermal residual stress caused by cure volume shrinkage. Epoxy-sizing swelling could counteract the cure volume shrinkage of the matrix.
- 4. Finite element analyses was very useful for analyzing the interfacial shear stress distribution during matrix shrinkage. The results from finite element analyses

were consistent with the experimental results that larger shrinkage produces higher von Mises effective stress.

- 5. DGEBA epoxy sizing provides a beneficial interphase between the carbon fiber and vinyl ester resin. First of all it provided the ability to form chemical bonds with the composite matrix resin and the surface of carbon fiber reinforcement. Second, the epoxy vinyl ester was made from DGEBA epoxy which should be compatible to the DGEBA sizing material. The small styrene monomers can interdiffuse into the slightly cross-linked epoxy sizing material before the matrix is fully cured. The swelling of the sizing with styrene diffusion may be critical for counteracting the matrix volume shrinkage and further more eliminate the residual stress. The optimum sizing thickness is 90~100nm. Nano-indentation test and nano-indentation scratch test are useful techniques for measurement of interphase profile.
- 6. Modified interphase strength could be qualitatively predicted. By comparing the ITS interfacial shear strength (IFSS) values, more accurate interphase properties can be obtained.

7.5 REFERENCES

- 1. D. Hoyns. and L. T. Drzal, "Hydrothermo-Mechanical Response and Surface Treated and Sized Carbon Fiber/Vinyl Ester Composites", ASTM Symposium on the Fiber Matrix and Interface Properties, 1994
- 2. S. M. Corbin, M.S. Thesis, Department of Chemical Engineering, Michigan State University, 1998
- 3. Rich, M., Corbin, S., and Drzal, L., "Adhesion of Carbon Fibers to Vinyl Ester Matrices", Proceedings of the 12th International Conference of Composite Materials, Paris, ICCM12, 1999
- 4. M. B. Launikitis, "Vinyl Ester Resin", Hand Book of Composite, pp.38-49
- 5. L. S. Penn and T. T. Chiao, "Epoxy Resins", Hand Book of Composite, pp.57~88
- 6. L. Xu and L. T. Drzal, "Influence Of Matrix Cure Volume Shrinkage on the Adhesion between Vinyl Ester and Cardon Fiber", Proceedings of the 2003 Adhesion Society, pp.415-417, 2003
- 7. Xu, L. and Drzal, L., "Adhesion Improvement between Vinyl Ester and Carbon Fiber", Proceedings of the 13th International Conference of Composite Materials, Beijing, ICCM13, 2001.
- 8. Xu, L., Drzal, L., Al-Ostas, A., and Schalek, R., "Improvement Of Adhesion Between Vinyl Ester Resin and Carbon Fibers by A Controlled and Designed Interphase", Proceeding of the 2002 Adhesion Society/WCARP-II Meeting, 2002
- 9. http://www.fuchem.com
- 10. Livermore Software Technology Corporation, LS-DYNA Keyword User's Manual, Version 940, 1997
- 11. A. Ten Busschen, **Ph.D thesis**, Delft University of Technology, the Netherlands, 1996
- 12. Weitzsacker, L., Xie, M. and L. T. Drzal, "Using XPS to Investigate Fiber/Matrix Chemical Interactions in Carbon Fiber Reinforced Composites", Surf. Interf. Anal. 25, 53-63, 1997

- 13. R. P. Brill and G. R. Palmese, "An investigation of vinyl-ester—styrene copolymerization cure kinetics using Fourier Transform Infrared Spectroscopy", J. App. Poly. Sci., Vol. 76, pp1573-1582, 2000
- 14. C. P. Hsu and L. J Lee, "Free-radical crosslinking copolymerization of styrene/unsaturated polyester resins: 3. Kinetics-gelation mechanism" Polymer, Vol. 34, pp. 4516-4523, 1993

CHAPTER 8

CONCLUSIONS AND RECOMMENDATIONS

8.1 CONCLUSIONS

Derakane 411-C50 vinyl ester resin is a mixture of vinyl ester and styrene monomer which polymerizes by a free radical polymerization. The interface between this resin and AS4 carbon fiber is much more complex than that between epoxy and AS4 carbon fiber. From this study, several conclusions can be made.

Application of a slightly cross-linked epoxy-amine polymer on the carbon fiber surface is found as an effective way to increase the adhesion between carbon fiber and vinyl ester resin. The sizing thickness on the carbon fiber surface can be controlled by the concentration of sizing solution. The optimum sizing thickness is 90~100nm that brought a substantial increase in the value of interfacial shear strength (IFSS) measured by micro-indentation more than 30%. Finite element analysis result was compatible with the micro-indentation result. The maximum value of IFSS happens when the sizing thickness is about 90~100nm. At thicknesses greater than this value, no improvement is detected because of the low modulus of the epoxy sizing. Inter-diffusion of the styrene into the epoxy sizing creates an interphase which is stronger than the epoxy sizing material itself.

DGEBA epoxy sizing provides a beneficial interphase between the carbon fiber and vinyl ester resin. First of all it provided much more possibilities to form chemical bonding to the surface of carbon fiber reinforcement surface. Second, the epoxy vinyl ester was made from DGEBA epoxy which should be compatible to the DGEBA sizing material. Third styrene monomers are very small which could penetrate the slightly cross-linked epoxy sizing material. Nano-scratch measurement found that the inter-diffusion distance could be up to 1.5 microns. Last but not the least, the epoxy sizing on the fiber surface is very important for the relaxation of thermal residual stress caused by cure volume shrinkage.

Cure volume shrinkage of vinyl ester resins are generally determined by the average molecular weight of the vinyl ester monomer and the content of styrene monomer. Normally larger average molecular weight of the vinyl ester monomer and lower the content of styrene monomer result in small cure volume shrinkage. The shrinkages were also related to the catalysts of the free radical polymerization and time-temperature schedule of the process. Different cure temperature and catalysts of produce different heats of reaction, cross-link density and degrees of micro-gel formation and/or micro-phase-separation resulting in different cure volume shrinkage. The cure volume shrinkage of vinyl ester could introduce residual interfacial tensile stress which would decrease interfacial shear strength (IFSS) values The greater the shrinkage the more significant the effect. While the bulk moduli of the vinyl ester resin measured by nano-indentation increase as the cure volume shrinkages increase, the material mechanical properties increase as well. Finite element analyses was very useful for analyzing the interfacial shear stress distribution during matrix shrink. The results from finite element

analyses were consistent with the experimental results that larger shrinkage produced a higher von Mises effective stress.

Preferential adsorption of the components of the vinyl ester system, the promoter (CoNap), the accelerator (DMA), or the styrene monomer does not make a major difference on the interfacial shear strength value measured. However, changes in the initiator and the concentration of initiator (CHP-5) cause changes in the polymerization of the vinyl ester system. Optimum fiber-matrix adhesion could be obtained by properly select the initiator and adjusting the amount of initiator. The contributions of styrene and vinyl ester in D411-C50 to the adhesion between the fiber and matrix are different especially for fibers with the lightly cross-linked DGEBA-T403 sizing. The small styrene monomers diffuse into the DGEBA-T403 sizing material and provide a strengthened interphase.

Modified interphase strength could be qualitatively predicted. By comparing the ITS interfacial shear strength (IFSS) values, more accurate interphase properties can be obtained.

8.2 RECOMMENDATIONS

While most of the experimental work presented in this study is completed, the mechanical properties of the composite material with engineered interphase are not provided here. Though using three point flexural tests increased strength were found for composites with an engineered interphase and composites with low shrinkage vinyl ester. The error in these measurements was high as a result of deficient fabrication conditions. Once these sources of error are brought under control, (e.g. fiber volume percentage, the

control of the fiber distribution, and etc.), more accurate mechanical properties of the composites could be collected in the future.

Nano-indentation and nano-scratch techniques were introduced to profile the interphase gradient between epoxy sizing and vinyl ester resins. The effects of tip size, both for indentation and scratch were found. Especially for nano-scratch, the effect of the indenter size were accurately simulated by a C++ program. The inter-difusion between polymers was measured though it was only a range at this point. For example, the inter-diffusion distance between vinyl ester and slightly cross-linked epoxy in this study would be 391nm~1521nm. According to Einstein's equation,

$$l^2 = 2Dt$$

where l is the inter-diffusion distance, D is inter-diffusion coefficient and t is the diffusion time. Assume diffusion time t=geltime=20mins=1200seconds, $D=(l^2/2t)$, D would be $6.37 \times 10^{-13} \sim 9.64 \times 10^{-12} \text{cm}^2/\text{s}$. According to literature the inter-diffusion coefficient, D, for low molecular weight polymers and oligomers could be in the range of $10^{-5} \sim 10^{-10} \text{cm}^2/\text{s}$ [131] while normal polymer could be in the range of $10^{-8} \sim 10^{-17} \text{cm}^2/\text{s}$ [131]. Although the inter-diffusion could be profiled by the nano-scratch technique, the large range of values indicated further improvement is required.. The scratch size of the Berkovich scratch indenter would be smaller if a smaller load was applied but the smaller the load the more noisy the data. More work needs to be done until an accurate measurement of the inter-diffusion distance can be measured.

The modeling of the interphase strength presented in CHAPTER 7.4 is a first step to incorporate interphase properties, such as chemical bonding and residual stress at the

interphase, into the interfacial shear strength. To solve the whole puzzle, more generalized empirical data for samples of various fiber and matrix combinations are required.

Appendix I

EVALUATION OF FIBER/MATRIX ADHESION

The interphase is where the fiber and matrix bonded together. The bond strength often refers to fiber/matrix adhesion. For fibers without sizing, the contributions to the adhesion could be chemical reaction or interdiffusion of element between fiber and matrix, or van der Waals force, electrostatic attraction, acid-base interaction including H-bond, or mechanical interlock. For fiber with organic coating the situation is rather complex. Beside the interactions mentioned above, the entanglement between the molecules of the sizing and matrix and the interdiffusion [1-4] between compatible sizing and matrix polymers could be one of the important contribution to the adhesion. On the other side, voids, contaminates, etc., and thermal residual stress could be negative contribution to the adhesion.

Direct measurement of the interphase strength, normally refers to adhesion, is very difficult. Therefore, the level of adhesion is assessed practically by the interphase strength value, the interfacial shear strength (IFSS), obtained from destructive mechanical tests. These tests could be classified into three groups, fiber pullout test, single fiber fragmentation test and microindentation test. The microindentation test has attracted much attention because it is an in situ testing method conducted on a real composite, thus allowing for evaluation of the processing or environmental exposure encountered either during manufacturing or in service. The interfacial shear strength value obtained by these

[5-8]. A strong correlation has also been found between the interfacial shear strength and such thermodynamic parameters as surface free energy [9-11] or specific enthalpy of adsorption [11,12]. Therefore, it seems to be possible to obtain information about fibermatrix adhesion from micromechanical experiments. However, there is a problem concerned with correct treatment of experimental data. The attempts made to compare bond strength value obtained by different micromechanical techniques even for the same polymer-fiber pair turned out to be unsatisfactory because the large scatter in the results.

I-1 From Stress Transfer Point of View

For fiber reinforced polymeric composites, a high-modulus fiber embedded in a low modulus matrix. As mentioned in Chapter 2, the matrix holds the fiber together and transmits the applied load to the fiber through a "layer" between fiber and matrix—the interphase. The topic of load transfer from the matrix to the fiber has been treated by a number of researchers. These range from simplified physical model such as Kelly-Tyson model [13] to a number of models in terms of thermo-mechanical properties and microfailure mechanics.

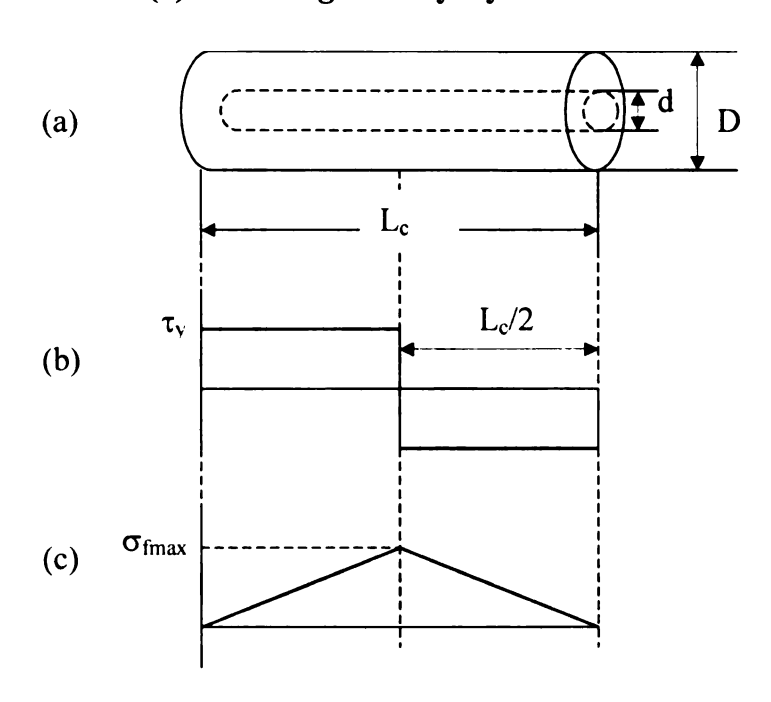
a) Kelly-Tyson Equation [13-16]

Assumptions

1. Fiber is linear elastic and isotropic surrounded by rigid plastic isotropic matrix.

- 2. Perfect bonding between fibers and matrix.
- 3. The transfer of tensile stress from matrix to fiber by means of interfacial shear stress τ_i which is a constant equal to the matrix yield stress in shear.
- 4. Each fiber has two ends which are free from tensile stress.

Fig. I.1 Variation of interfacial shear stress τ (b) and fiber normal stress σ_f (c) with distance along the fiber of a representative volume element (RVE) (a) according to Kelly-Tyson model [16]



A simple idea of force balance gives the solution of interfacial shear stress, see Fig. I.1, as:

$$\tau_y \pi dL_c = \pi \frac{d^2}{4} \frac{\sigma_{f \text{ max}}}{L_C/2}$$
I.1

So,

$$\tau_y = \frac{d}{L_c} \frac{\sigma_{f \max}}{2}$$
 I.2

where $2L_c$ is the "critical transfer length" and σ_{fmax} is the maximum stress in the fiber center. To achieve the maximum stress in the fiber center, the fiber length should at least not be shorter than the critical transfer length.

b) Shear Lag Model and Modified Shear Lag Model [16.17]

Assumptions

- 1. Both fiber and matrix are linear elastic and isotropic.
- 2. Perfect bonding between fibers and matrix, the transfer of tensile stress from matrix to fiber by means of interfacial shear stress.
- 3. The lateral stiffness of the fiber and matrix are the same. In other words, identical axial strain in the fiber and matrix.
- 4. Each fiber has two ends which are free from tensile stress.

Because both fiber and matrix are linear elastic, so that the interfacial shear stress is proportional to the different between u and v, where u is the axial displace ment at a point the same in the fiber and v is the axial displacement the matrix would have at the same point in the represented volume element (RVE) with no fiber present. The rate of change of the fiber axial load P is given by,

$$\frac{dP}{dx} = H(u - v) \tag{I.3}$$

where H is a propotionality constant to be determined from geometrical and material property data. Differentiating Eq. I.3, then

$$\frac{d^2P}{dx^2} = H\left(\frac{du}{dx} - \frac{dv}{dx}\right) = H\left(\frac{P}{A_f E_f} - e\right)$$
 I.4

where the expression $\frac{du}{dx} = \frac{P}{A_f E_f}$ is taken from elementary mechanics of materials

and $\frac{dv}{dx} = \varepsilon_m$ is the matrix strain with no fiber present. Solve this second order differential equation, the interfacial shear stress τ at point x is

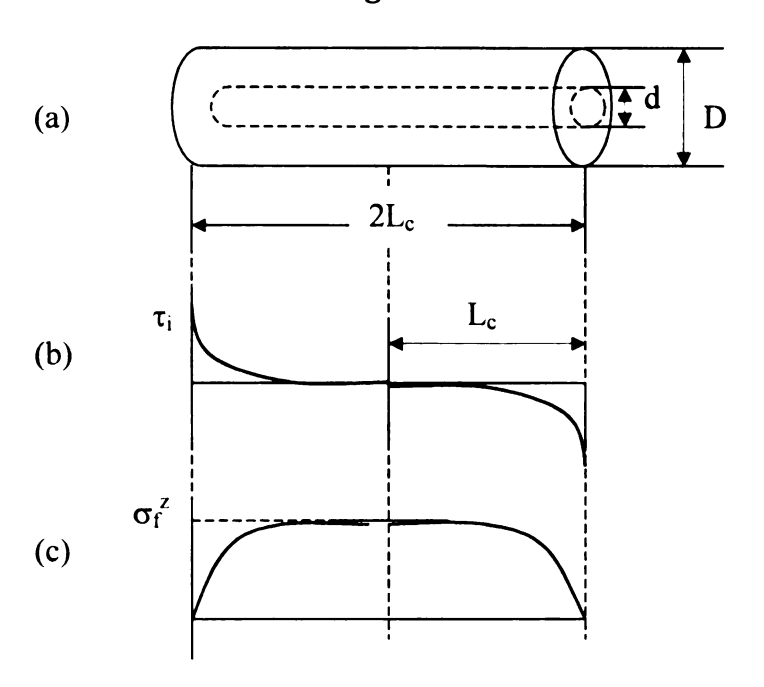
$$\tau = E_f \varepsilon_m \left(\frac{G_m}{2E_f \ln \left(\frac{D}{d} \right)} \right)^{\frac{1}{2}} \frac{\sinh \beta (0.5L - x)}{\cosh \beta 0.5L}$$
I.5

where E_f is the tensile modulus of the fiber, G_m is the shear modulus of the matrix,

and
$$\beta^2 = \frac{2\pi G_m}{A_f E_f \ln(D/d)}$$
.

The solution can be decried by the following figure, Fig. I.2.

Fig. I.2 Variation of interfacial shear stress τ_i (b) and fiber normal stress σ_f^z (c) with distance along the fiber of a RVE (a) according to Cox's shear lag model [16]

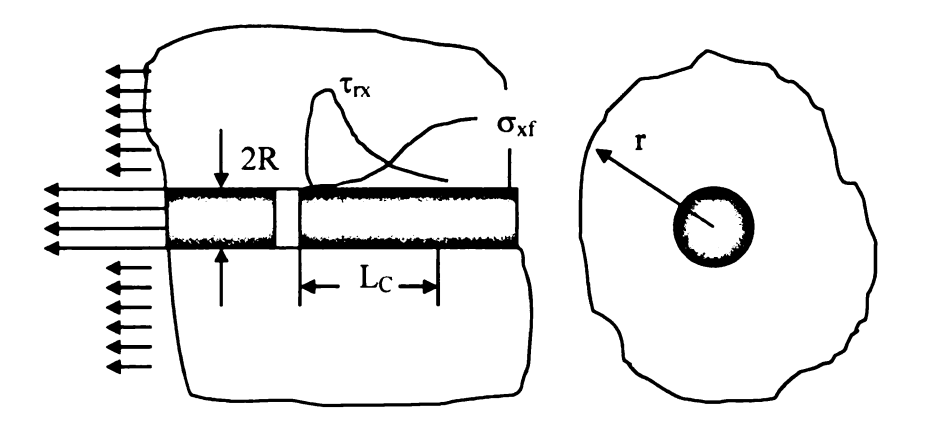


Dow modified Cox's model, assuming that the matrix axial displacement is not constant as opposed to the original assumption of Cox. Rosen further refined the model by considering that the matrix encapsulating the fiber is surrounded by a material having the average properties of the composites. Using the same idea employed by Rosen, Whitney and Drzal [17] also proposed a two-dimensional thermo-mechanics model. The significance of Rosen's work lies in the attempt of quantifying the efficiency of the stress transfer across the interface with respect to the fiber length by introducing the concept of "ineffective length". While the great wok done by Drzal et al. is to use Weibull modulus to evaluate the statistic nature of the critical transfer length.

c) Stress Analysis Model [17]

Whitney and Drzal also proposed a two-dimensional thermo-mechanics model of stress transfer based on superposition of solutions for two axisymmetric problems of the exact far field solution and the approximate local transient solution. The model is based on a single broken fiber sorrounded by an unbounded matrix as Fig. I.3.

Fig. I.3 Stress analysis model [17]



Assumptions

- 1. Both fiber and matrix are linear elastic and the matrix is isotropic while the fiber is transversely isotropic.
- 2. Perfect bonding between fibers and matrix, the transfer of tensile stress from matrix to fiber by means of interfacial shear stress.
- 3. Axisymmetric behaviors for both fiber and matrix.
- 4. Each fiber has two ends which are free from tensile stress.

The model is based on superposition of the solutions to two axisymmetric problems, an exact far field solution and an approximate transient solution. Axisymmetric behavior is assume with the origin of an x, r axis system at the broken end of the fiber (Fig. I.3). The results are summarized here. The axial normal stress, σ_x , in the fiber is independent of d and is of form

$$\sigma_x = [1 - (4.75x^{-} + 1)e^{-4.75x^{-}}]A_1\varepsilon_0$$
 I.6

where $\bar{x} = x/L_c$, ϵ_0 is the far field strain, and A_1 is a constant dependent on material properties, the expension strain and the far field axial strain. The interfacial shear stress is given by the relationship

$$\tau_{xr} = -4.75 \bar{x} \mu A_1 \varepsilon_0 \)e^{-4.75 \bar{x}}$$
 I.7

where

$$\mu = \sqrt{\frac{G_m}{E_{1f} - 4\nu_{12f}G_m}}$$
 I.8

I-2 From Physical-Chemical Interactions Point of View

The modern view of the origin of intermolecular forces is the presence of both polar and non-polar interactions between different molecules. The non-polar one is well accepted as London dispersion force and Fowkes and co-workers [18-23] have led the argument that polar forces (which include hydrogen bonds) are actually Lewis acid-base interactions. So

$$W_A = W^D + W^{ab}$$

where W is the energy of adhesion and superscript D and ab denotes dispersion and acidbase interaction respectively.

a) Schultz's Tentative Model

A tentative model correlating the total work of adhesion with the interfacial shear stress was proposed by Schultz et al. First, a linear relationship between interfacial shear strength τ and the thermodynamic work of adhesion, W_A was found for poorly polar matrix fiber reinforced composites from experimental work ^[24,25]. Then for more polar matrixes, a linear relationship between interfacial shear strength τ measured by fragmentation and the specific interaction parameter, A, was found ^[26,27]. The specific interaction parameter A can be considered as being a specific enthalpy of Lewis acid-base interaction, $-\Delta H^{ab}$, at the fiber-matrix interface. And according to Fowkes, the work of adhesion can be defined in the follow way ^[28]:

$$W_A = W^D + W^{ab}$$

$$= 2(\gamma_f^D \gamma_m^D)^{\frac{1}{2}} - f\Delta H^{ab} n^{ab}$$
I.10

where γ refers to surface free energy, subscribe f and m denotes fiber and matrix respectively, superscript D corresponds to dispersion interaction, f is a correction factor (near unity) to transform enthalpy value to free energy values, and n^{ab} is the number of acid-base site per unite surface area of interface which cannot be directly measured.

After applying equation I.10 with an estimated value of $n^{ab}=6x10^{-6}$ mol/m² [28] to the result of linear relationship between τ and A, a linear relationship between τ and W_A came out again. It is therefore possible to write:

$$\tau = \alpha W_A$$
 I.11

The previous work [103] gave a relation: $\frac{d}{L_c} = \left(\frac{E_f}{E_m}\right)^{\frac{1}{2}}$. Comparing with Kelly-

Tyson equation, $\tau_y = \frac{d}{L_c} \frac{\sigma_f}{2}$, Schultz and et al approximate that:

$$\alpha \approx \left(\frac{E_f}{E_m}\right)^{\frac{1}{2}}$$
I.12

where E_f is the tensile modulus of the fiber, G_m is the shear modulus of the matrix.

b) Gutowski's Theoretical Model

The work of adhesion, W_A , equals to the work required to separate the two materials at their interface is given by Dupre equation:

$$W_A = \gamma_1 + \gamma_2 - \gamma_{12}$$
 I.13

Where γ is the surface free energy, subscribe 1, 2 and 12 refers to materials 1, materials 2 and interface respectively. According to Fowkes, $W_A = W^D + W^{ab}$ and $W^D = 2(\gamma_1^D \gamma_2^D)^{\frac{1}{2}}$, so

$$W^{ab} = \gamma_1 + \gamma_2 - \gamma_{12} - 2(\gamma_1^D \gamma_2^D)^{\frac{1}{2}}$$
I.14

Then use Schultz's semi-experimental expression [29] for acid-base interaction,

$$-U_{12} = \gamma_1 \left(\frac{3}{\gamma_1 / \gamma_2} - \frac{1}{\psi_1^2 (\gamma_1 / \gamma_2)^2} \right)$$
 I.15

Where $-U_{12}$ is the energy of interaction which is equal to the work of adhesion W_A here and $\psi_1 = (\gamma_{C(1)}/\gamma_1)^{1/2}$. The free energy of any material is given by [30],

$$\gamma = \frac{h\overline{\omega}_o}{32\pi^2 r_o^2}$$
 I.16

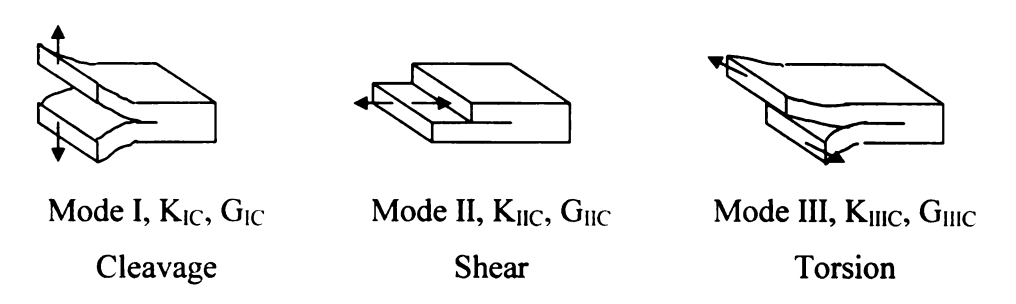
Gutowski began with the interaction force, F_{12} , between two materials. $F_{12} = -dU_{12}/dr$, put equation I.14 into equation I.15 and differential, then put equation I.16 back get the relationship between the interaction force and the surface free energies if the materials as below:

$$F_{12} \propto \gamma_1 \left[\frac{3}{(\gamma_1/\gamma_2)^2} - \frac{2}{\psi_1^2 (\gamma_1/\gamma_2)^3} \right]$$
 I.17

I-3 Measurement of the Interfacial Shear Strength [31-40]

A number of testing methods was developed for measuring fiber-matrix adhesion using single or groups of fibers. For each method, first of all, a mathematics relation was set up. Most of them were based on the theoretical consideration of micromechanics models discussed in section I-1, the Kelly-Tyson model and/or shear lag model or other model extended there from. Then a fracture mode is necessary for a failure criterion. Among the three typical failure modes shown at Fig. I.4, the interphase fracture is normally considered as a combination of mode I and mode II. Even stress intensity factor criterion (K_{IC} , the critical stress intensity factor for mode I, K_{IIC} is for mode II and so on) and strain energy release rate criterion (G_{IC} , the critical strain energy release rate for mode I, G_{IIC} is for mode II and so on) in general deals with a more fundamental aspect of the interface debond problem, the tensile fracture strength criterion or the maximum shear stress criterion has an important advantage in that the interfacial shear strength, whether for bonded, partially debonded or debonded region, can be directly determined from the experimental results of the tests.

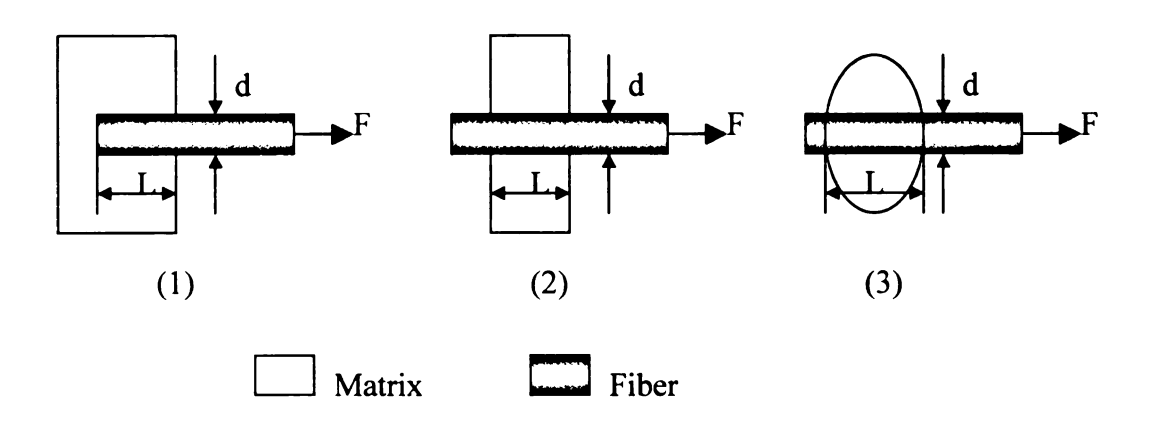
FigI.4 Fracture Mechanics



a) Fiber Pull-out Technique

In the fiber pull out experiments, Fig.I.5, one end of a single fiber is embedded in a block of matrix. The free end is gripped and an increasing load is applied as the fiber is pulled out of the matrix while the load and displacement are measured.

Fig. I.5 Schematic diagram of the single-fiber pull-out method for measuring fiber-matrix adhesion [107]



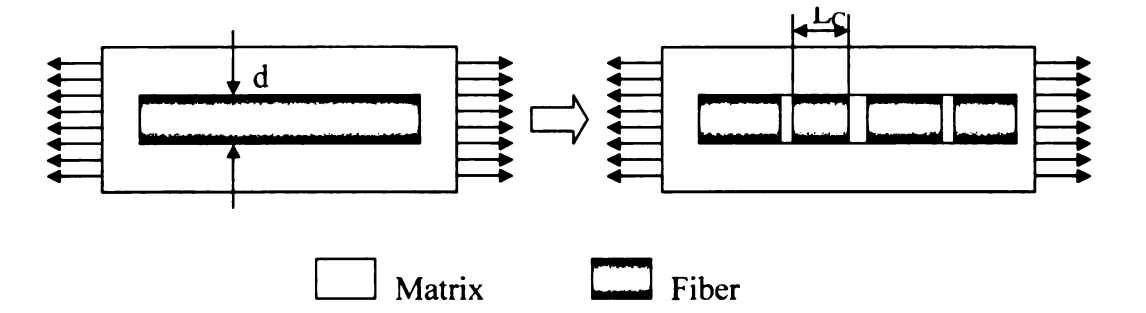
From each load and displacement curve the force at debonding , F, and the embedded length, L, were derived and the interfacial shear stress, τ , is calculated using the simple Kelly-Tyson Equation, equation I.18.

$$\tau = \frac{F}{d\pi L}$$
 I.18

The interfacial shear stress, τ , measured here reflects a combination of adhesion and friction due to coulomb force (Coulomb force also can be considered as one of the interaction force contributed to adhesion).

b) Single Fiber Fragmentation Technique

Fig. I.6 Schematic diagram of the single-fiber fragmentation method for measuring fiber-matrix adhesion [107]



In single fiber fragmentation test, Fig.I.6, the fiber is totally encapsulated in a matrix coupon, a tensile load is applied to the coupon. The interfacial shear stress transfers the coupon tensile to the encapsulated fiber through the interface. As the load is increased on the specimen, shear forces are transmitted to the fiber tensile. The fiber tensile stress increases to the point where the fracture strength is exceed and the fiber breaks inside the

matrix. This fragmentation process is repeated as the sample strain is increased producing shorter and shorter fiber fragments within the coupon until the remaining fragment lengths are no longer sufficient in size to produce further fracture through this stress-transfer mechanism. The final fiber fragment length, also called critical length, is measured. The interfacial shear stress can be calculated based on the final fiber fragment length using either Kelly-Tyson model or shear lag model.

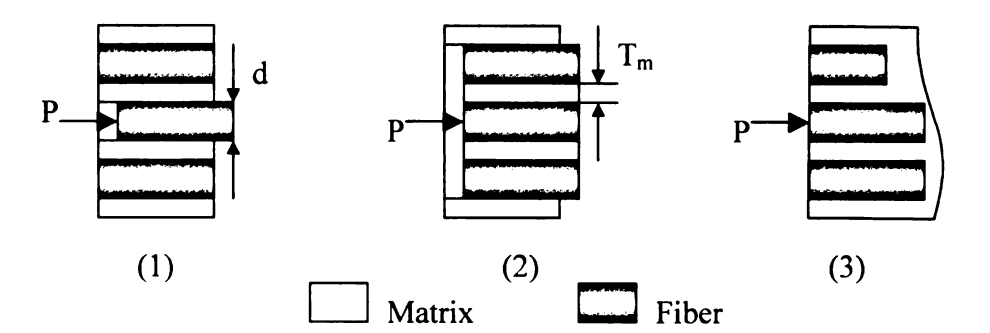
In practice, there is a distribution of the final fiber fragment lengths. Based on Kelly-Tyson model, Drzal et al use Weibull statistic to fit the data as shown

$$\tau = \left(\frac{\sigma_f}{2\beta}\right) \Gamma\left(1 - \frac{1}{\alpha}\right)$$
 I.19

where α and β are the scale and shape parameters from the Weibull distribution, Γ is the gamma function.

c) Micro-indentation

Fig. I.7 Schematic diagram of the microindentation method for measuring fiber-matrix adhesion [38]



The microindentation technique (or push-out test as opposed to the pull-out test) is a single fiber test capable of examining fibers embedded in the actual composite. It can determine the interphase strength due to fatigue or environmental exposure, or possibly monitor the interphase properties of parts in service. The test utilizes a microhardness indenter with various tip shape and sizes to apply a compressive force to push against a fiber end into metallographically polished surface of a matrix block. In the first approach, Fig. I.7 (1), a load is applied continuously to compress the fiber into the specimen surface. The embedded fiber length and the specimen thickness are delicately controlled. In the second approach, Fig. I.7 (2), very thin slice specimens of known embedded fiber lengths are employed to distinguish debonding and post debonding frictional push-out in a continuous loading. This technique has become most popular in recent years among various of specimen geometry and loading method. In the third version of test, Fig. I.7 (3), a selected fiber is loaded using spherical indenters in steps of

increasing force, and the interface bonding is monitored microscopically between steps, until debonding is observed.

The interfacial shear stress is calculated from [40,41]:

$$\tau_{deb} = \sigma_{adj} \left(\frac{\tau_{\text{max}}}{\sigma_{app}} \right)_{FEM}$$
1.20

where τ_{deb} is the maximum shear stress for debonding, σ_{adj} is the adjusted compressive stress applied to the fiber end at debonding and σ_{app} is the applied stress, $(\tau_{max}/\sigma_{app})_{FEM}$ is the ratio of the maximum interface shear stress to the applied stress from the linear axisymmetric finite element.

The finite element result are compared with those obtained from an analytical solution of the Hertz contact problem of a point load on a half-space with imaginary boundaries. Good agreement was found:

$$\tau = \frac{\sigma}{2} \left(\frac{G_m}{E_f}\right)^2 \left(\frac{d}{T_m}\right)^2$$
 I.21

where E_f is the tensile modulus of the fiber, G_m is the shear modulus of the matrix, τ is the interfacial shear stress, σ is the stress applied to the fiber end, d is the diameter of the fiber and T_m is the distance to the nearest neighbor.

REFERENCES

- 1. H. Ho and L. T. Drzal, "Non-linear Numerical Study of the Single-Fiber Fragmentation Test, Part I: Test Mechanics", Composites Engineering, 5, No. 10-11, 1231-1244 (1995).
- 2. H. Ho and L. T. Drzal, "Non-linear Numerical Study of the Single-Fiber Fragmentation Test, Part II: A Parametric Study", Composites Engineering, 5, No. 10-11, 1245-1259 (1995).
- 3. H. Ho and L. T. Drzal, "Evaluation of Interfacial Mechanical Properties of Fiber Reinforced Composites Using the Microindentation Method", accepted for publication in Composites, Part A (1998)
- 4. J. Rich, S. Corbin, and L. T. Drzal, "Adhesion of Carbon Fibers to Vinyl Ester Matrices", Proceedings of International Conference on Composite Materials, ICCM-12, Paris, France, July 5-10, 1999.
- 5. Hoecker, K. Friedrich, H. Blumberg and J. Karger-Kocsis, Comp. Sci. Tech., Vol.54, pp.317, 1995
- 6. H. D. Wagner, H. E. Gallis and E. Wiesel, J Mater. Sci., Vol.28, pp.2238, 1993
- 7. G. S. Sheu and S. S. Shyu, J. Adhesion Sci. Tech., Vol. 8, pp.1027, 1994

- 8. H. J. Jacobasch, K. Gruncke, P. Uhlmann, F. Simon and E. Mader, Composite Interfaces, Vol. 3, pp. 293, 1996
- 9. H. Simon, Ph.D thesis, University de Haute Alsace, Mulhouse, France, 1984
- J. Schultz, L. Lavielle and H. Simon, "Science and new applications of carbon fibers", Proc. Tntern. Symp., pp. 125, 1984
- 11. J. Schultz and L. Lavielle and C. Martin, J. Adhesion, Vol. 23, pp. 45, 1987
- 12. J. Schultz and L. Lavielle, "Inverse Gas Chromatography", Amer. Chem. Soc. Symp. Ser., Vol391, pp.185, 1989
- 13. H. L. Cox, "The elasticity and strength of paper and other fibrous materials", British J. App. Phys., Vol. 3, pp.72-79, 1952
- 14. P. K. Mallick, Fiber-Reinforced Composites, Marcel Dekker, Inc., New York, 1993
- 15. D. Hull and T. W. Clyne, T.W., An Introduction to Composite Materials, 2nd edition, Cambridge university press, New York 1996
- L. T. Drzal, "The Epoxy Interphase in Composites", review chapter in Advances in Polymer Science II, 75, K. Dusek, ed., Spring-Verlag, 1985
- 17. J. M. Whitney and L. T. Drzal "Three Dimensional Stress Distribution Around An Isolated Fiber Fragment", ASTM STP 937, Toughened Composites, 179-196, 1987
- 18. F. M. Fowkes, "Acid-base Interaction in Polymer adhesion.", Physical-chemical Aspect of polymer surfaces, (Mittal ed), Plenum Press, New York 1983
- 19. W. B. Jensen, "Acids, Bases, and Adhesion." Chemtech. v12, 755 1982
- V. Gutmann, The Donor-Acceptor Approach to Molecular Interaction. Plenum Press, New York 1978

- 21. R. G. Pearson, "Hard and Soft Acids and Bases.", Am. Chem. Educ. v64(7) 563
- 22. R. S. Drago, G. C. Vogel and T. E. Needham, "A Four-parameter Equation for Predicting Enthalpies of Adduct Formation.", J. Am. Chem. Soc. v93, 6014, 1971
- 23. L. H. Lee, "The Chemistry and Physics of Solid Adhesion.", Fundamentals of Adhesion, Plenum Press, New York 1991
- 24. H. Simon, Ph.D thesis, University de Haute Alsace, Mulhouse, France, 1984
- 25. J. Schultz, L. Lavielle and H. Simon, "Science and new applications of carbon fibers", **Proc. Tntern. Symp.**, pp. 125, 1984
- 26. J. Schultz and L. Lavielle and C. Martin, J. Adhesion, Vol. 23, pp. 45, 1987
- 27. J. Schultz and L. Lavielle, "Inverse Gas Chromatography", Amer. Chem. Soc. Symp. Ser., Vol391, pp.185, 1989
- 28. F. M. Fowkes, J. Adhesion Sci. Tech., Vol.1, pp7, 1987
- 29. L. T. Drzal, M. Madhukar and M. C. Waterbury, "Surface Chemical and Surface Energetic Alteration of the IM6 Carbon Fiber Surface and Its Effect on Composite Properties", 14th Annual Meeting of the Adhesion Society, Hilton Head, SC (1992).
- 30. L. T. Drzal, "The Role of the Fiber/Matrix Interphase on Composite Properties", Vacuum, 41, 1615-1618, 1990
- 31. L. T. Drzal and M. Madhukar, "Fiber-Matrix Adhesion and Its Relationship to Composite Mechanical Properties" J. Matr. Sci., 28, 569-610, 1993
- 32. G. S. Sheu and S. S. Shyu, J. Adhesion Sci. Tech., Vol. 8, pp.1027, 1994

- 33. L. T. Drzal and P. Herrera-Franco, "Composite Fiber-Matrix Bond Tests", Chapter in the Engineered Materials Handbook: Adhesives and Sealants, 3, 392-405, 1990
- 34. M. C. Waterbury and L. T. Drzal, "On the Determination of Fiber Strengths by In-Situ Fiber Strength Testing", J. Comp. Tech. Res., 13, 22-28, 1991
- 35. V. Rao, P. Herrera-Franco, A. D. Ozzello and L. T. Drzal, "A Direct Comparison of the Fragmentation test and the Microbond Pull-Out Test for Determining the Interfacial Shear Strength", J. Adhesion, 34, 65-77, 1991
- 36. P. Herrera-Franco and L. T. Drzal, "Comparison of Methods for the Measurement of Fiber-Matrix Adhesion in Composites", Composites, 23, 2-27, 1992
- 37. P. Herrera-Franco, W-L. Wu, M. Madhukar and L. T. Drzal, "Contemporary Methods for the Measurement of Fiber-Matrix Interfacial Shear Strength", Polymer, 1991
- 38. P. Herrera-Franco, V. Rao, L. T. Drzal and M.Y.M.Chang, "Bond Strength Measurement in Composites-Analysis of Experimental Techniques", Composites Engr. 2, 31-45, 1992
- P. J. Herrera-Franco, M. Chiang and L. T. Drzal, "The Microbond Technique for Measurement of Fiber-Matrix Interfacial Shear Strength -A Theoretical Analysis-", Proceedings of ANTEC '92, Detroit, MI, 1992
- 40. The Interfacial Testing System (ITS), The Dow Chemical Company, Freeport,
 Texas
- 41. J. F. Mandell, D. H. Grande, T. H. Tsiang and F. J. McGarry, ""Modified microdebonding test for direct in situ fiber/matrix bond strength determination in

fiber composites", Composite Materials:Testing and Design, ASTM STP893,
American Society for Testing and Materials, 1986, pp. 87-108

Appendix II

C++ PROGRAM FOR NANO-SCRATCH TEST

```
#include <stdio.h>
#include <math.h>
#include <stdlib.h>
#define NULL 0
#define FALSE 0
#define TRUE 1
#define PIE 3.1415926
      float Ydisplacement offset, Sdis offset, rad;
      float Ydis, Sdis, Los, Ylf, Ycof, Thcof, Plcof, P2cof, Shratio;
      int Step, Count, AveCount, Condition;
      float SumYdis, SumSdis, SumLos, SumYlf, SumYcof, BaseYdis;
      float AveLos, AveYlf, AveYcof, AveYdis, AveSdis;
      FILE *fp r, *fp w;
      bool First;
float function of d(int Con, float d, float s)
      float theta, beta;
      switch (Con)
      case 1:
            return 0;
            break;
            }
      case 2:
                  if(d<=Ydisplacement offset)</pre>
                        return Plcof;
                  else if (d \ge (sqrt(3)/2)
*Shratio*fabs(s)+Ydisplacement offset))
                        return P2cof;
                  else return (Plcof * ((s*Shratio)*(s*Shratio)-
4.0/3.0*(d-Ydisplacement offset)*(d-Ydisplacement offset))+P2cof *
4.0/3.0* (d-Ydisplacement offset)*(d-
Ydisplacement offset))/((s*Shratio)*(s*Shratio));
```

```
//break:
      case 3:
            s=s-Sdis offset;
            if(d<=Ydisplacement offset)</pre>
                        return Plcof;
            else if ( d > Ydisplacement offset && d <= (sqrt(3)/2)
*Shratio*fabs(s)+Ydisplacement offset))
                  theta= PIE/6-asin((Ydisplacement offset+rad -
d)/(2*rad));
                  return
4/(sqrt(3)*(s*Shratio)*(s*Shratio))*(Plcof*(sqrt(3)/4*(s*Shratio)*(s*Sh
ratio) -theta*rad*rad+sin(theta)*cos(theta)*rad*rad-
sqrt(3)*rad*rad*sin(theta)*sin(theta))+
                        P2cof*(theta*rad*rad-
rad*rad*sin(theta)*cos(theta)+sqrt(3)*rad*rad*sin(theta)*sin(theta)));
            else if (d > (sqrt(3)/2)
*Shratio*fabs(s)+Ydisplacement offset) && d <= Ydisplacement offset +
rad - 2*rad*sin(PIE/6-asin(Shratio*fabs(s)/(2*rad))))
                  theta= PIE/6-asin((Ydisplacement offset+rad -
d)/(2*rad));
                  beta=acos(1-(d-sqrt(3)/2*Shratio*fabs(s)-
Ydisplacement_offset)/rad);
                  return
4/(sqrt(3)*(s*Shratio)*(s*Shratio))*(Plcof*(sqrt(3)/4*(s*Shratio)*(s*Sh
ratio)-theta*rad*rad*rad*(Ydisplacement offset+rad-d)*sin(theta)
+beta*rad*rad -rad*rad*cos(beta)*sin(beta))+
                        P2cof*(theta*rad*rad-
rad*(Ydisplacement offset+rad -d)*sin(theta)-
beta*rad*rad*rad*rad*cos(beta)*sin(beta)));
            else if ( d > Ydisplacement offset + rad - 2*rad*sin(PIE/6-
asin(Shratio*fabs(s)/(2*rad))) & d <= Ydisplacement offset + 2*rad)
                  return P2cof;
            else if ( d> Ydisplacement offset + 2*rad && d <= sqrt(3)/2
*Shratio*fabs(s)+Ydisplacement offset + rad + sqrt(rad* rad - 0.25 *
Shratio*fabs(s) * Shratio*fabs(s)))
                  //theta = acos((d-Ydisplacement offset-rad)/(1+rad));
```

```
theta=asin((d-Ydisplacement offset -rad)/(2*rad))-
1.0/6.0*PIE:
                  return
4/(sqrt(3) * (s*Shratio) * (s*Shratio)) * (Plcof*(sqrt(3) / 4*(s*Shratio) * (s*Sh
ratio) -(theta*rad*rad-
rad*rad*sin(theta)*cos(theta)+0.5*(2*rad*sin(theta)+Shratio*fabs(s))*(s
grt(3)/2*Shratio*fabs(s)-
sqrt(3)*rad*sin(theta))))+P2cof*(theta*rad*rad-
rad*rad*sin(theta)*cos(theta)+0.5*(2*rad*sin(theta)+Shratio*fabs(s))*(s
qrt(3)/2*Shratio*fabs(s)-sqrt(3)*rad*sin(theta))));
            else if (d > sqrt(3)/2)
*Shratio*fabs(s)+Ydisplacement offset + rad + sqrt(rad* rad - 0.25 *
Shratio*fabs(s) * Shratio*fabs(s)) && d <= Ydisplacement offset + 2*rad
+ sgrt(3)/2 *Shratio*fabs(s))
                  theta = acos((d-Ydisplacement offset-rad -
sqrt(3)/2*Shratio*fabs(s))/rad);
                  return
4/(sqrt(3) * (s*Shratio) * (s*Shratio)) * (Plcof*(sqrt(3)/4*(s*Shratio) * (s*Sh
ratio) - theta*rad*rad
+rad*rad*sin(theta)*cos(theta))+P2cof*(theta*rad*rad-
rad*rad*sin(theta)*cos(theta)));
            else
                  return Plcof;
      default:
            return 0;
            //break;
};
main()
{
      printf("Condition = ");
      scanf("%d", &Condition);
      printf("Ydisplacement offset = ");
      scanf("%f", &Ydisplacement offset);
      printf("Sdis_offset = ");
      scanf("%f", &Sdis offset);
      printf("Radius = ");
      scanf("%f", &rad);
      printf("Shratio = ");
      scanf("%f", &Shratio);
```

```
printf("Plcof = ");
      scanf("%f", &Plcof);
      printf("P2cof = ");
      scanf("%f", &P2cof);
      printf("\nStep = ");
      scanf( "%d", &Step);
      if((fp r=fopen("original.txt", "r"))==NULL)
            printf("Error Open Read!\n");
            exit(-1);
      }
      if((fp w=fopen("output.txt", "w"))==NULL)
            printf("Error Open Write!\n");
            exit(-1);
      First=TRUE;
      SumYdis=0;
      SumSdis=0;
      SumLos=0;
      SumYlf=0;
      SumYcof=0;
      Count=1;
      AveCount=0;
      while (fscanf (fp r, "%f %f %f %f %f", &Ydis, &Sdis, &Los, &Ylf,
&Ycof)!=EOF)
      {
            if(First)
            {
                  First=FALSE;
                  BaseYdis=Ydis;
            }
            Sdis=Sdis/1000;
            if( (Ydis-BaseYdis) <= (Step * 0.001) * Count)</pre>
                  SumYdis += Ydis;
                  SumSdis += Sdis;
                  SumLos += Los;
                  SumYlf += Ylf;
                  SumYcof += Ycof;
                  AveCount++;
            else //
                  if(AveCount!=0)
```

```
AveYdis=SumYdis/AveCount;
                        AveSdis=SumSdis/AveCount;
                        AveLos =SumLos/AveCount;
                        AveYlf =SumYlf/AveCount;
                        AveYcof=SumYcof/AveCount;
                        Thcof=function_of_d(Condition, AveYdis,
AveSdis);
            11
                        Thcof=0;
                        fprintf(fp w,"%11.6f %11.6f %11.6f
%11.6f %11.6f %11.6f\n", AveYdis, AveSdis, AveLos, AveYlf, AveYcof,
Thcof, AveYcof-Thcof);
                        Count=(int)((Ydis-BaseYdis)*1000/Step)+1;
                        SumYdis=Ydis;
                        SumSdis = Sdis;
                        SumLos = Los;
                        SumYlf = Ylf;
                        SumYcof = Ycof;
                        AveCount=1;
                  }
            } //else
      } //while
      if(AveCount!=0)
            AveYdis=SumYdis/AveCount;
            AveSdis=SumSdis/AveCount;
            AveLos =SumLos/AveCount;
            AveYlf =SumYlf/AveCount;
            AveYcof=SumYcof/AveCount;
            Thcof=function_of_d(Condition, AveYdis, AveSdis);
            fprintf(fp w,"%11.6f %11.6f %11.6f %11.6f %11.6f
11.6f\n", AveYdis, AveSdis, AveLos, AveYlf, AveYcof, Thcof, AveYcof-
Thcof);
      }
      fclose(fp_r);
      fclose(fp_w);
      return 0;
}
```

Appendix III

RELATIONSHIP BETWEEN LINEAR SHRINKAGE AND VOLUMETRIC SHRINKAGE^[1]

Shrinkage can induce significant stresses in the composite already before loading. While when the material in the liquid state, no stress will be build up. Even when the material in one region is solidified, the surrounding material can still flow and shrinkage induced stress is limited. The main shrinkage caused residual stress is caused by the volume shrinkage after the main domain become a kind of solid. Here we refer this volume shrinkage as ΔV .

For a specific change of volume $\Delta V/V_o$ (V_o is a volume at which the stress caused by volume shrinkage begin to build up) and a deformation state, for an arbitrarily large deformation:

$$\Delta V/V_0 = J_1 + J_2 + J_3$$

Where, $J_1+J_2+J_3$ are the strain invariants, and

$$J_1 = \varepsilon_x + \varepsilon_y + \varepsilon_z$$

$$J_2 = \varepsilon_x \varepsilon_y + \varepsilon_y \varepsilon_z + \varepsilon_x \varepsilon_z$$

$$J_{3} = \begin{vmatrix} \varepsilon_{x} & \frac{1}{2}\gamma_{xy} & \frac{1}{2}\gamma_{xz} \\ \frac{1}{2}\gamma_{xy} & \varepsilon_{y} & \frac{1}{2}\gamma_{yz} \\ \frac{1}{2}\gamma_{xz} & \frac{1}{2}\gamma_{yz} & \varepsilon_{z} \end{vmatrix}$$

For a small strain,

$$\Delta V/V_0 \approx J_1$$

$$J_1 = \varepsilon_x + \varepsilon_y + \varepsilon_z = (\varepsilon_{x0} + \varepsilon_{xr}) + (\varepsilon_{y0} + \varepsilon_{yr}) + (\varepsilon_0 + \varepsilon_{zr})$$

$$\varepsilon_{xr} = \varepsilon_{yr} = \varepsilon_{zr} = 0$$
 and $\varepsilon_{x0} = \varepsilon_{y0} = \varepsilon_{z0} = \varepsilon_0$

So:
$$\Delta V/V_0 = 3\varepsilon_0 = 3\varepsilon^S$$

where ε^S is the linear strain caused by cure shrinkage.

REFERENCES

1. A. Ten Busschen, **Ph.D thesis**, Delft University of Technology, the Netherlands, 1996